JAERI-Tech
2004-071

RESEARCH AND DEVELOPMENT OF REMOTE MAINTENANCE EQUIPMENT FOR ITER DIVERTOR MAINTENANCE

February 2005

Nobukazu TAKEDA, Satoshi KAKUDATE
and Masataka NAKAHIRA

日本原子力研究所
Japan Atomic Energy Research Institute

本レポートは，日本原子力研究所が不定期に公刊している研究報告書です。
入手の問合わせは，日本原子力研究所研究情報部研究情報課（〒319-1195　茨城県那珂郡東海村）あて，お申し越しください。なお，このほかに財団法人原子力弘済会資料センター（〒319-1195　茨城県那珂郡東海村日本原子力研究所内）で複写による実費頒布をおこなっております。

This report is issued irregularly.
Inquiries about availability of the reports should be addressed to Research Information Division, Department of Intellectual Resources, Japan Atomic Energy Research Institute, Tokai-mura, Naka-gun, Ibaraki-ken, 319-1195, Japan.

編集兼発行　　日本原子力研究所

JAERI-Tech 2004-071

Research and Development of Remote Maintenance Equipment for ITER Divertor Maintenance

Nobukazu TAKEDA, Satoshi KAKUDATE and Masataka NAKAHIRA

Department of ITER Project
Naka Fusion Research Establishment
Japan Atomic Energy Research Institute
Naka-shi, Ibaraki-ken

(Received October 19, 2004)

To facilitate easy remote maintainability, the ITER divertor is divided into 60 cassettes, which are transported in the toroidal and radial directions for replacement through maintenance ports located every 90 degrees using the divertor remote maintenance equipment such as in- and ex-vessel transporters. The cassette of 25 tons has to be transported and installed in the vacuum vessel with a positioning accuracy less than 2 mm in the limited space of the vacuum vessel and maintenance port under the intense gamma radiation field. Based on these requirements, the following design and tests were performed. (1) Link mechanism was studied to apply to the transportation of the heavy cassette in the restricted space. A compact mechanism with links for transportation of heavy cassette is designed through the optimization of the link angle taking account of space requirement and force efficiency. As a test result, the lifting capacity of 30 tons (larger than the cassette weight of 25 tons) using two link mechanisms has been demonstrated in the limited space. (2) Compact link mechanism was also studied to apply for locking of the cassette through the optimization of the link angle taking account of space requirement and force efficiency. As a test result, the final positioning accuracy of 0.03 mm for the 25 tons-cassette installation on the vacuum vessel from the initial positioning error of 5 mm has been demonstrated, so that the test result satisfies the requirement less than 2 mm using the link mechanisms in the limited space. (3) Sensor-based control using simple sensors such as optical fiber sensor for divertor maintenance was tested using the full-scale mock-up of divertor cassette and remote maintenance equipment. As a result, it is found that the positioning accuracy of 0.16 mm has been achieved by the optical fiber sensor and this value is sufficient for sensor-based control. In addition, the maintenance operation has been carried out through the human-machine interface, simulating the remote maintenance equipment, divertor, vacuum vessel and port by the virtual reality.

Keywords: ITER, Fusion, Tokamak, Divertor, Remote Maintenance, Sensor-based Control, Human-machine Interface, FMEA, Fail Safe

ITERダイバータ遠隔保守機器の開発

日本原子力研究所那珂研究所ITER開発室
武田　信和・角舘　聡・中平　昌隆

（２００４年１０月１９日受理）

ITERのダイバータは、保守を容易にするために60個のカセットに分割されており、真空容器内および真空容器外搬送装置等のダイバータ遠隔保守機器を用いて、真空容器内を周方向と半径方向に搬送した後、９０度毎に設けられた保守ポートを経由して交換される。25トンのダイバータカセットは、強い放射線環境の下で、真空容器と保守ポートの狭隘な空間内での搬送と2mm以下の精度での設置が要求されている。これらの要求に基づき、以下の設計および試験を実施した。（１）限られた空間での大重量カセットの搬送にリンク機構を適用するための検討を行った。空間的制約と駆動力効率を考慮してリンク角度を最適化し、コンパクトな搬送用機構を設計した。試験の結果、２つの搬送用機構を用いてカセット重量の２５トンを超える３０トンの搬送に必要な持ち上げ力を達成した。（２）搬送用機構と同様にリンク角度を最適化し、コンパクトなリンク機構をカセットの固定に用いるための検討を行った。試験の結果、２５トンのカセットを真空容器に設置する際に、初期の位置誤差が5mmの状態から最終的な位置決め精度として0.03mmを達成した。これにより、リンク機構を用いることで、限られた空間で要求性能である2mmの精度を満足した。（３）ダイバータカセットと搬送装置の実規模試験体を用いて、光ファイバセンサ等のシンプルなセンサによるセンサベース制御の試験を行った。試験の結果、光ファイバセンサを用いて、0.16mmの位置決め精度を達成し、センサベース制御としては十分な水準の精度を得た。また、仮想現実（バーチャルリアリティ）によって遠隔保守機器、ダイバータ、真空容器およびポートを模擬したヒューマンマシンインタフェースを用いた試験も実施した。

那珂研究所：〒311-0193　茨城県那珂市向山801-1

Contents

目次

1. INTRODUCTION

The ITER is a fusion experimental reactor aiming to demonstrate the scientific and engineering feasibility of fusion energy, as shown in Fig. 1-1 [1]. The divertor, which is one of major components in the fusion reactors and whose function is to exhaust helium and other impurities, is classified into the scheduled maintenance component in the ITER, so that the reliable maintenance technology is a fundamental requirement. To facilitate easy maintainability, the divertor is divided into 60 cassettes which are transported in the toroidal and radial directions for replacement through maintenance ports located every 90 degrees using in- and ex-vessel transporters, as shown in Fig. 1-2. The cassette has to be installed in the vacuum vessel with a positioning accuracy less than 2 mm while the cassette is a heavy component (about 25 tons in weight) and the space for the maintenance is quite limited in the vacuum vessel and maintenance port [2]. In addition, 14 MeV neutron caused by fusion reaction induces activation of structural material and emission of gamma ray, so that the maintenance activity has to be performed remotely. The design conditions are summarized in Table 1-1.

Based on the above background, there are the following critical issues to be solved for the remote maintenance of the heavy divertor cassette with a high positioning accuracy in the restricted vacuum vessel and maintenance port under the intense gamma radiation field.

(1) Compact remote handling transporter is required to replace the divertor cassette of 25 tons in the in the restricted vacuum vessel and maintenance port.

(2) Compact locking mechanism is required to fix rigidly and precisely the divertor cassette on the vacuum vessel within 2 mm in order to withstand the electromagnetic forces and seismic loads.

(3) Sensor-based control using simple sensors with radiation resistance is required because the ITV camera cannot be applied to a regular tool due to high radiation.

(4) Human-machine interface is required for easy remote handling by the operators in order to provide the imaginary visual information of the cassette, vacuum vessel and remote maintenance equipment by the virtual reality.

(5) Remote handling equipment is required to provide some countermeasures such as fail-safe mechanisms overcoming the accidents in the high radiation field.

This report describes the results of design and technical development of the divertor remote handling equipment for ITER. In the Chapter 2, the compact mechanisms of the transportation and locking are described for the heavy divertor cassette handling with high positioning accuracy in the restricted space of the vacuum vessel and maintenance port. In the Chapter 3, the design and test results of the sensor based control, human-machine interface and fail-safe are described. Chapter 4 describes the conclusions of this report.

Table 1-1 Requirements for Divertor Remote Maintenance

Atmosphere	Dry nitrogen, 1 bar
Dose Rate	3×10^{-4} Gy/hr
Dimensions of cassette	5 m × 1 m × 2 m
Weight of cassette	25 tons
Installing accuracy	less than 2 mm

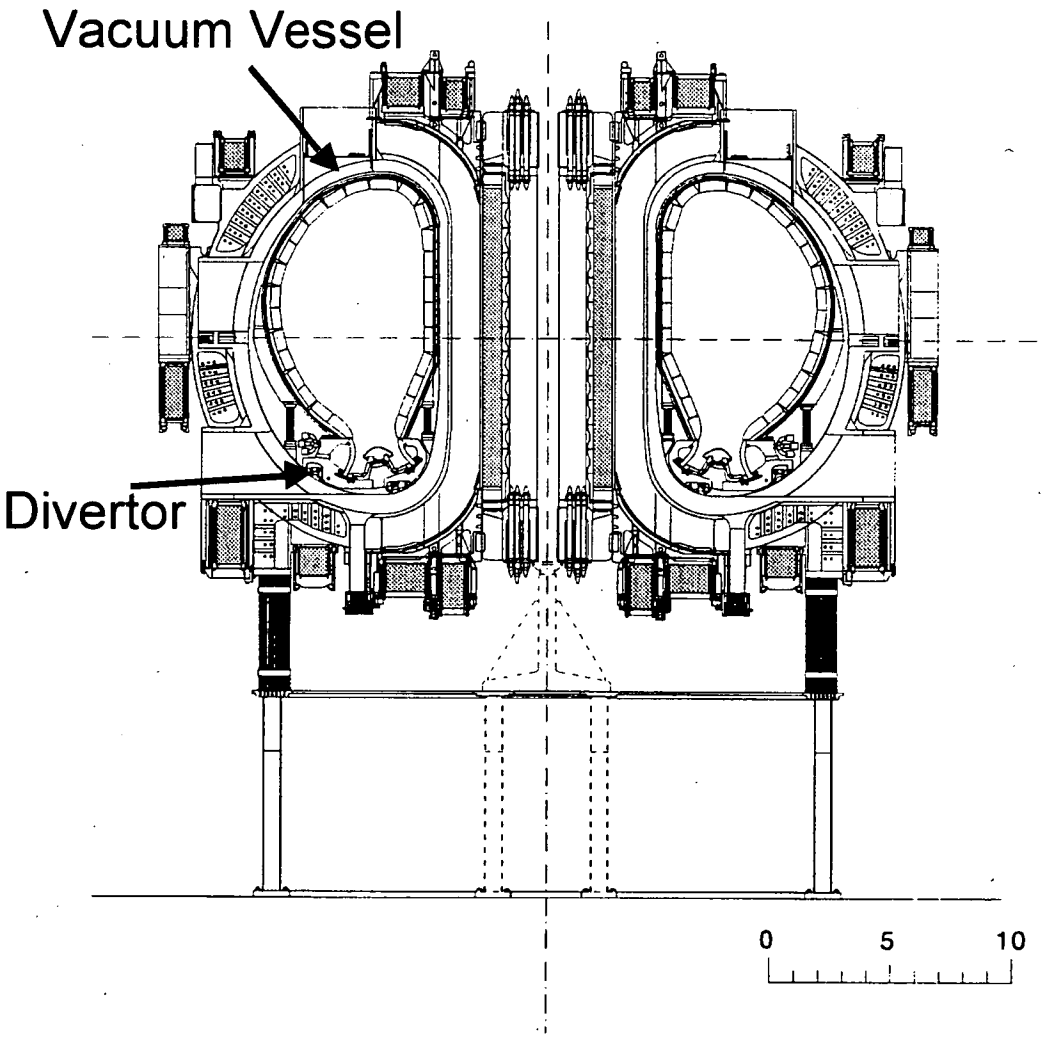

Fig. 1-1 Overall Layout of ITER

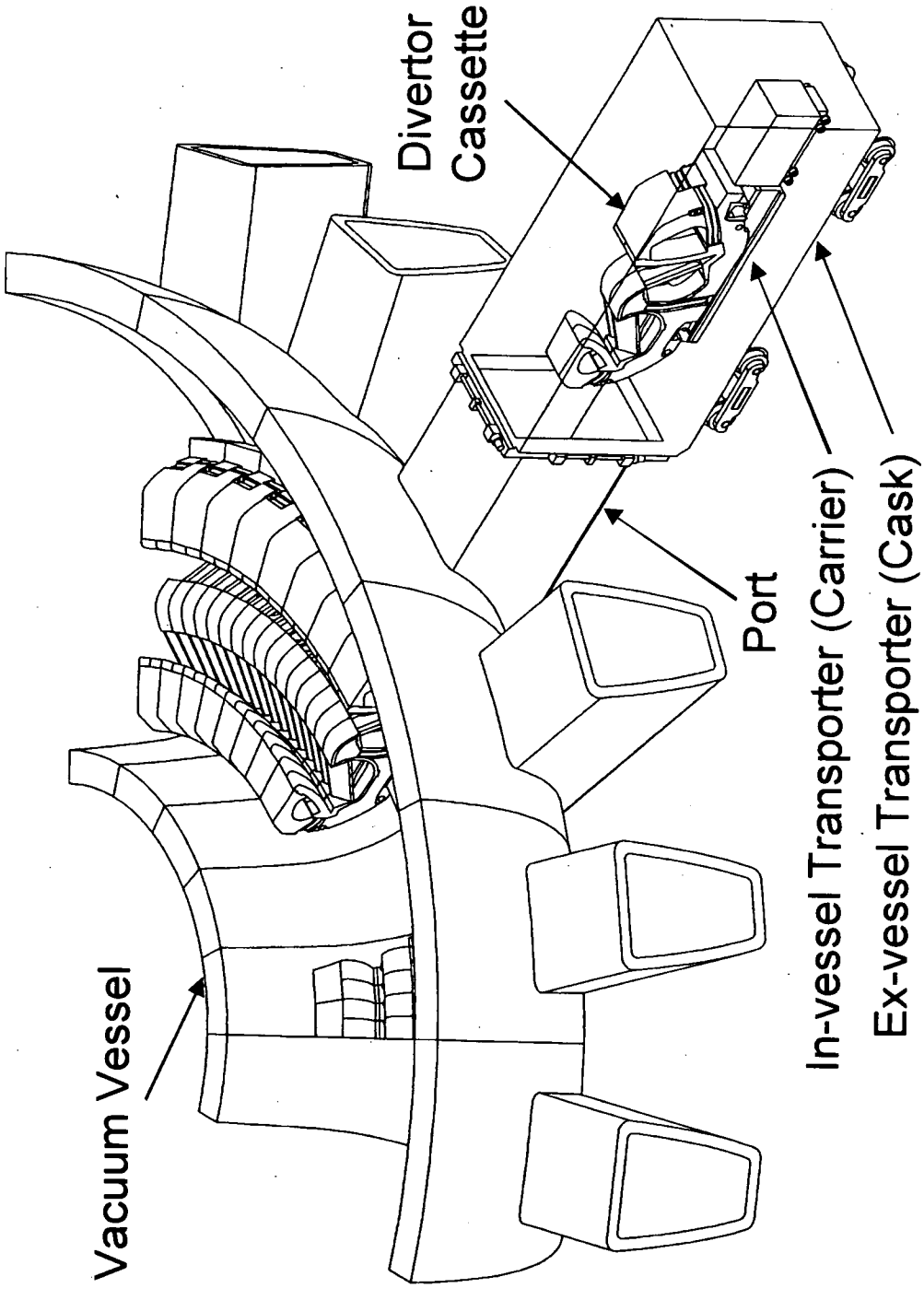

Fig. 1-2 Concept of Divertor Maintenance in ITER

2. LINK MECHANISM FOR TRANSPORTATION AND LOCKING OF HEAVY COMPONENTS

2.1 Basic concept of divertor maintenance in ITER

In the ITER, the divertor is divided into 60 parts, which are colled "cassettes", for deployment and removal. The cassette must be installed in the vacuum vessel with the accuracy of less than 2 mm while weight of each cassette is almost 25 tons. In order to satisfy both requirements, the toroidal rails were adopted to the maintenance system. The rails guide the cassette to its installed position and support it their. The cassettes are fixed to the rails using the locking system, which sustains the severe electromagnetic loads, accommodates thermal expansion and aligns the cassette within a final tolerance of 2 mm. The rails are used for transportation also. The cassettes are transported through the "maintenance ports" located every 90 degrees using in-vessel transporters and ex-vessel transporters.

The in-vessel transporters are categorized into two types: a cassette toroidal mover (CTM) and radial carriers. The former moves cassette between the installed position and the maintenance port toroidally (movement "A" in Fig. 2-1) and the latter carries radially between the vacuum vessel and the ex-vessel transporter (movement "B" in Fig. 2-1). There are three types of the radial carriers: the Central Cassette Carrier (CCC), the Second Cassette Carrier (SCC) and the Regular Cassette Carrier (RCC). The CCC is used for the cassettes located nearest to the maintenance port (Central Cassette), SCC for those located at both sides of the Central Cassette (Second Cassette) and RCC for other cassettes (Regular Cassette). All the radial carriers cannot move by themselves but is pushed by a tractor. There is laid two radial rails on the floor of the maintenance port for radial movement of the carriers.

2.2 Selection of suitable mechanism for maintenance of heavy components

The maintenance system of the divertor cassette needs two main functions: transportation and locking. Regarding the transportation, the function can be separated into two subfunctions: lift in the vertical direction and movement in the horizontal direction. By this separation of function in transportation, efficiency of the total system can be optimized and the mechanism can be compact. The compactness of the mechanism is quite important because the working space is limited. The vertical lift needs a jack-up system which achieves large output force while the horizontal movement needs only rollers which reduce friction force and a drive whose traction force is larger than rolling friction force. The locking of the divertor cassette also needs relatively strong output force which can overcome the sliding friction force for the alignment of the position. In addition, the locking system

must sustain the external loads on the cassette such as electromagnetic force and seismic load. The required output force and the expected external load are summarized in Fig. 2-2 and 2-3, respectively. Therefore, both of transportation and locking systems need some mechanism which is compact and enables large output force.

There are other requirements other than compactness and output force. The required characteristics for the mechanism used for the divertor maintenance system (including two requirements mentioned above) are as follows:

- compactness (because of limited space)
- large power (25 tonf for jack-up system and 7.5 tonf for locking system)
- radiation hardness (3×10^{4} Gy/hr)
- fail safe (it is difficult to fix failure externally)
- simplicity (complex system is not reliable)

For the jack-up system, following mechanisms can be used but most of them are not adequate because of requirements mentioned above:

- oil cylinder (not radiation-hard)

  Radiation reduces viscosity of oil and so the oil can leak into the vacuum vessel. This kind of impurity must be excluded from the plasma.
- hydraulic cylinder (not compact)

  Rubber O-ring cannot be used in the radiation field so the metal bellows must be used. This makes mechanism large.
- rack-and-pinion mechanism (not fail safe)

  Once the rack or pinion is broken, the jack cannot sustain its position.
- worm gear mechanism (not compact)

  The system becomes relatively large if the same output force is achieved.
- link mechanism (satisfies all the requirements)

Therefore, the link mechanism is selected not only for the jack-up system but also for the locking system because it has similar requirements. Figure 2-4 shows concept of jack-up system, or mechanical jack, and the locking system using the link mechanism.

2.3 Mechanical jack for in-vessel transporter

The mechanical jack must be equipped by all of in-vessel transporters other than the RCC because the CTM lifts up and down the cassette instead of the RCC. In this section, design of the mechanical jack for the SCC is discussed. The SCC needs two mechanical jacks, inboard and outboard, which must move in the toroidal direction also (see Fig. 2-5).

Requirements for the mechanical jack can be summarized as follows:

- Lift up force: 15 tonf
- Transfer efficiency of force: larger than 1

- Dimension: 240 mm (W) x 246.4 mm (H)

The requirement for dimension is quite strict so the mechanism must be as compact as possible.

As shown in Fig. 2-6, larger angle of link can achieve higher transfer efficiency of force and power. In order to make the transfer efficiency of force higher than one, the angle of link must be larger than 45 degree.

On the other hand, larger angle of link increase horizontal movement of the center of the link as shown in Fig. 2-7. The horizontal movement affects on the compactness directly so it must be reduced as possible.

In order to satisfy these two requirements, the angle of link must be as small as possible and larger than 45 degrees. Considering the arrangement with motors and gears, the range of angle was decided between 45 and 70 degrees. The actual mechanism is shown in Fig. 2-8.

2.4 Locking system

The locking system of the divertor cassette has to be capable of sustaining the external loads, such as the electromagnetic force or the seismic loads, acting vertically, radially and toroidally on the cassette, while keeping a flexiblility to accommodate thermal expansion due to high temperature in the normal operation. In addition, a positioning capability is also required to align the cassette with an accuracy of 2 mm. To satisfy these requirements, a link mechanism with tapered pins or plates was adopted as a locking system of the cassettes mounted to the toroidal rail. In this section, design of the inboard locking system for the Central Cassette is discussed.

Figure 2-9 shows a structural concept of the locking system developed for the Central Cassette. The locking system is composed of pins connected to a link mechanism with ball screw which can be handled by the wrenches equipped by the CCC. Since the toroidal rails are interrupted in the Central Cassette position, the locking pins are designed to insert toroidally into the toroidal rail segment. In the inboard region, two tapered pins are inserted into the inboard rail segments, so that the Central Cassette is moved inward along the angle of the tapered pins and is tightly fixed to the inboard vacuum vessel bank so as to bear the electromagnetic loads. In the outboard region, on the other hand, two straight pins are inserted into the outboard rail segments to fix the cassette and to allow radial movement by sliding so as to accommodate the thermal expansion. The angle of the tapered pins can also provide a positioning capability to align the cassette into the final position within the required precision.

The functions of the locking system for the divertor cassette can be summarized as follows:

- Positioning during cassette installations (with an accuracy of 2 mm)
- Support of external loads such as electromagnetic force, seismic load and so on
- Absorption of thermal expansion due to temperature differences in cassettes and vacuum vessel
- Remote locking and unlocking

Design conditions for the inboard locking system can be summarized as follows:

- Propelling force for alignment: 7.5 tonf (See Fig. 2-2)
- External loads: ~400 tonf (Downward) (See Fig. 2-3)
- Maximum positioning error to be aligned:
- Transfer efficiency of force: larger than 1
- Dimension: 475 mm (W) x 170.5 mm (H) x 666 mm (Toroidal, Outboard)

As shown in Fig. 2-10, smaller angle of link can achieve higher transfer efficiency of force and power. In order to make the transfer efficiency of force higher than one, the angle of link must be less than 45 degree.

On the other hand, the insertion stroke of the locking pin, which is decided by the maximum positioning error and the angle of the taper, must have a margin for unexpected errors. Assuming this margin as 5 mm, the angle at start of insertion must be larger than 37 degrees as shown in Fig. 2-11.

In order to satisfy these two requirements, the angle of link must be as small as possible and larger than 37 degrees. Considering the arrangement in the cassette, the angles at start of insertion and at maximum insertion position were decided as 37 and 14 degrees, respectively.

2.5 Result of test for mechanical jack and locking system

The mechanical jack and the locking system were tested using the dummy cassette, whose weight was same as the actual cassette, 25 ton. As shown in Table 2-1, the mechanical jack operated well with the normal motor torque as assumed. The inboard locking system was tested using the wrench of the CCC. The cassette was put on the vacuum vessel by the CCC with different radial misalignments: 1, 3 and 5 mm. Results of the test are summarized in Table 2-2. The locking system could align the cassette with accuracy of 0.03 mm. The maximum required torque for the wrench was 690 kgf•cm.

As a result, the mechanical jacks and the locking system were successfully designed and fabricated using the link mechanism.

Table 2-1 Performance test for mechanical jack

Load (tonf)	Stroke (mm)	Maximum motor torque (kgf•cm)			
		Inboard		Outboard	
0	15	0.7	1.1	0.6	0.6
25	15	13.0	14.0	5.7	5.7

Table 2-2 Performance test for locking system

Initial (mm)	Final (mm)	Maximum wrench orque (kgf•cm)
1	0.03	690
3	0.02	670
5	0.02	670

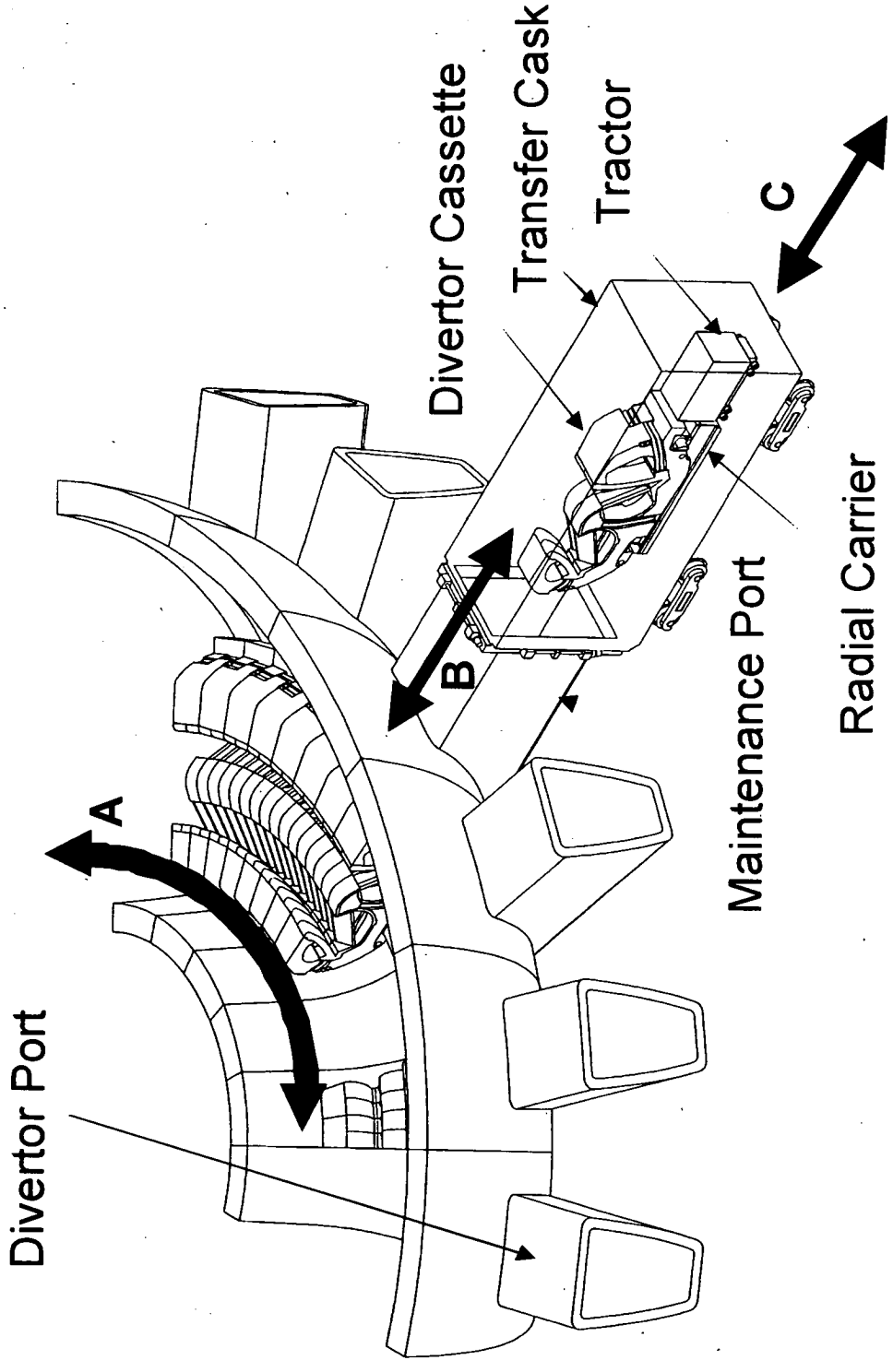

Fig. 2-1 Concept of divertor maintenance system in ITER

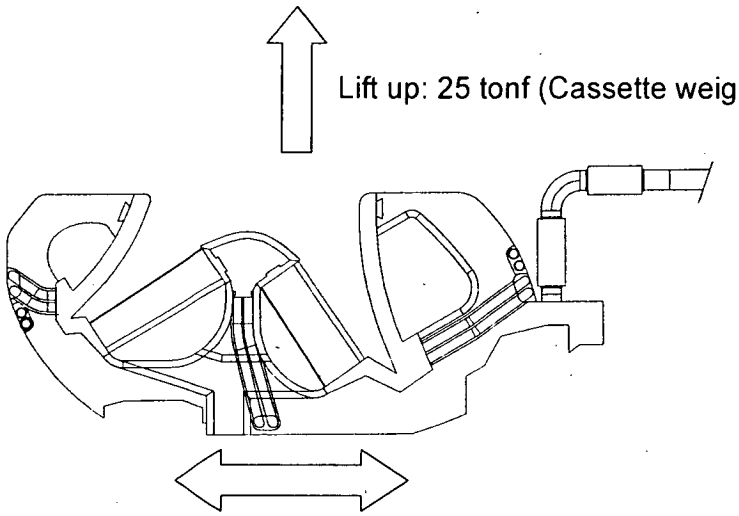

Fig. 2-2 Required Output Force for Transportation and Locking of Divertor Cassette

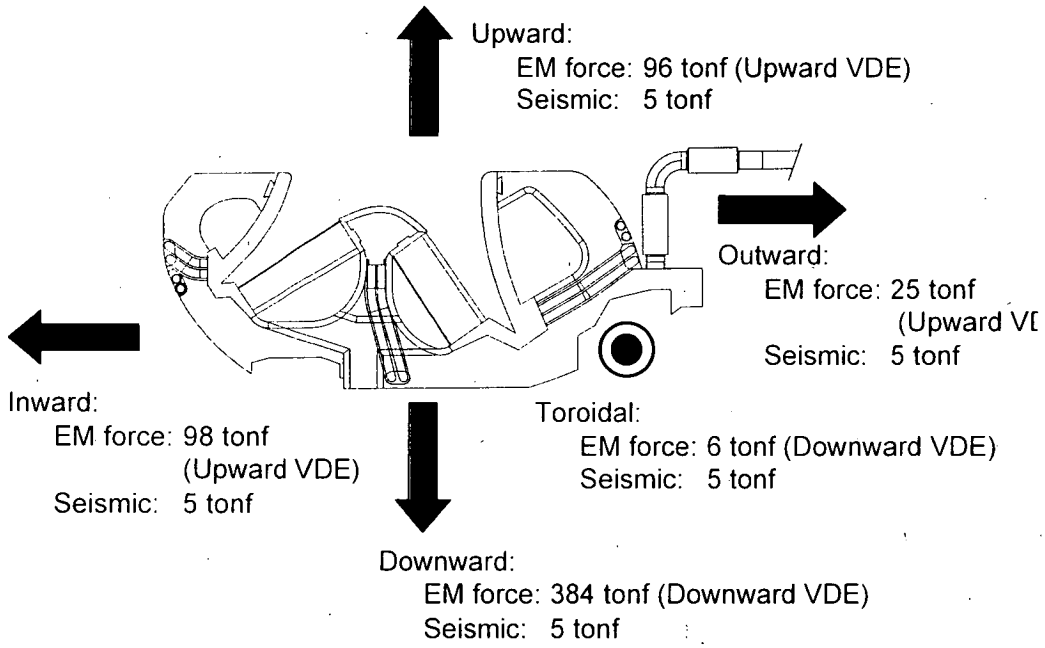

Fig. 2-3 External Loads Applied on Divertor Cassette

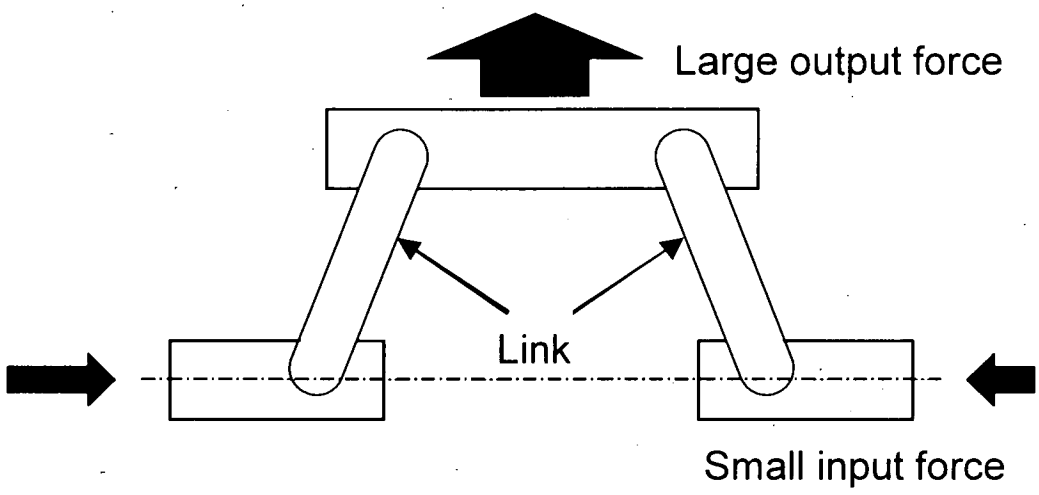

(a) Mechanical Jack System

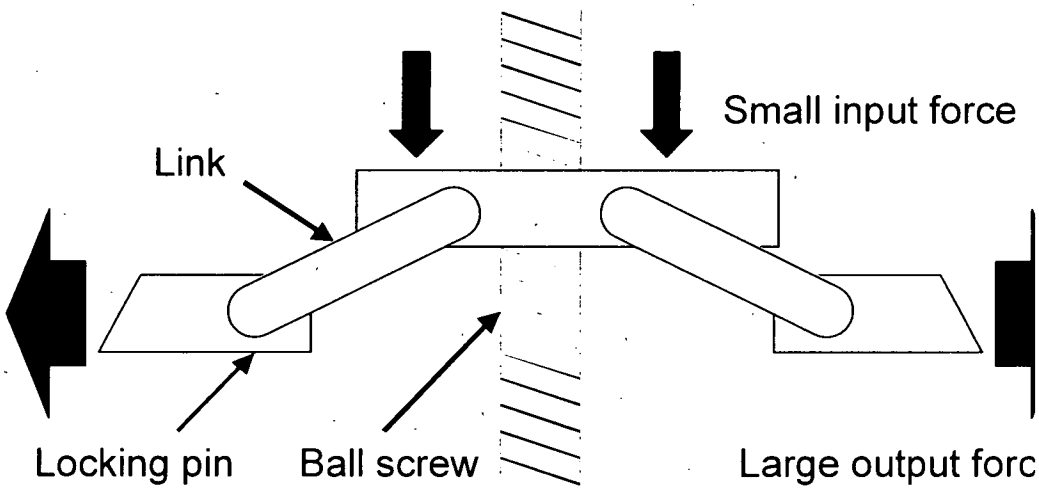

(b) Locking System

Fig. 2-4 Concept of Mechanical Jack System and Locking System Using Link Mechanism

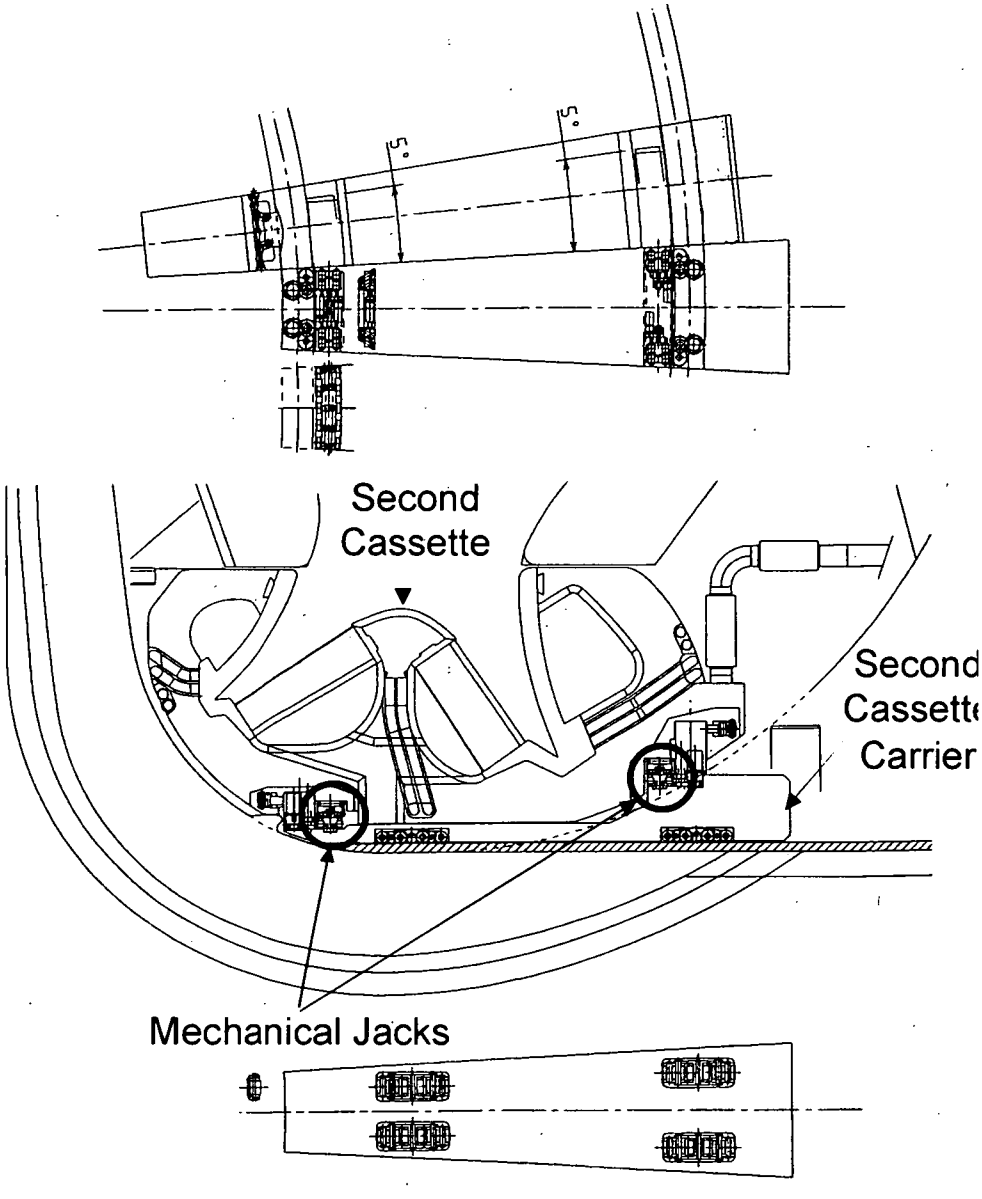

Fig. 2-5 Mechanical Jacks for Second Cassette Carrier

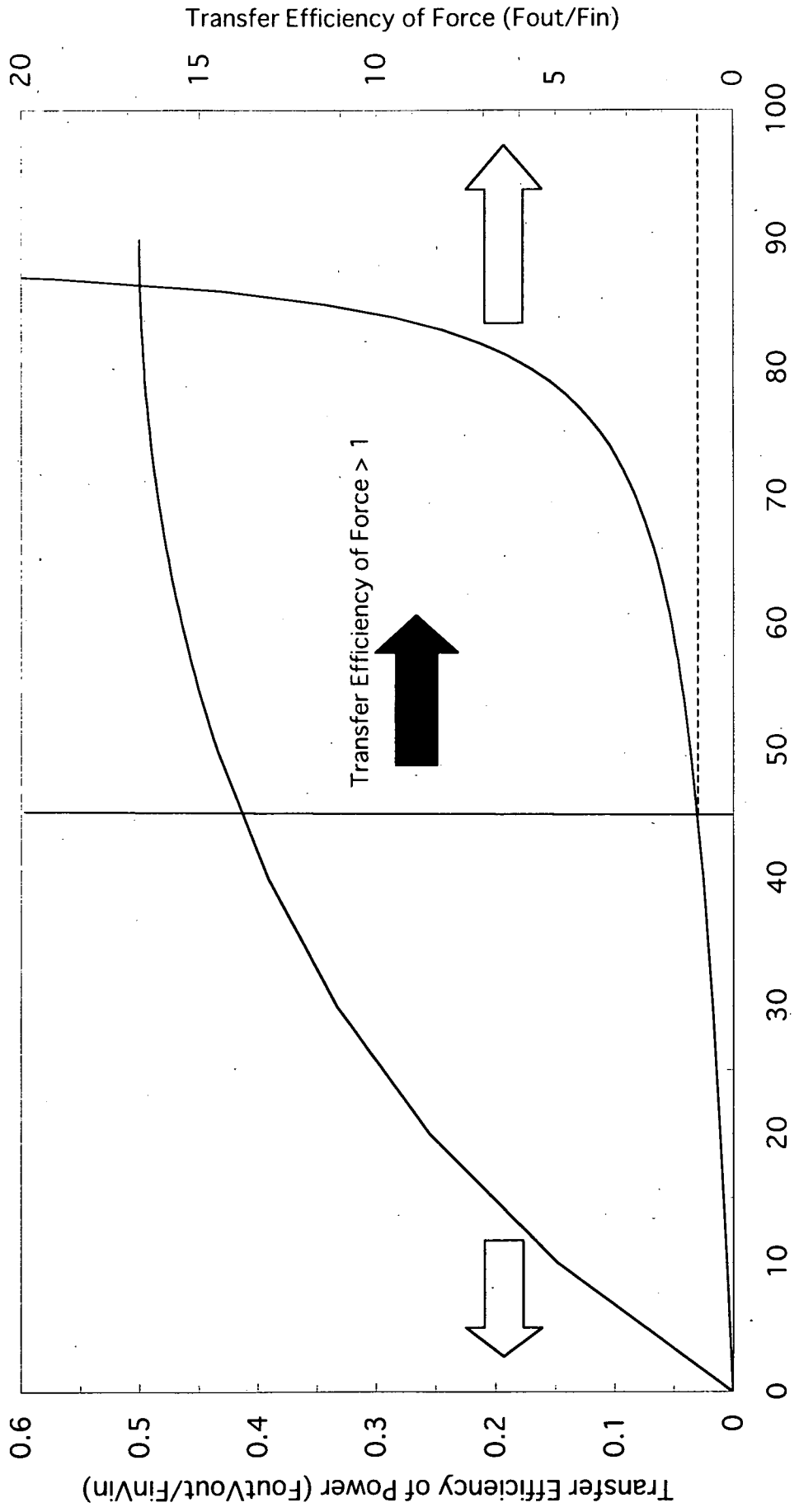

Fig. 2-6 Transfer Efficiency of Power and Force of Link Mechanism

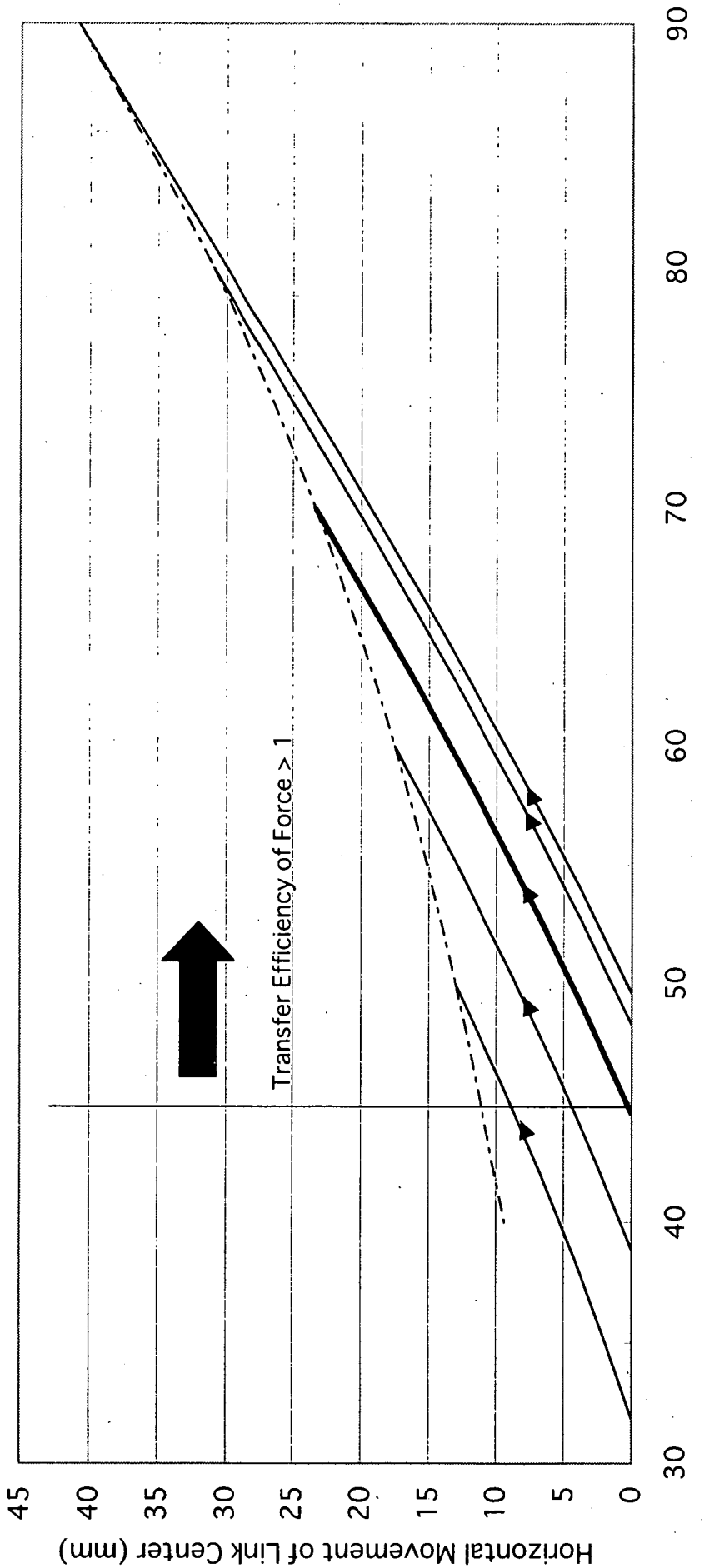

Fig. 2-7 Angle of Link and Its Horizontal Movement of Link (Jackup 15 mm)

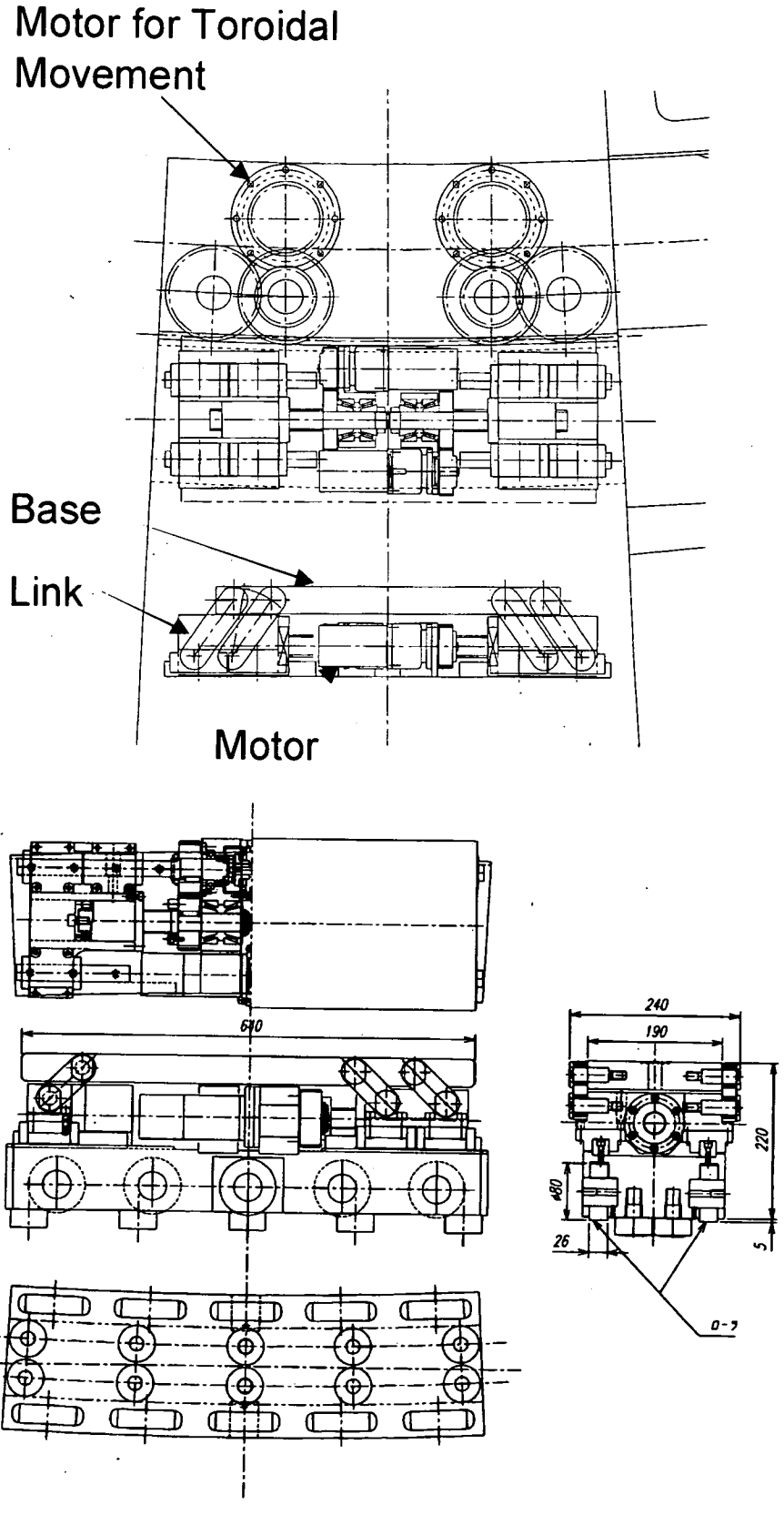

Fig. 2-8 Designed Jack-up System for Second Cassette Carrier (Inboard)

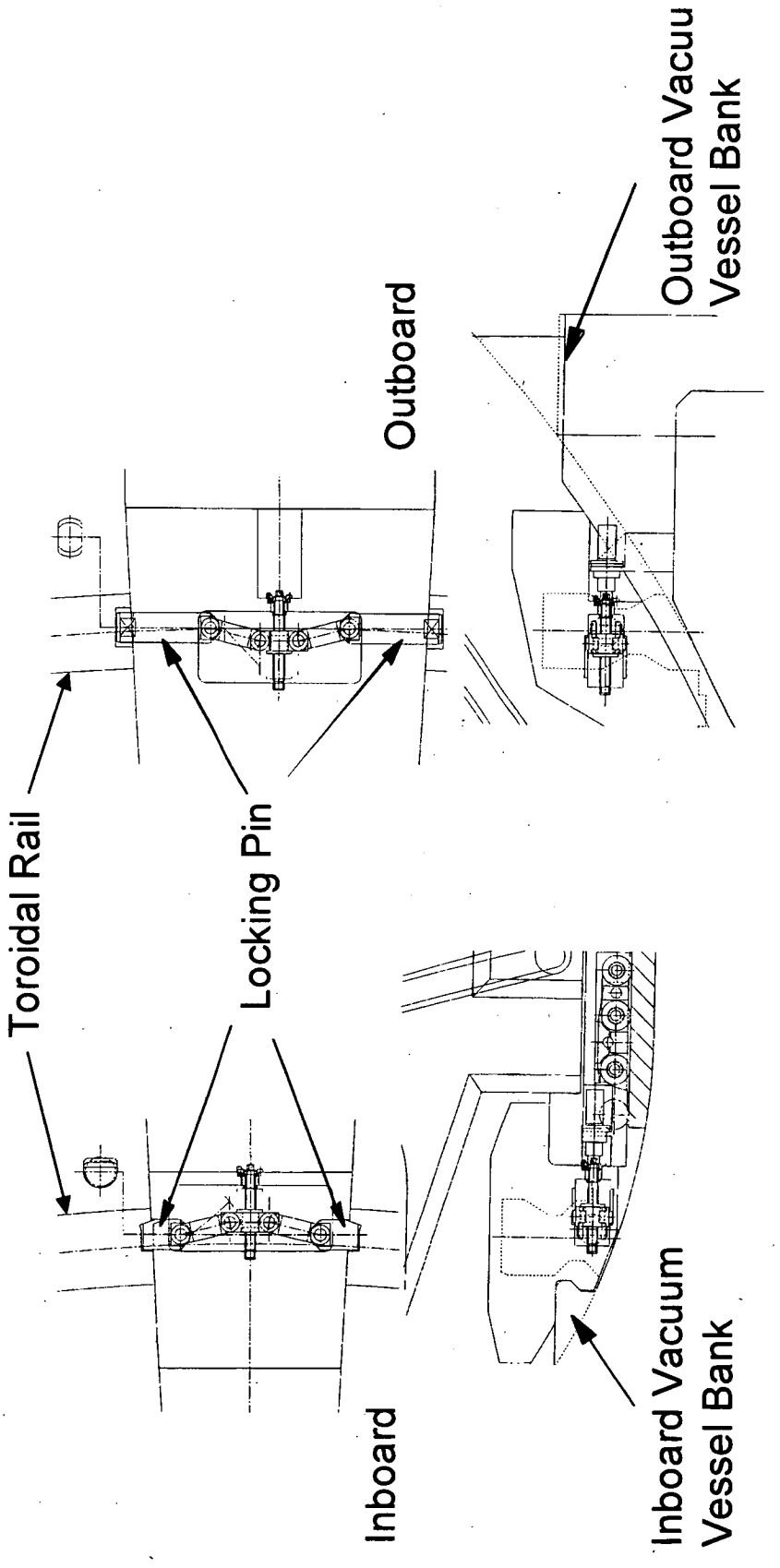

Fig. 2-9 Concept of Central Cassette Locking System

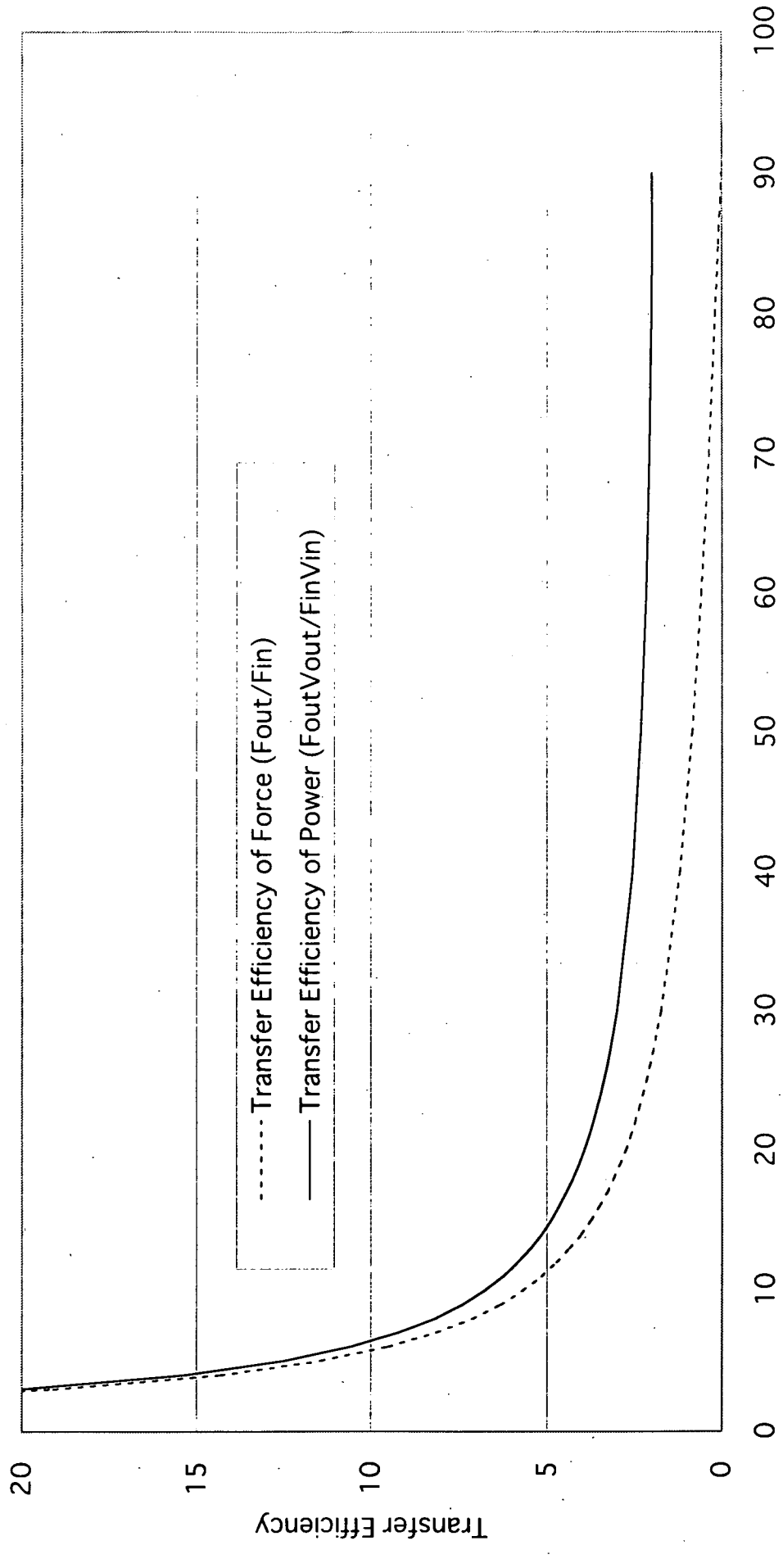

Fig. 2-10 Transfer Efficiency of Power and Force of Link Mechanism

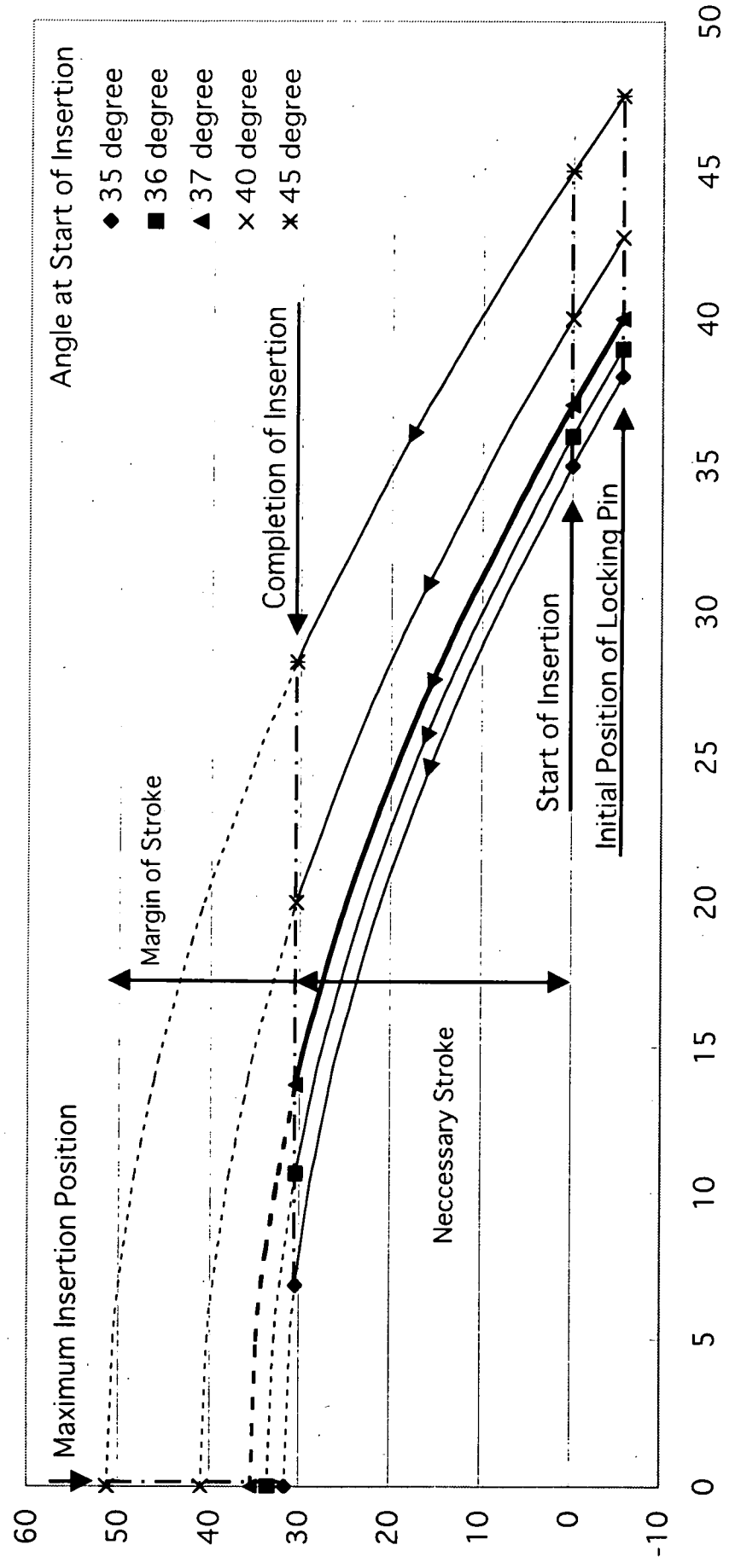

Fig. 2-11 Relation between Angle of Link and Insert Stroke of Locking Pin

3. DETAILED DISCUSSIONS ON R&D OF DIVERTOR MAINTENANCE SYSTEM

3.1 Assessment of "Fail-safe" Behavior and Rescue Procedures of the SCM

3.1.1 Failure Mode and Effect Analysis for SCM

A failure mode and effects analysis (FMEA) was executed for the SCM with the following assumptions, in order to examine a rescue system of the remote maintenance equipment of a divertor cassette.

a. Object of analysis is the SCM.

b. Tractor, SCC, a controller, a wiring harness, transported cassette itself and a reactor structure (especially baffle adjacent to the cassette and toroidal rails) were examined as subsystems.

c. A failure is considered to be single fault, and combined failure is not considered.

d. A failure does not depend on operation and its situation of a system and a subsystem.

Fig. 3-1 shows a reliability block diagram where the system of the SCM is resolved into subsystems, components of subsystems and parts of components and they are classified by their functions. The analysis is performed until the level of parts shown in Fig. 3-1.

As the first step, failure modes of the subsystems are categorized into four modes: "Inability of motion", "Decrement of driving power", "Decrement of speed" and "Lowering of positioning accuracy"; and effects of failure, methods to detect failure and methods of rescue are analyzed for each subsystem. The result is shown in Table 3-1.

It is the failure at the transit position between the SCM and the installation position that affects seriously. The rescue system must move the cassette in the worst case.

If the cassette at the transit position can be removed by the rescue system and if the fork retreats on the SCM, the rescue of SCM is enabled by equipping the transfer cask with a tractive mechanism, which pulls back the SCM into the transfer cask in case of failure. . The current TRC, however, cannot be actuated by the external mechanism because of a breaking force of the driving mechanism, unless the engagement between the lack and the pinion is released. The following solutions are effective:

- Selecting a reduction gear ratio so as to be actuated backward
- Selecting a break whose breaking torque is small so as to be actuated by an excessive force
- Arranging a torque-limiting coupling in the driving system so as not to transmit an excessive torque to the motor, reduction gear and break with the

coupling slipped

The cassette is included in the subsystems because the deformation of the cassette and reactor structure make severe problems, and the following results are found:

- It is possible that the transportation of the cassette is disturbed by the deformation of structure, such as the guide rail where the fork moves and the interface between the cassette and the toroidal rail where the electromagnetic force acts. The deformation is critical to the current system so it is recommended that an inspection system is introduced and operated to confirm the integrity of the positions mentioned above before the maintenance operation.
- It is suggested that the integrity is confirmed by observing defects, dusts and deformation on the guide rail.
- It is possible that the transportation of the cassette is disturbed by the deformation of the buffles and the toroidal rails. It can be observed from inside of the tokamak so the status should be confirmed by the in-vessel viewing system before the operation.

In case that the CTM is used, the inspection tool can be kept by a manipulator installed on the CTM and can confirm the integrity of the reactor structure.

On the other hand, the SCC is complicated comparing to the TRC so the FMEA is proceeded into the deeper level. The failure modes of components are classified into four modes: "Inability of motion", "Decrement of driving force", "Decrement of speed" and "Lowering of positioning accuracy" and the effects of failure, methods to detect failure and methods of rescue are analyzed.

It is confirmed again that the failure of the fork at the transit position between the SCM and the installation position affects most seriously. When the cassette is removed by the rescue system, it should be moved to the installing position so as to secure the accessibility of the rescue system to the SCC from the port side and reactor side.

It is advisable that the jack-up and pushing mechanisms of the fork can move the cassette to the SCC or the installing position even in case of failure in order not to leave the cassette in the worst condition, that is , at the transit position. Regarding this point, the current fork system do not have a break for the jack-up mechanism because of space restriction. It is desirable, however, that the fork can sustain the cassette with jacked up even in case of power cut so as not to leave the cassette at the transit position. The electromagnetic break is installed relatively near the motor and its breaking torque is small, so it is easy to force the brake to actuate externally. From this viewpoint, it cannot be said that the break in the actuating mechanism makes the rescue difficult. It is considered, therefore, that the break should be installed also in the jack-up mechanism so as to keep the position even in case of failure.

Furthermore, it is confirmed again that the failure of the fork driving mechanism stops function of whole system if it happens during deployment of the fork.

Therefore, the FMEA has been proceeded into the level of the parts composing the jack-up and driving mechanisms of the fork; and the considerable failure mode, effect of failure, method to detect failure, failure level and failure frequency has been listed up and estimated for each part.

As the failure frequencies are not obtained from the providers, they are defined qualitatively. It is assumed that the failure of the servo motor on control and the depletion of the grease under radiation are frequent.

The former can be restored by the adjustment and repair in the control device located outside of the tokamak. It is effective to modify the motor driver in advance to enable adjustment after error to ease the criteria of error or to change the parameter such as the torque limit and so on. In addition, resistance to an encorder error can be increased by modifying the motor to enable the driving operation without speed control.

The other failures rarely happen after the inspection for the design. Most of them are breakdowns of some parts in rotating systems. However, it is critical if it happens once. The rescue scenario, where the driving mechanism is rotated by an external actuator, becomes impossible. The rescue scenario is needed that the fork driving mechanism is released from the fork and the fork is pulled back to the SCC, and/or that the fork driving mechanism is replaced by the blanket manipulator.

There is a possibility that the mechanism is broken by operation error while it is considered to happen rarely. The breakdown of the mechanism is critical so the design is necessary that the components are not broken by the excessive motor torque. In addition, the interlock is needed for the excessive motor torque.

3.1.2 Rescue procedures of the SCM

(1) Rescue of TRC

The concept of the rescue of the TRC is shown in Fig. 3-2. As considered in Section 0, the basic concept of the rescue for the TRC is to tract it back to the port (here the conditions required for rescue, such as location of the fork and the cassette, is assumed as satisfied).

The rescue TRC is transported by the rescue cask and is introduced from it. The structure of the rescue TRC can be same as the normal TRC except the radial driving mechanism whose torque must be improved. The connector between the normal and rescue TRC should be automatic as that of trains. The TRC and SCC retracted by the rescue TRC to the cask.

(2) Rescue of SCC

For the rescue of the SCC, two mechanisms are considered: the mechanism that moves

the cassette at the transit position and the mechanism that retract the fork to the SCC to enable withdrawal to the cask

As the first step of rescue, the method to actuate the failed mechanisms compulsorily by an external power assuming that the actuator such as motor does not work while the mechanisms are not broken mechanically. The rescue mechanisms installed on the SCC are shown in Fig. 3-3. Bits to be engaged with nut runners are projected at the jack-up and driving mechanisms of fork so that the external power can be input from the bits. Those positions are at the periphery of the SCC so that the external power can access easily even if the fork moved bi-directionally. The both mechanisms have two motors for each and the two motors are connected by chains in order to synchronize.

From viewpoint of space, it is difficult to prepare the structure enough stiff to support the nut runner which input the external power. Therefore, a hole is prepared near the rescue bit and the nut runner inserts a rod to the hole when it insert its socket wrench to the bit in order to sustain the reaction force caused by rotating the bit.

Fig. 3-4 shows the concept of the SCC rescue manipulator with the nut runner on the tip, introduced from the port. A support arm is installed on the above mentioned rescue TRC and equipped with the radial movement mechanism. The articulated manipulator is attached to the support arm.

Fig. 3-5 shows a concept that the SCC is rescued by using the vehicle manipulator. The rescue manipulator is attached to the tip of the vehicle manipulator. During the rescue of the SCC, the movable area of the vehicle manipulator is restricted because of the interference with the buffles so the vehicle manipulator cannot be operated freely. Therefore, the rescue manipulator must cover the movable area. Specifications, such as the arm length and degree of freedom, of the rescue manipulator are more severe than that from the port.

If the mechanisms of the SCC are broken and the cassette is almost on the SCC, the rescue mentioned above, from the port and with the vehicle manipulator, cannot be operated. In this case the toroidal moving tool shown in Fig. 3-6 should be used to move the cassette to the installing position and the SCM can be rescued.

If the mechanisms of the SCM is broken, the cassette on the SCM must be moved and the fork must be resolved and stored on the SCC. The SCC can be withdrawn to the port using the rescue TRC if the cassette is not on the SCC and the fork is stored on the SCC.

3.1.3 Effect of dust

During the operation of ITER, it is concerned that the dust is produced by the contact of the plasma to the first wall and pours to the rail through the gap of 10 mm between the cassettes. The appearance of the dust is various: lies on the rail, adheres to the rail and so on. The most fundamental solution is to cover the rail from the dust as shown in Fig. 3-7. The cover is a plate projected from the side of the cassette above the toroidal rail and receives the

dust. The vertical position of the cover should differ between right and left so that the covered areas overlap each other. The cover can prevent the dust which has heavy weight and/or adheres to the rail from pouring directly to the rail. Therefore, only the light dust needed to be considered in the following study.

As shown in Fig. 3-8, the light dust can be removed by equipping the fork with a brush and a scraper installed in the commercial linear guide. The scraper must be installed with a gap between it and the rail because it interferes with the rail if there is a step caused by misalignment of the rail. The width of the gap depends on the misalignment. On the other hand, the brush can be composed of wires and/or fibers so it can comply with the step. First, the scraper removes the relatively heavy dust and the rest of dust is removed by the brush.

If the dust is very heavy, the fork itself removes the dust instead of the scraper and brush do. (The possibility is, however, lowered by the cover.) By removing the dust without load on the fork, the driving force can be used to remove it.

If the rail deforms, the reason of an excessive motor torque cannot be judged whether the dust removal force makes the driving force excessive or the interference between the fork and the rail does.

It can be said that the observation system of the rail is necessary to confirm the status of the dust and the deformation of the rail. There is a space for the fiber scope in the lower part of the fork in 1998 design as shown in Fig. 3-9. The deformation and status of the dust on the rail can be observed with the fork running on the rail.

On the other hand, the cross section of the fork reduced by 1/4 in area in the 2001 design so it is difficult to install the fiber scope in the fork. It is possible that the manipulator on the CTM can observe the status of the toroidal rail with the fiber scope. However, if the CTM is next to the second cassette, the opening of the toroidal rail is occupied by the CTM so the manipulator cannot access. The observation must be done when there is a space between the second cassette and the CTM.

3.2 Definition & validation of sensor based control of the SCM

It is considered that the toroidal rail where the fork moves has a radial positional error originating in the installation misalignment, distortion caused by electromagnetic force and thermal deformation. Aiming at the positional errors of the rail at the insertion of the fork and during traveling of that, this study investigates sensor-based control of the SCM to avoid the failure caused by both of positional errors.

3.2.1 Selection of sensor

Under the D-T operation, inside of the vacuum vessel is high radiation field even in the maintenance period. Therefore, the control system can use only the radiation-hard sensors

as shown in Table 3-2.

In order to take measures against the positional error at the insertion of the fork, the opening of the toroidal rail is detected by sensors. In the same time, the radial position of the toroidal rail can be determined by a radial position of the TRC. In this case, the only needed information is a binary information on the opening of the rail, whether it exists or not. A fiber-type optoelectric on/off switch, by which the sensor head can be minimized most, is selected. A separated-amplifier-type eddy current on/off switch is also a candidate. At the detecting distance in this case, however, the eddy current switch becomes larger than the optoelectric switch.

In the optoelectric switch, the thru-beam type cannot be used because of object arrangement, and the reflective type is selected. The detecting distance is 10-20 mm and the fiber should be flexible considering installation in a narrow space. From these conditions, the sensor head FU-66Z, whose detecting distance is 45 mm, is selected from the FS01 series of the Keyence Corp. The sensor head is M4 size and 15 mm in length, and the connected fiber can be bent with a minimum radius of only 2-mm.

Regarding the radial positional error during traveling of the fork, sensors attached to the fork watch the inboard and outboard side walls of the toroidal rail and observe whether the width between both walls gets narrower or not. The detecting distance is 0-10 mm and the required resolution is less than 0.5 mm because the gap between the guide roller and the wall is 0.5 mm in the 1998 design. The suitable sensor is a switch which can detect if the gap between the fork and the wall of the rail becomes shorter than the set value, or a sensor which can output a distance as a analog value. The selectable sensor is a optoelectric switch or eddy current distance sensor because they are well-developed.

In the optoelectric switch, the above mentioned FU-66Z of the Keyence Corp. can be used because it is compact enough.

A diameter of the sensor head of the eddy-current-type distance sensor varies as a detecting distance. The relation between the diameter of the sensor head and the detecting distance is shown in Table 3-3. The combination of the EX500 and EX-016 is applicable considering the detecting distance and the size of the sensor head.. The EX200 is acceptable also (EX500: resolution 0.03%FS, linearity +-0.3%FS; EX200: resolution 0.04%FS, linearity +-1%FS). In this case, however, sensors are installed in a small space so the EX500 is better because it considers the mutual interference.

3.2.2 Design of control system

The following two objectives are to be:

- Inserting position for the fork (edges of the guide rails at the opening of the toroidal rail)
- Abnormal approach of the side walls while the fork travels toroidally

In this study, the situation is simulated partially:

- Only the inboard fork and the TRC is actuated.
- The outboard fork is kept in the center of the SCC.

It is not confirmed strictly how the operation sequence is changed according to the sensor signal and how to deal with the abnormal approach of the side wall during the fork insertion. Therefore, the control sequence must be easy to be changed and so the software is produced with avoiding the implement to higher level, that is, the VME. The judgement of the input data, decision of the action and the indication of the next action are managed by an operator.

(1) Hardware

As modification of the hardware, the fiber sensor and the sensor amp are installed and the control device is modified so that the DI board can input the sensor signal.

- Fiber sensor and amp

The optical fiber FS01 series of the Keyence Corp. is used.

- Wiring

The wiring outline is shown in Fig. 3-10. The wiring route is same as the existing route between the SCM and the control device. The cables are fixed temporary using the mount base etc.

(2) Software

a. Current system

A personal computer (PC) is used as a sequential control device and keeps teaching points and programs which indicate the order of the actions. Actually, the program has only a order of the teaching points. In execution, the operator selects and launches a program through the huhuman-machine interface. After the completion of execution is confirmed, the PC sends a command indicating an action one by one to the position controller (VME) . The VME executes the action one by one according to the command sent from the PC and reports to the PC after completion. Therefore, the PC manages the sequence of the actions and the VME controls the machine action by action according to the indication of action.

The operator elects and judges the sequence of actions. The current system do not have conditional branches according to the concept that the divertor cassette can be transported by a fixed sequence of actions.

b. Modification of software

The current system is a fixed sequence of actions which do not have conditional branches. The following two modification is done so that the sequence can be changed by the sensor signals:

- Interrupt the action and stop when the sensor signal turns on.
- Selection the next action according to the sensor signal

Actually, the selection of the next action is done by the operator in order to keep the flexibility of the system during the test phase.

(a) Modification of sequencial control device (PC)

- Treatment of sensor signal
- Movement of TRC to the calculated point
- Relative movement
- Display of sensor status

(b) Modification of VME

- Observation of torque
- Interrupt execution by sensor signal
- Calculation of TRC position / action
- Notification of sensor information to PC

3.2.3 Modification of machine

The current fork do not have enough space because of the arrangement of guide rollers so the sensors measuring the radial position of the toroidal rail cannot be installed at the ideal locations. If the fork is newly designed, the sensors can be put at the locations shown in Fig. 3-11. Concept of the arrangement is:

- The guide rollers for the vertical direction are moved to the center and a space is made for the sensors A and B (photoelectric switch) detecting the radial position of the toroidal rail.
- Between the guide rollers for the vertical direction, the sensors C, D (eddy-current-type distance sensor) detecting the side walls of the toroidal rail are installed.

Sensor A: Optoelectric switch detecting radial position of the toroidal rail (inboard)

Sensor B: Optoelectric switch detecting radial position of the toroidal rail (outboard)

Sensor C: Eddy-current-type distance sensor detecting side walls of the toroidal rail (inboard)

Sensor D: Eddy-current-type distance sensor detecting side walls of the toroidal rail (outboard)

Sensors are installed on the SCC as shown in Fig. 3-12. The installation position is not same as the ideal and actual positions because of spatial restriction. Therefore, the target for the sensor is not at the actual position as shown in Fig. 3-13.

The electrical wiring outline between the sensor and the control device is shown in Fig. 3-14.

For the software, the control flow chart is shown in Fig. 3-15.

For the validation test, the jigs for the toroidal rail is manufactured to simulate deformation of the rail as shown in Fig. 3-16 and Fig. 3-17

deformation of the rail as shown in Fig. 3-16 and Fig. 3-17

The photographs of the modified and tested part are shown in Fig. 3-18 to Fig. 3-25.

3.2.4 Validation test

Detection of radial position of toroidal rail

The TRC was moved from 1903.5 mm to 2503.5 mm with 100% speed and the test for the outboard dog detection was performed. The results are summarized in Table 3-4. It was also clarified that the braking distance of the TRC is 11.5 mm. The arrangement of the sensors is shown in Fig. 3-26.

Next, the test with the combination of "Outboard Sensor False" and "Inboard Sensor True" was performed. The test was repeated 10 times. The results are shown in Table 3-5. Using the following procedures, the TRC can find the actual location, 2503.5 mm, with accuracy of less than 0.16 mm.

1. Move TRC to 2450.0 mm
2. Move till outboard sensor turns true.
3. Move till outboard sensor turns false. (S2:OF)
4. Move till inboard sensor turns true. (S1:IT)
5. Move to 2450.0 mm (to remove the backlash)
6. Move to WP1=0.5xS1+0.5xS2+1.13

Detection of abnormal distance of wall

The detection of abnormal distance of the side wall was tested. The eddy-current-type sensor was installed with the gap of 3 mm to the guide rail. The fork was inserted with the toroidal angle of 1.3 degree.

The detection of the abnormal approach of the side wall was tested with the guide rail jig which makes the width between the side walls narrower. The initial gap was 5.9 mm and the limitation was decided as 5.5 mm. The result was shown in Table 3-6. The servo noise was reduced with the shield of the sensor connected to the SCC and the measuring error decreased to 0.1 mm. As a result, the fork system could stop at the gap of 5.48 mm. Therefore, the accuracy is 0.02 mm. It can be said that the detection of the wall using the eddy-current-type distance sensor is effective.

3.3 Validation of Human-machine Interfaces of the SCC

3.3.1 Network connection to the supervising computer

The SCC control system is connected to the supervising computer and IGRIP computer through the LAN. The SCC controller composed of the position controller (VME) and the sequential controller (PC). The physical configuration of the network connection is shown

- Condition status of interlock position: from PC to VME
- Command of automatic operation: from supervisor to PC
- Position data: from PC to supervisor and IGRIP

TCP/IP is used for the connection protocol.

3.3.2 Remote Operation

The general format of the command exchanged in the network is show in Fig. 3-28. There are four command in this system: "RUN", "PAUSE", "STOP" and "DATA". The formats of each command are shown in Fig. 3-29 to Fig. 3-32, respectively.

The control system has three phases: "RUN", "PAUSE" and "STOP". The phase transit to other phase by receiving a command. The phase transition is shown in Fig. 3-33.

3.3.3 GUI with IGRIP

The GUI for the SCC is realized by using IGRIP. The position data sent by "DATA" command is received by the IGRIP computer and interpreted for the IGRIP. The model for the IGRIP is shown in Fig. 3-34.

Table 3-1 Initial FMEA for Divertor Cassette Maintenance System

Subsystem	Condition of Load and Operation	Failure Mode	Effect of Failure	Method to Detect Failure
Tractor	Cassette on the SCM	Inability to move	Stop of function	Error detection by servo driver
		Decrement of driving force	Stop of function if less than threshold, or lowering of performance	
		Decrement of speed	Lowering of performance	
		Lowering of positioning accuracy	Stop of function in case of installation	It is possible that the current system cannot det the failure. Backup systems are needed for the position sensor and so on.
			Operation can be continued in case of removal	
	No cassette on the SCM	Inability to move	Stop of function	Error detection by servo driver
		Decrement of driving force	Lowering of performance	
		Decrement of speed	Lowering of performance	
		Lowering of positioning accuracy	Operation can be continued in case of installation	It is possible that the current system cannot det the failure. Backup systems are needed for the position sensor and so on.
			Stop of function in case of removal	
	Cassettte on transition	Inability to move	The TRC is unable to be operated if the cassette is on transition. T	The TRC is not operated with the cassette on
		Decrement of driving force	TRC can be operated only after the cassette is moved to the SCM	transit position in the normal operation mode.
		Decrement of speed	the installing position. The further procedure depends on the final	Methods to detect failure depend on the cassett
		Lowering of positioning accuracy	cassette position and failure mode.	position.
SCM	Cassette on the SCM	Inability to move	All the system stop the function if the cassette is not on the cente the SCM.	Error detection by servo driver
		Decrement of driving force	Stop of function if less than threshold, or lowering of performance	
		Decrement of speed	Lowering of performance	
		Lowering of positioning accuracy	Stop of function in case of installation	It is possible that the current system cannot det the failure. Backup systems are needed for the position sensor and so on.
			Operation can be continued in case of removal	
	No cassette on the SCM	Inability to move	All the system stop the function if the fork is not on the center of SCM.	Error detection by servo driver
		Decrement of driving force	Stop of function if less than threshold, or lowering of performance	
		Decrement of speed	Lowering of performance	
		Lowering of positioning accuracy	Lowering of performance	It is possible that the current system cannot det the failure. Backup systems are needed for the position sensor and so on.
Controller	?	Inability to move	Stop of function	Possible to detect by self-check function
		Abnormal motion	Lowering of performance	Observation by an external system
Cable	?	Inability to move	Stop of function	Possible to detect by self-check function
		Abnormal motion	Lowering of performance	Difficult to investigate the cause
Cassette	?	Deformation	Stop of function or lowering of performance depending on the loca and level of deformation)	Rails and so on cannot be observed from outside another system is needed to confirm the status the cassette before the operation.
Reactor Struct	?	Deformation	Stop of function or lowering of performance depending on the loca and level of deformation)	Observation by an external system enables the p detection and dealing.

Table 3-2 Radiation-Hard Sensors

Sensor type	Measured value	Note
Mechanical limit switch	ON/OFF switch	Plastics should be replaced by ceramics etc.
Eddy current sensor	Distance sensor	Amp. should be placed out of vessel. Coil material should be replaced.
	ON/OFF switch	Amp. should be placed out of vessel. Coil material should be replaced.
Laser sensor	Distance sensor	Amp. should be placed out of vessel. Rad-hard fiber should be used for transmission.
	ON/OFF switch	Rad-hard fiber should be used for transmission.
Optoelectronic sensor	Distance sensor	Amp. should be placed out of vessel. Rad-hard fiber should be used for transmission.
	ON/OFF switch	Rad-hard fiber should be used for transmission.
Picture sensor	-	Rad-hard fiber should be used for transmission.

Table 3-3 Diameter and Detecting Distance of Eddy-Current-Type Distance Sensor

Provider	Type	Outer Diameter	Detecting Distance
Keyence	EX502/EX-008	M8	0-2mm
	EX505/EX-016	M16	0-5mm
	EX510/EX-022	M22	0-10mm
	EX201/EX-305	f5.4	0-1mm
	EX202/EX-110	M10	0-2mm
	EX205/EX-416	f14.5	0-5mm
	EX210/EX-422	f22	0-10mm
SUNX	PS930GA1/GSA5S	f5.4	0-1mm
	PS930GA2/GSA12M	M12	0-2mm

Table 3-4 Detection of Radial Position of Toroidal Rail

	Indicator	Position of sensor detection	Position of TRC stop
Inboard Sensor True	Green to Red	2254.84 mm	2266.33 mm
Inboard Sensor False	Red to Green	2280.85 mm	2292.36 mm
Outboard Sensor True	Green to Red	2464.85 mm	2476.34 mm
Outboard Sensor False	Red to Green	2491.34 mm	2502.84 mm

Table 3-5 Combination of "Outboard Sensor False" and "Inboard Sensor True"

	S1 (IT) (mm)	S2 (OF) (mm)	0.5xS1+0.5xS2+1.13 (mm)	Error (mm)
TRC Position	2491.492	2512.963	2503.358	0.1425
	2491.491	2513.266	2503.509	-0.0085
	2491.492	2513.261	2503.507	-0.0065
	2491.492	2513.261	2503.507	-0.0065
	2491.462	2512.963	2503.343	0.1575
	2491.467	2512.956	2503.342	0.1585
	2491.477	2513.261	2503.499	0.001
	2491.492	2513.261	2503.507	-0.0065
	2491.462	2513.255	2503.489	0.0115
	2491.492	2513.266	2503.509	-0.009

Table 3-6 Detection of Abnormal Approach

	Initial Status	At Detecting Position	At Stop Position
Total Gap (S3+S4)	5.90mm	5.48mm	-
Fork Position (degree)	0	1.23	1.3
Width between Guide Rail (measured by scale)	107.4mm	106.9mm	106.9mm

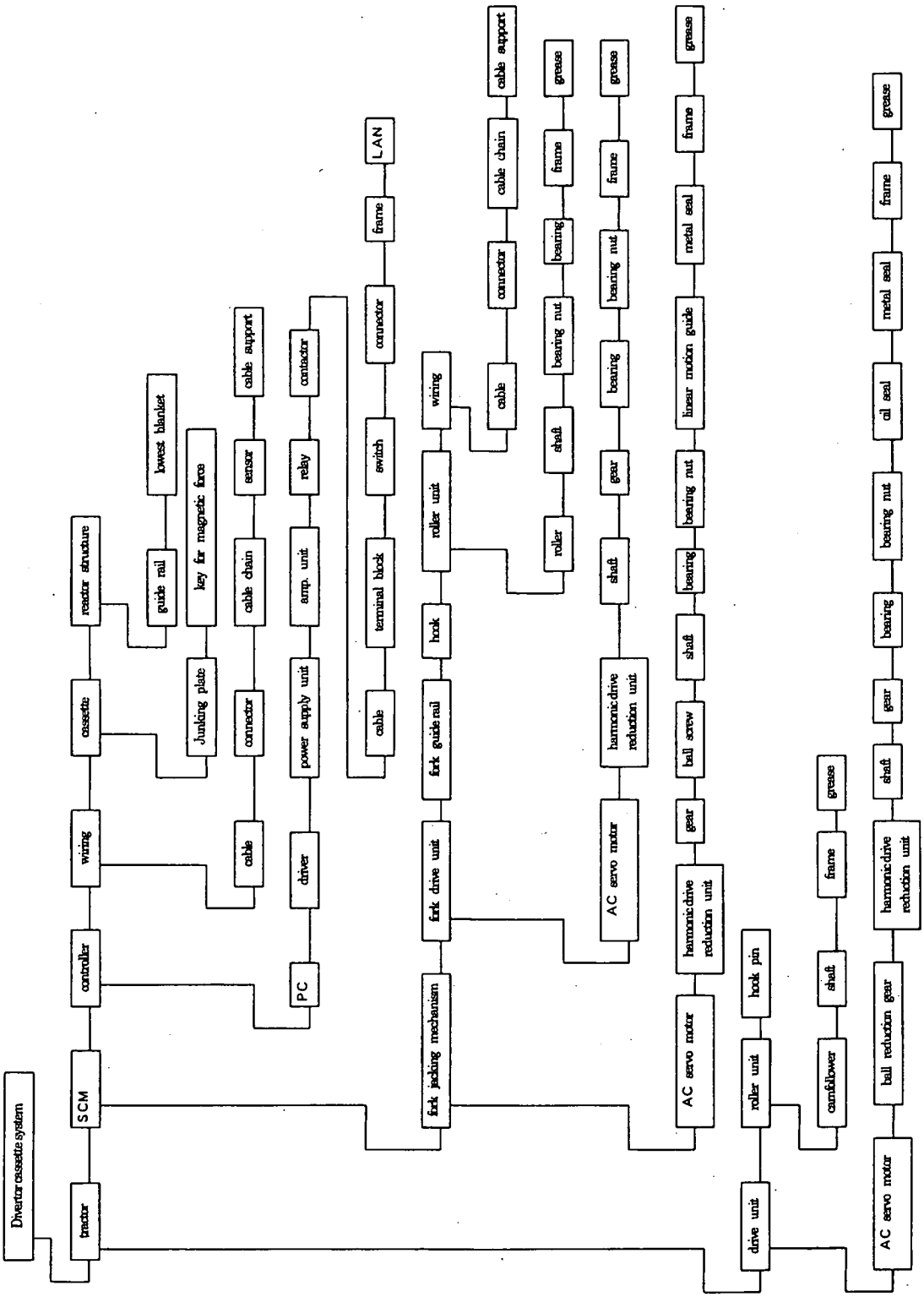

Fig. 3-1 Reliability Block Diagram

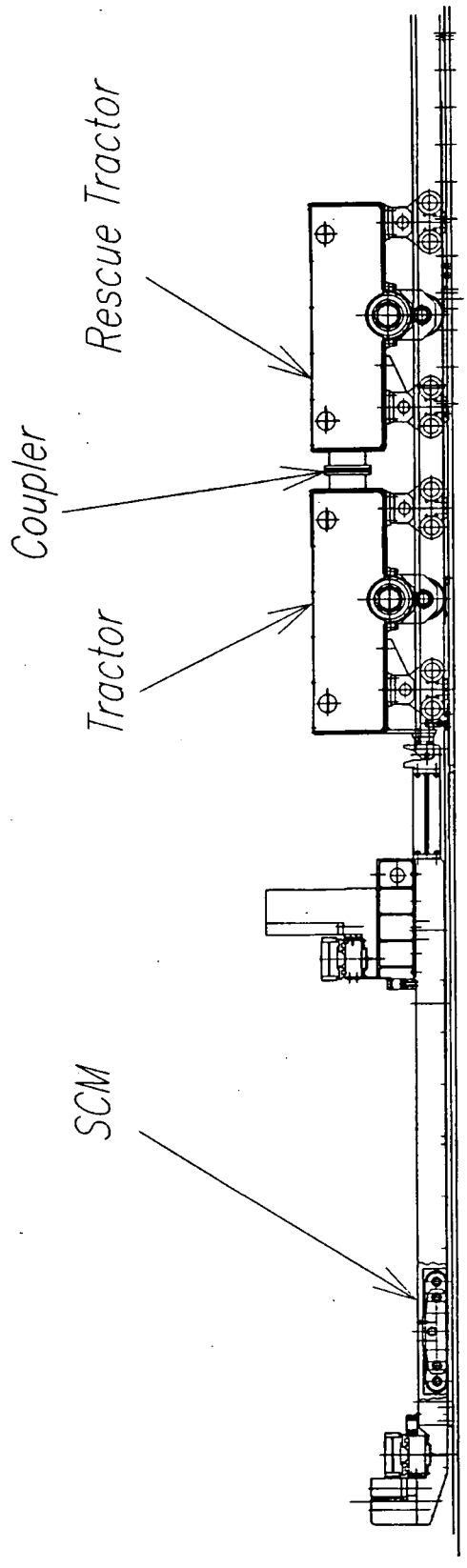

Fig. 3-2 Rescue Scenario of TRC

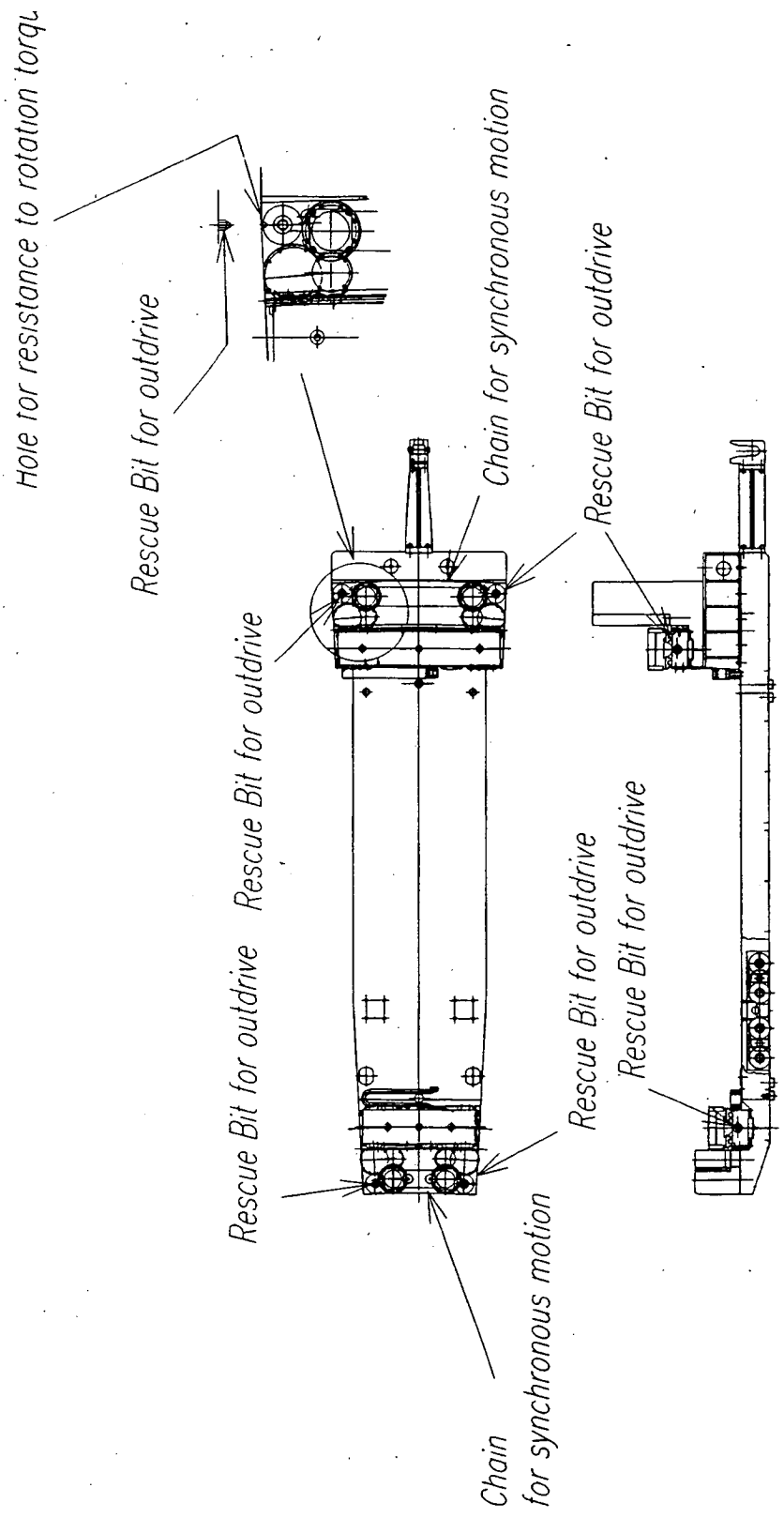

Fig. 3-3 Rescue Scenario of SCC

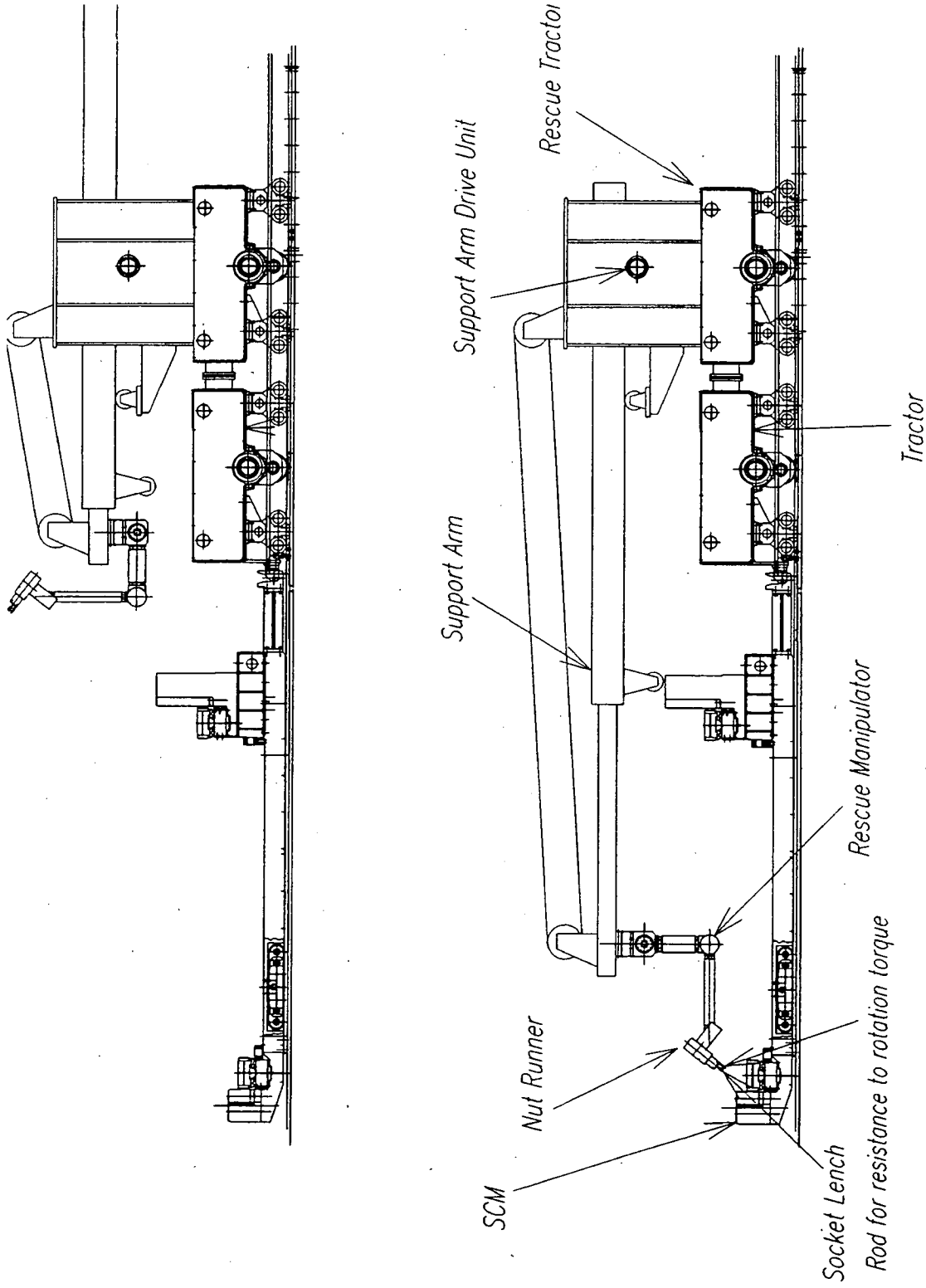

Fig. 3-4 SCC Rescue Manipulator

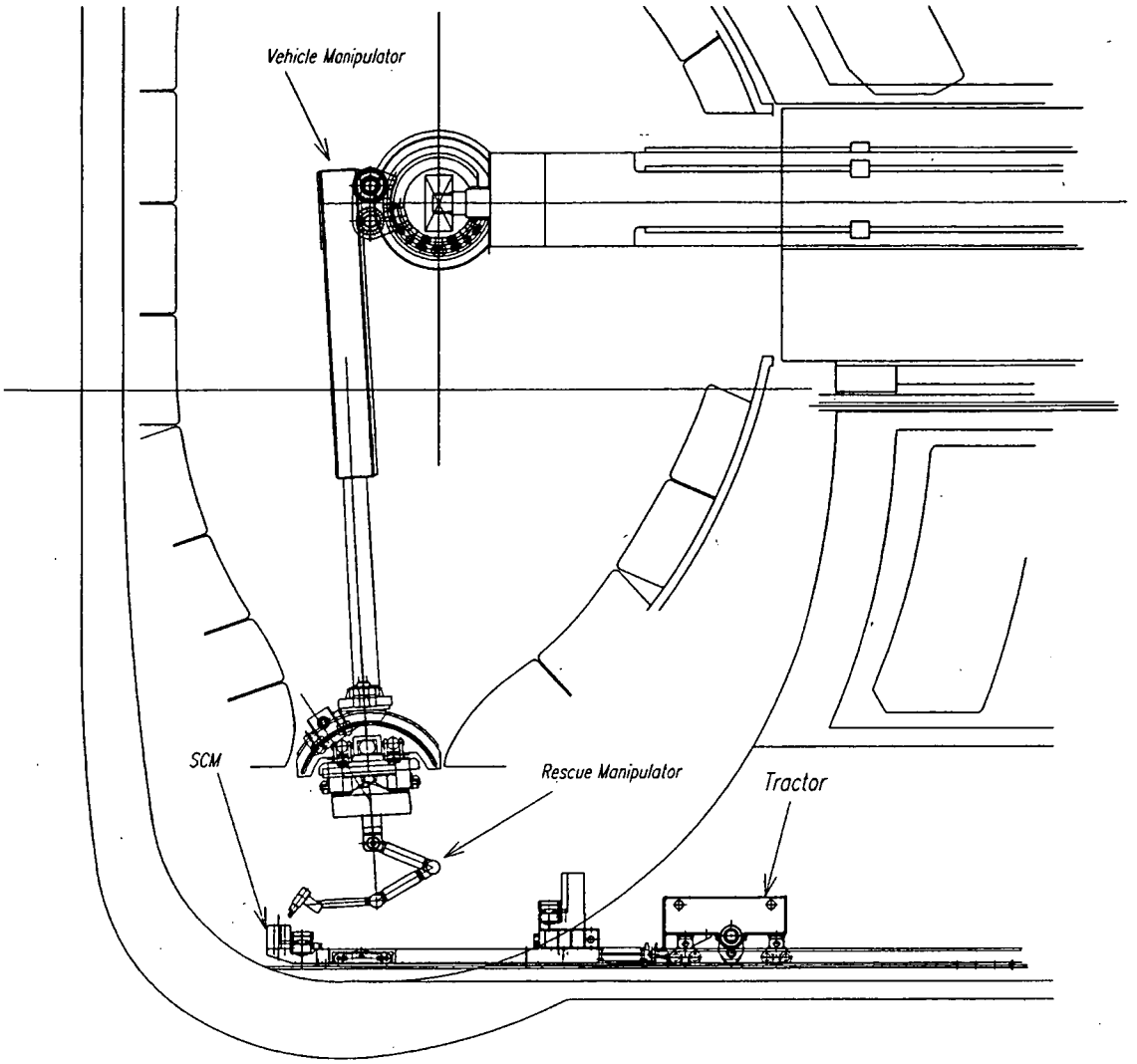

Fig. 3-5 SCC Rescue by Using Vehicle Manipulator

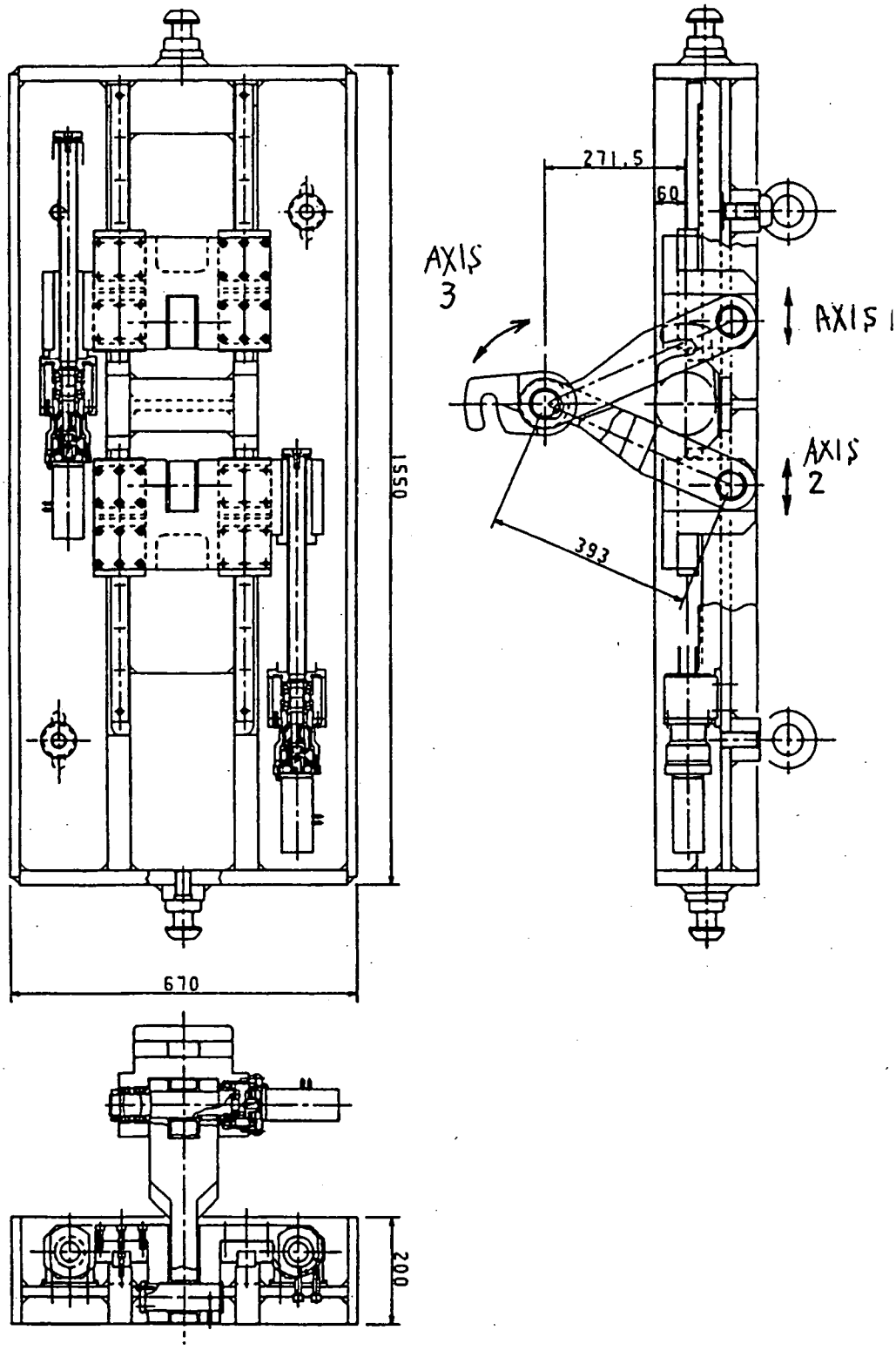

Fig. 3-6 Toroidal Moving Tool

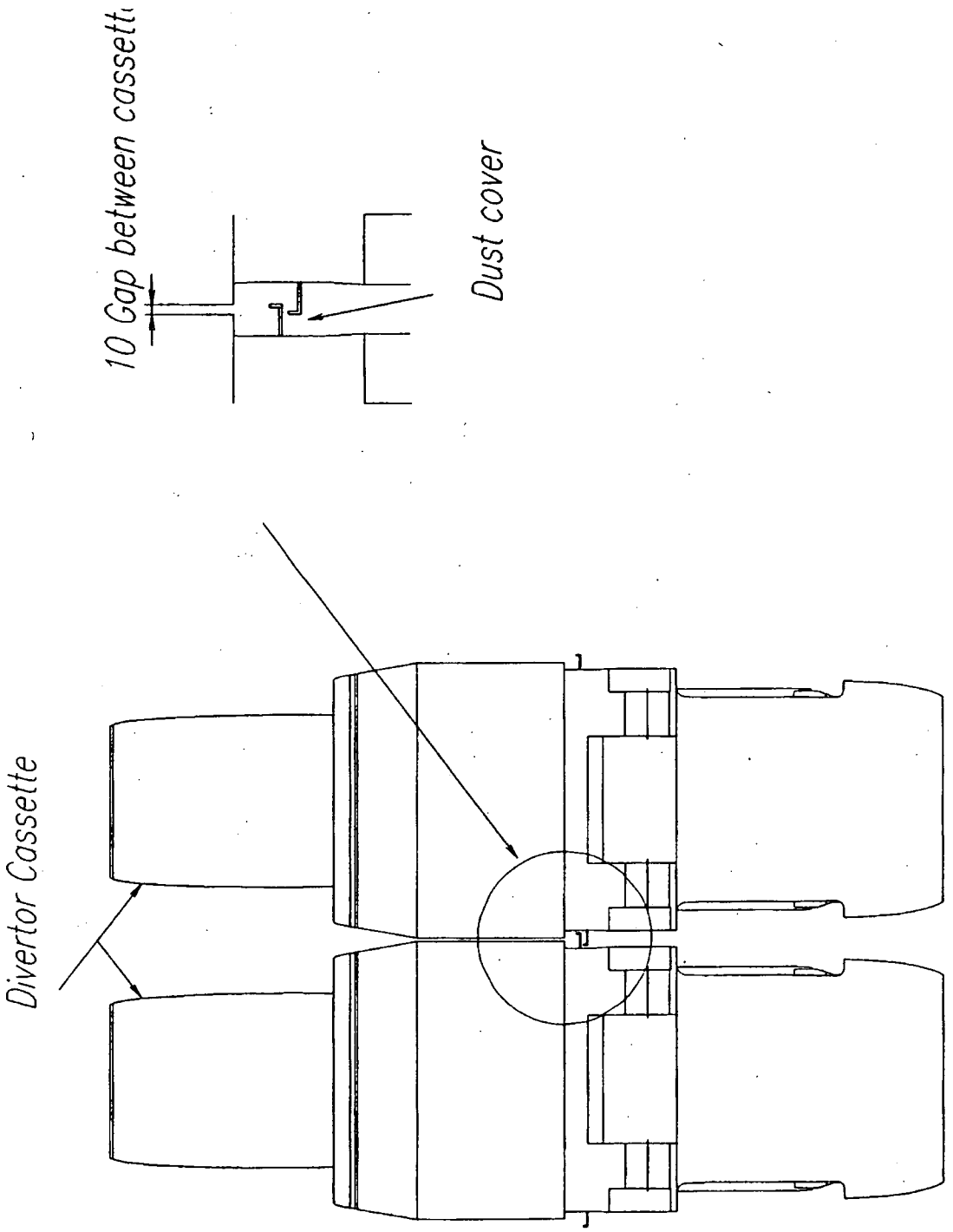

Fig. 3-7 Dust Cover

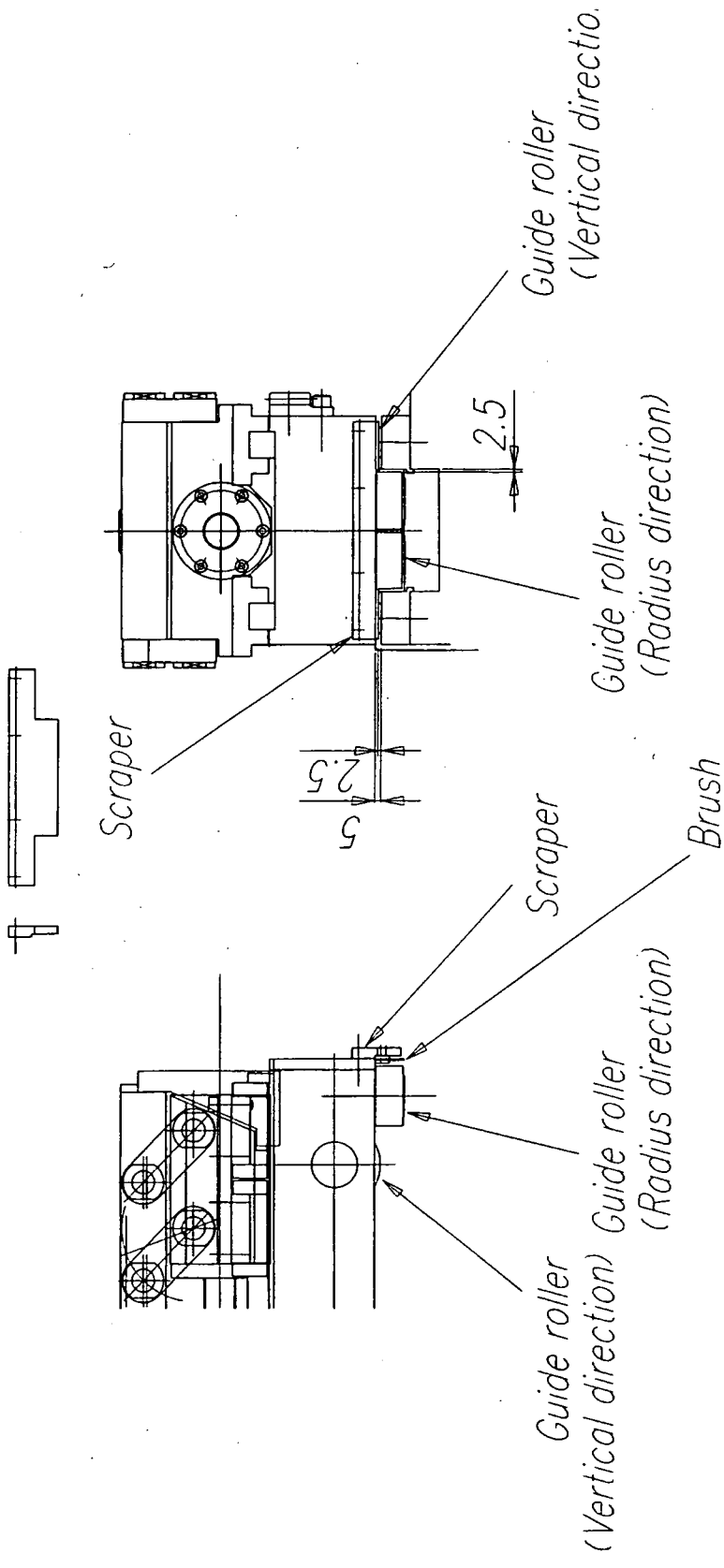

Fig. 3-8 Scraper and Brush

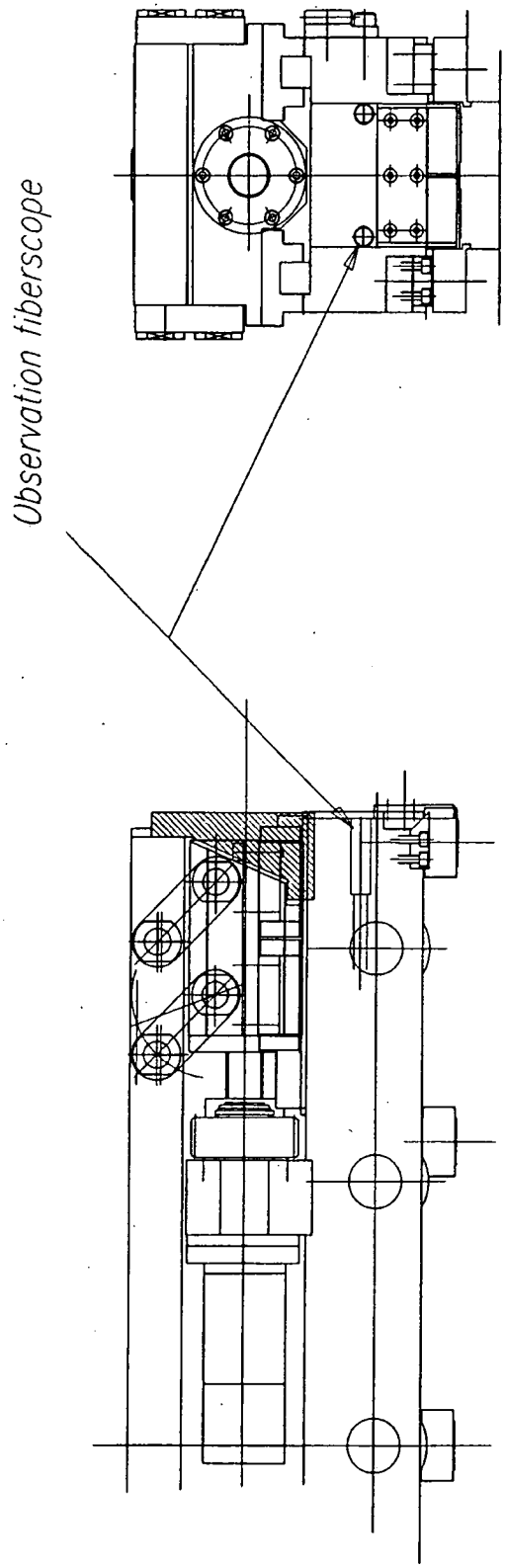

Fig. 3-9 Observation Fiber Scope

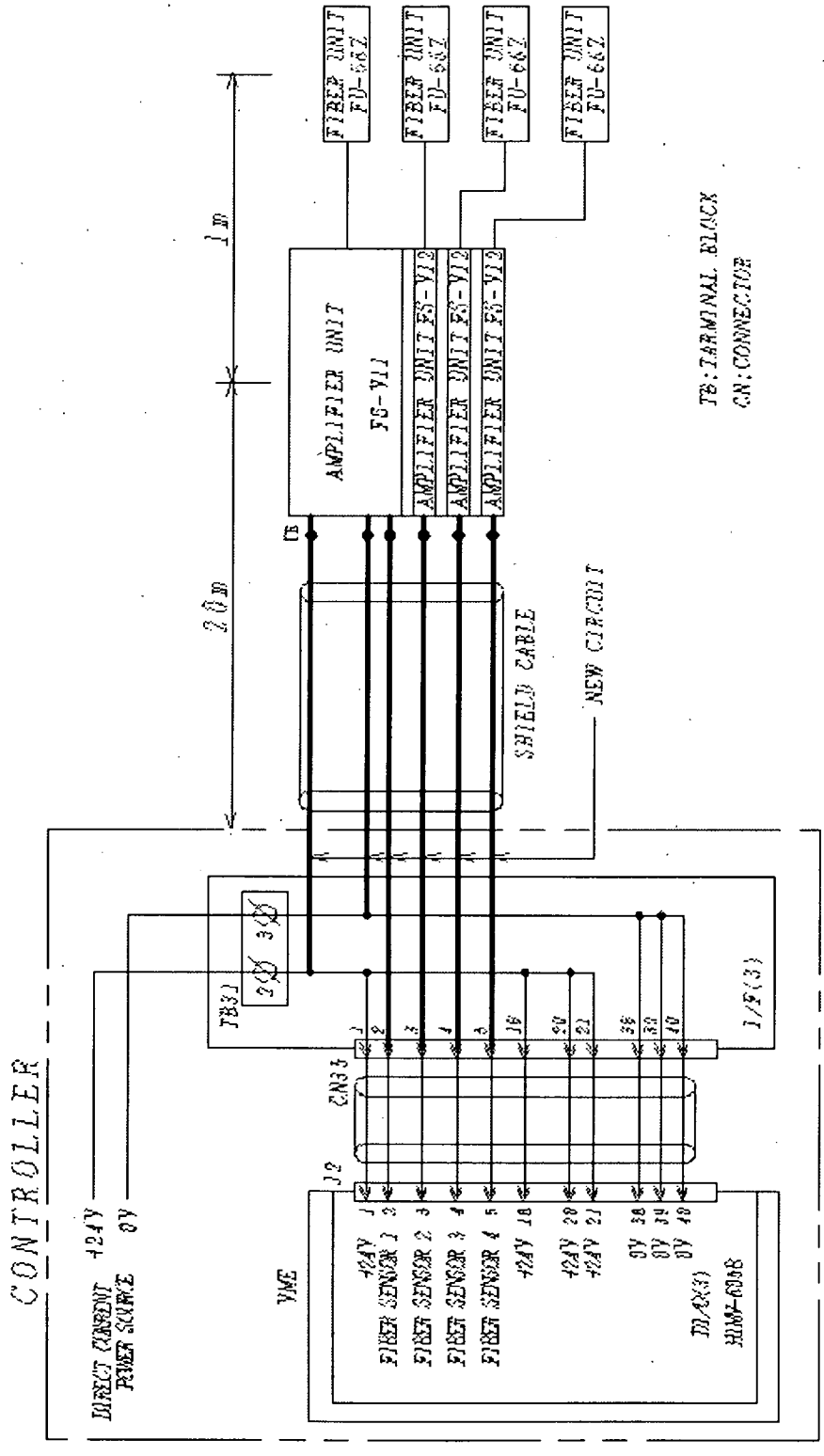

Fig. 3-10 Electrical Wiring Outline

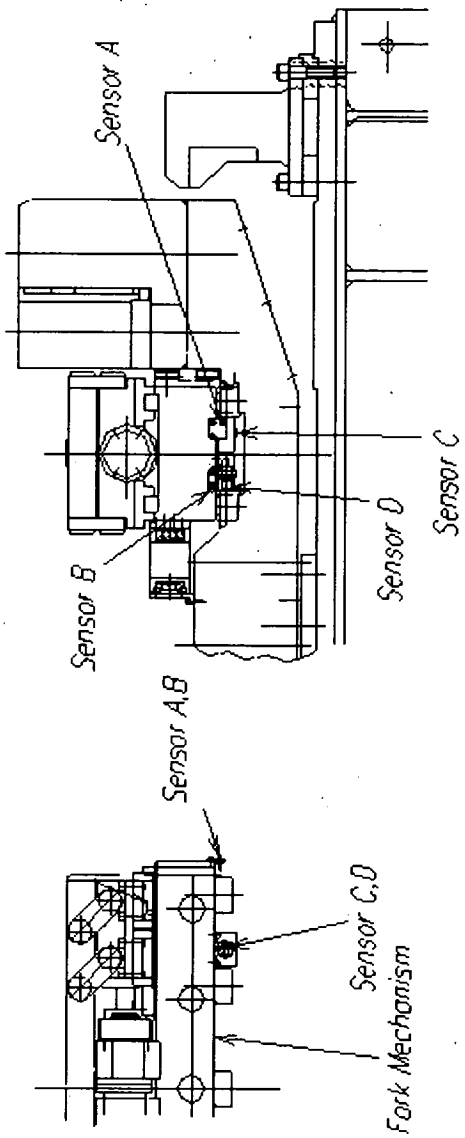

Fig. 3-11 Sensor Location

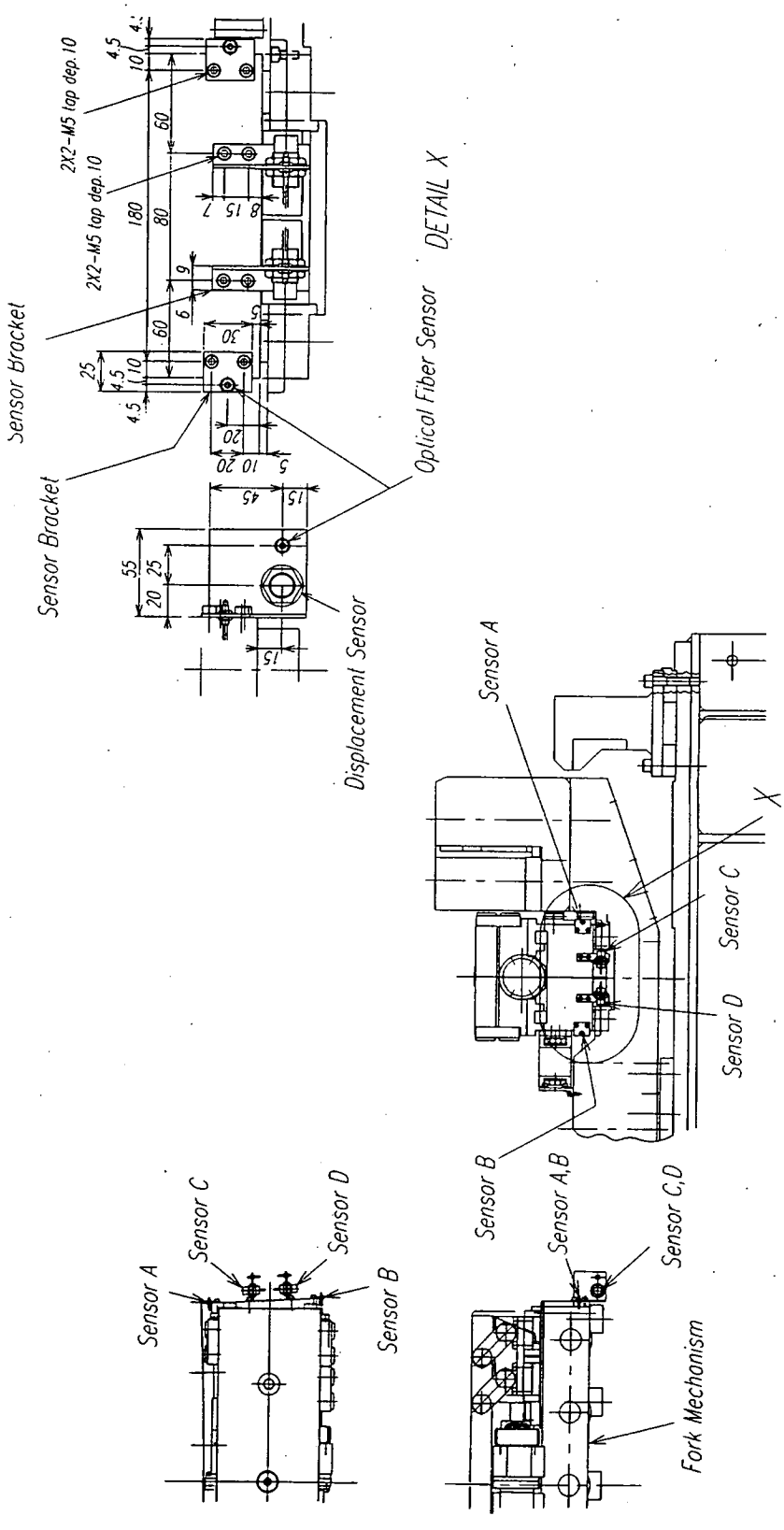

Fig. 3-12 Sensor Location

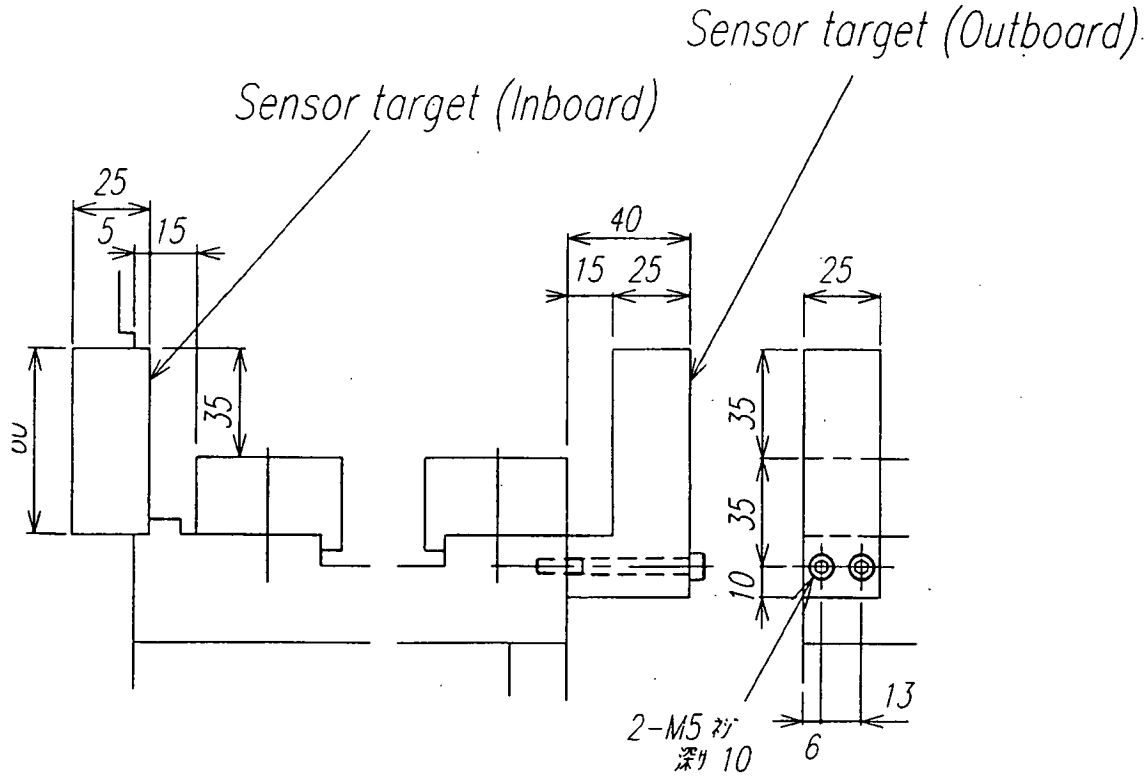

Fig. 3-13 Sensor Target

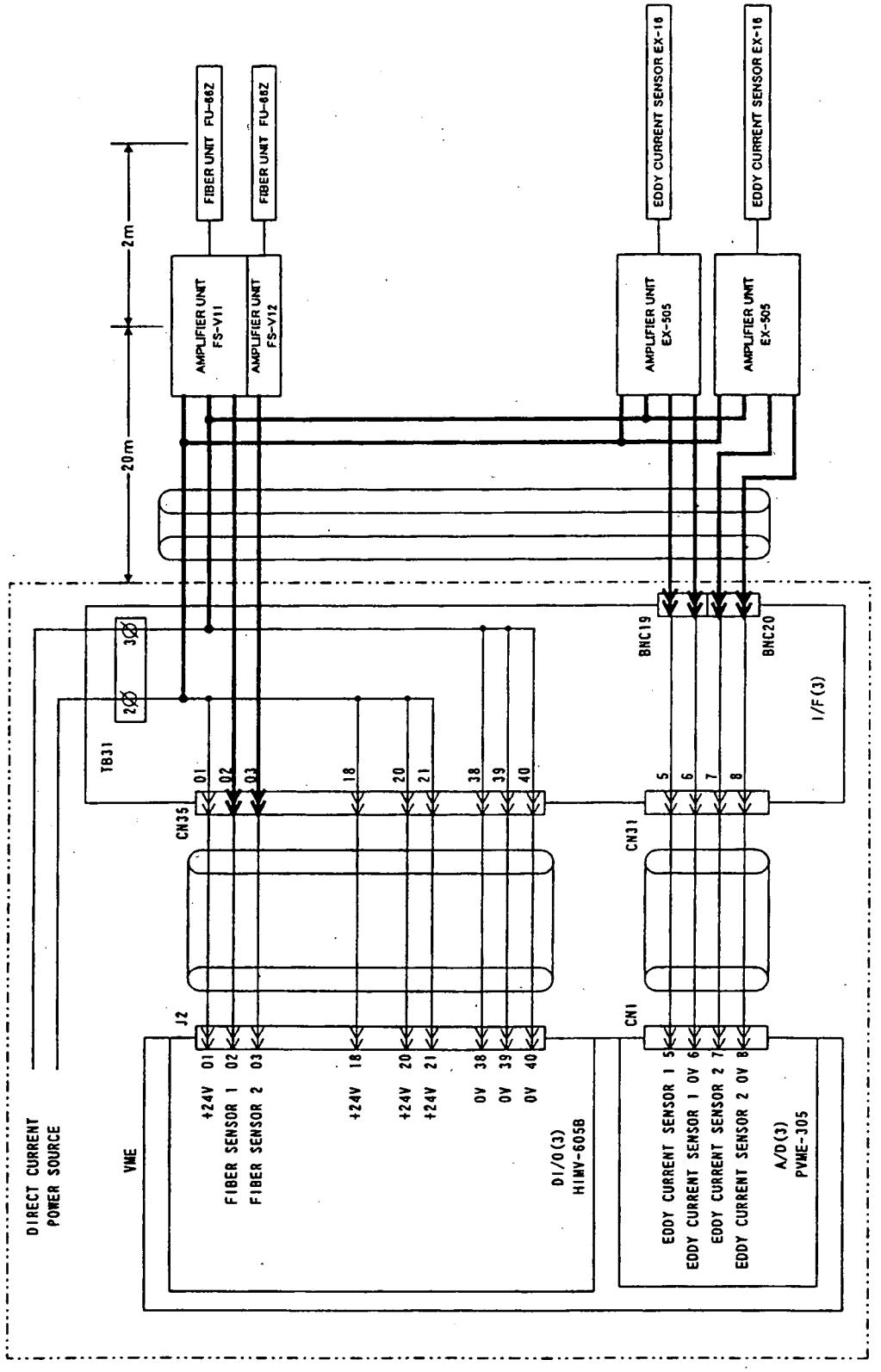

Fig. 3-14 Electrical Wiring Outline

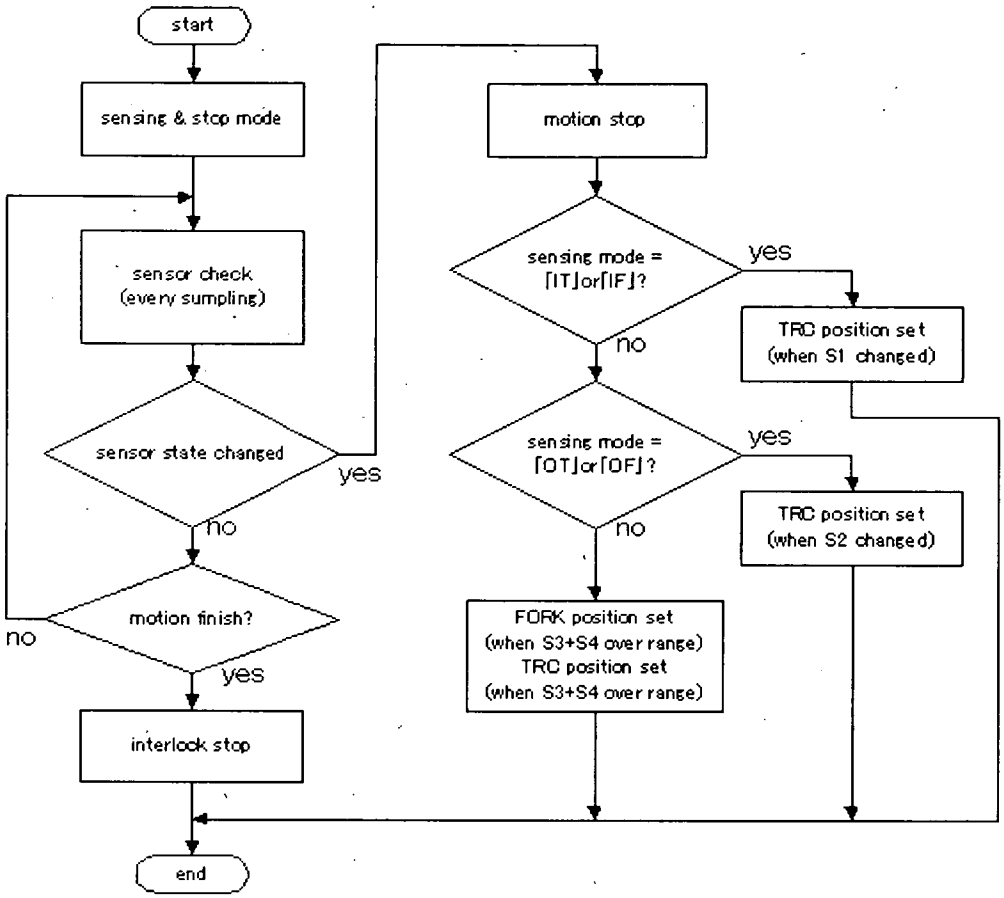

Fig. 3-15 Control Flow Chart

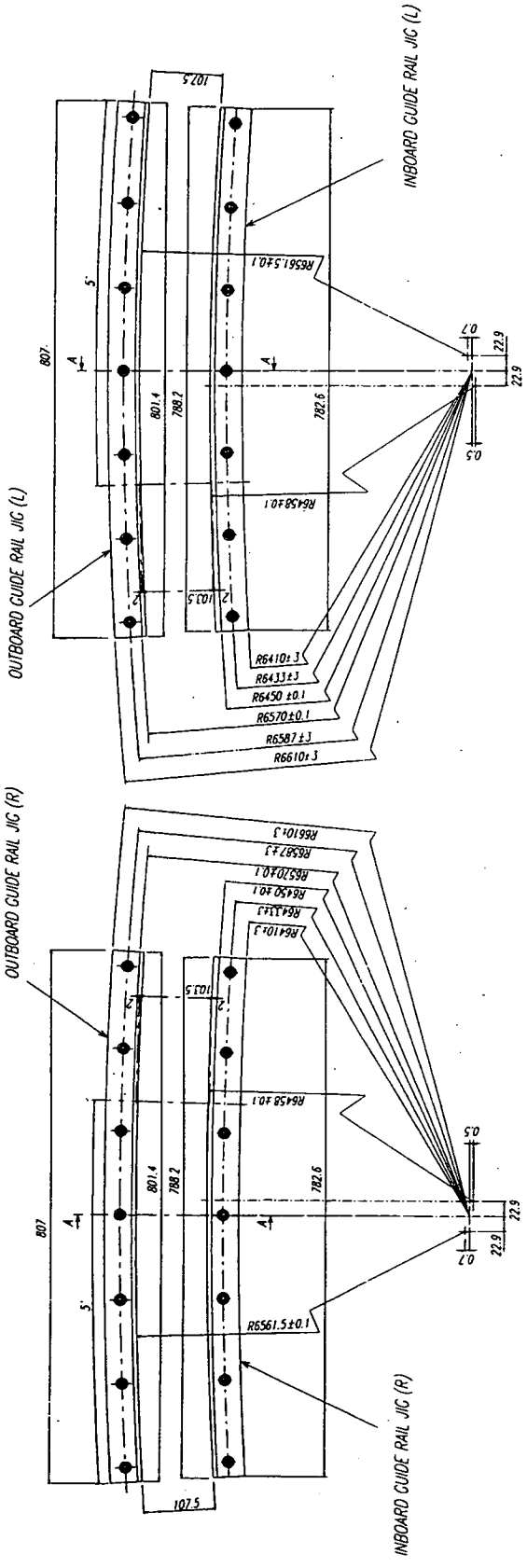

Fig. 3-16 Guide Rail Jigs

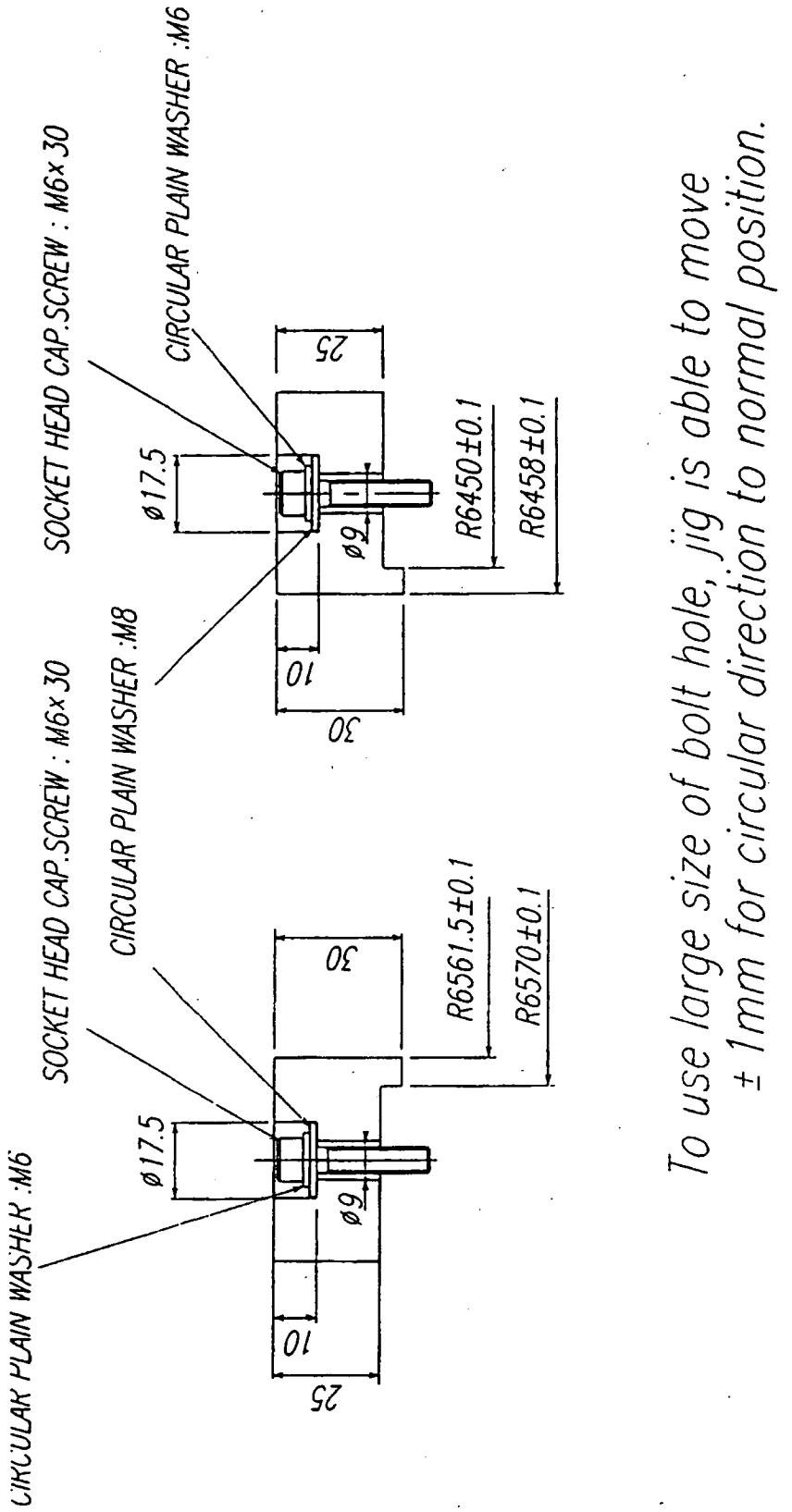

Fig. 3-17 Guide Rail Jig Attachment

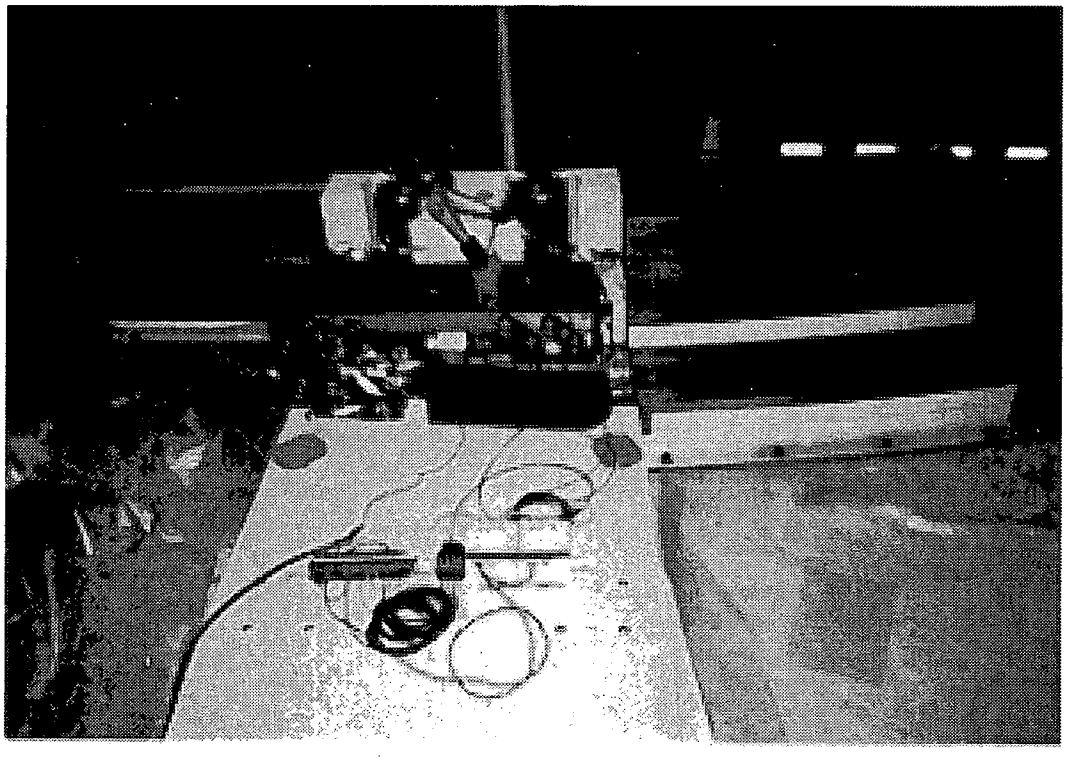

Fig. 3-18 Appearance of Test (Fork on SCC)

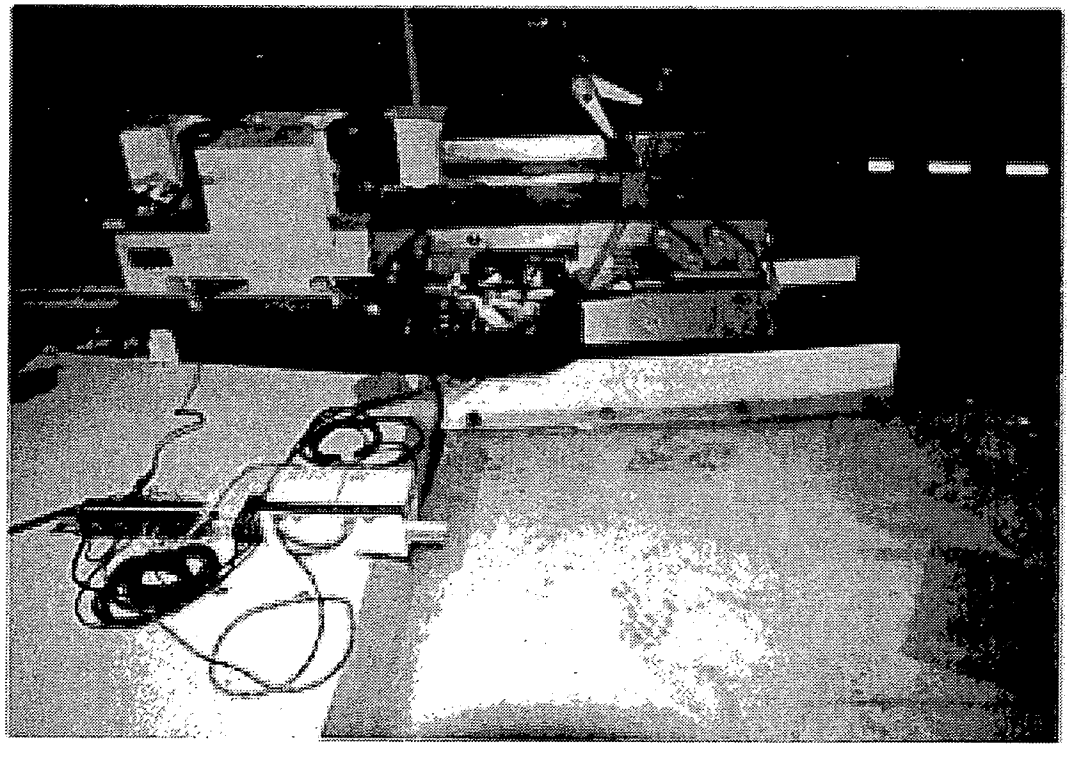

Fig. 3-19 Appearance of Test (Fork on Toroidal Rail)

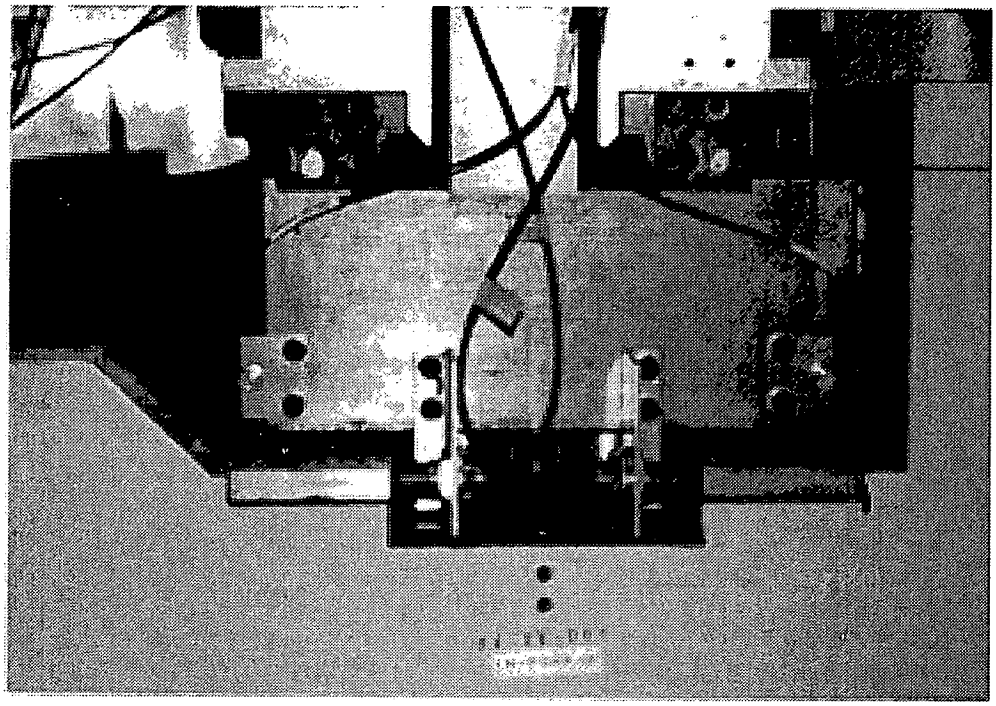

Fig. 3-20 Attached Sensors

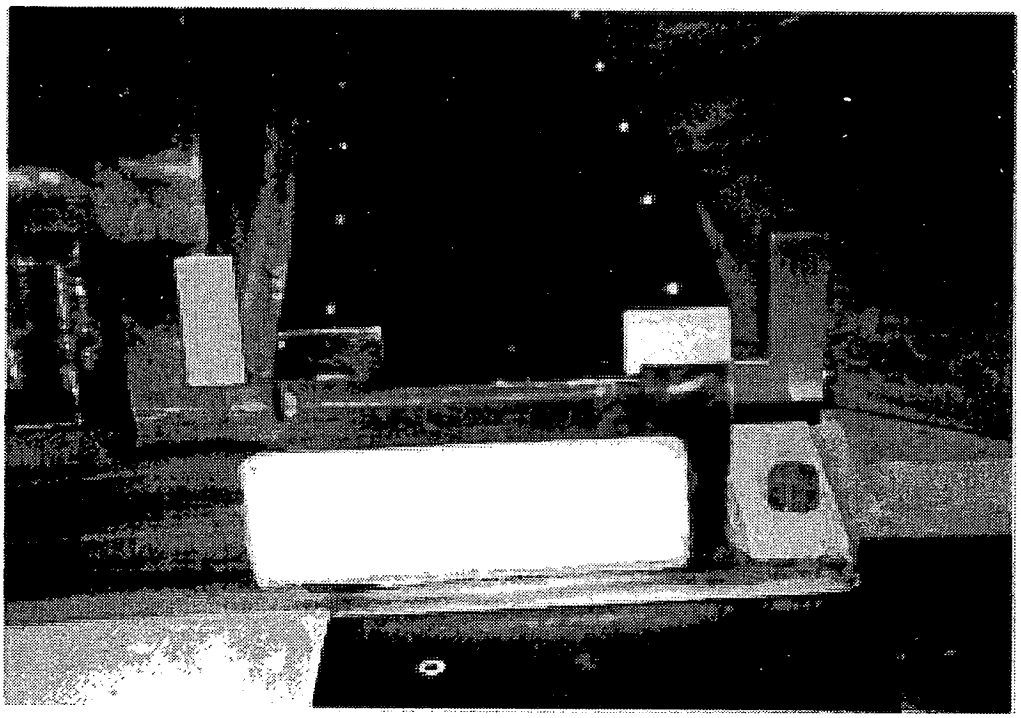

Fig. 3-21 Sensor Target

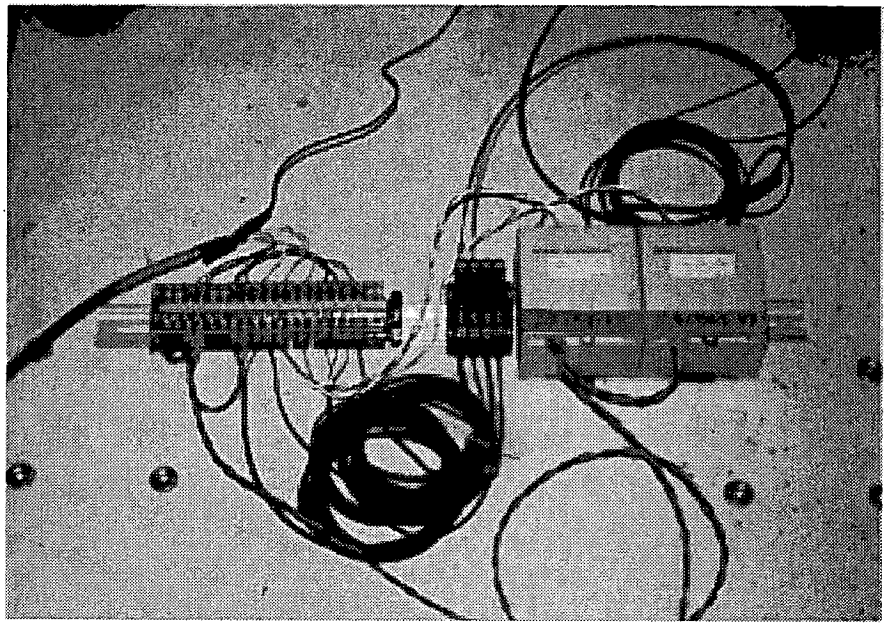

Fig. 3-22 Cabling for Test

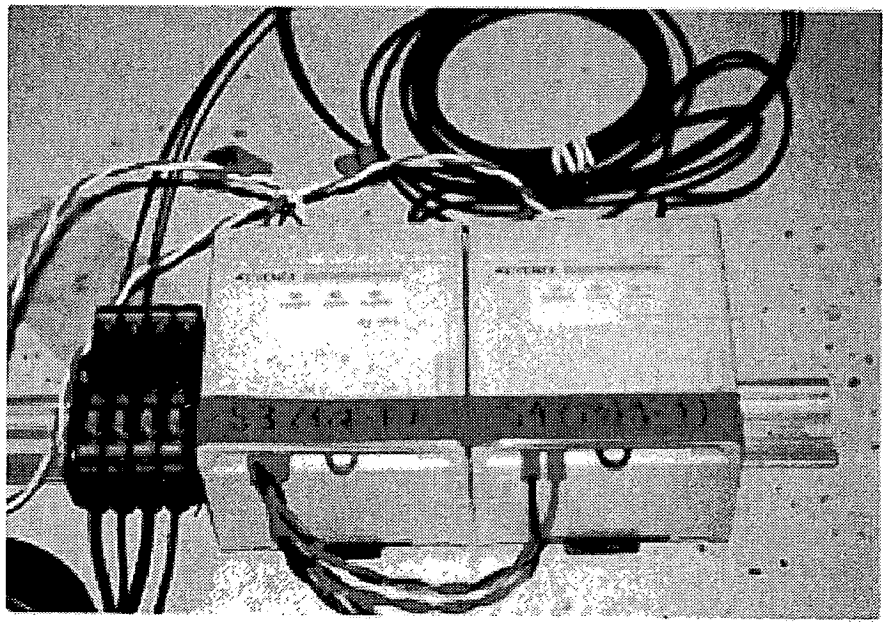

Fig. 3-23Censor Amplifier

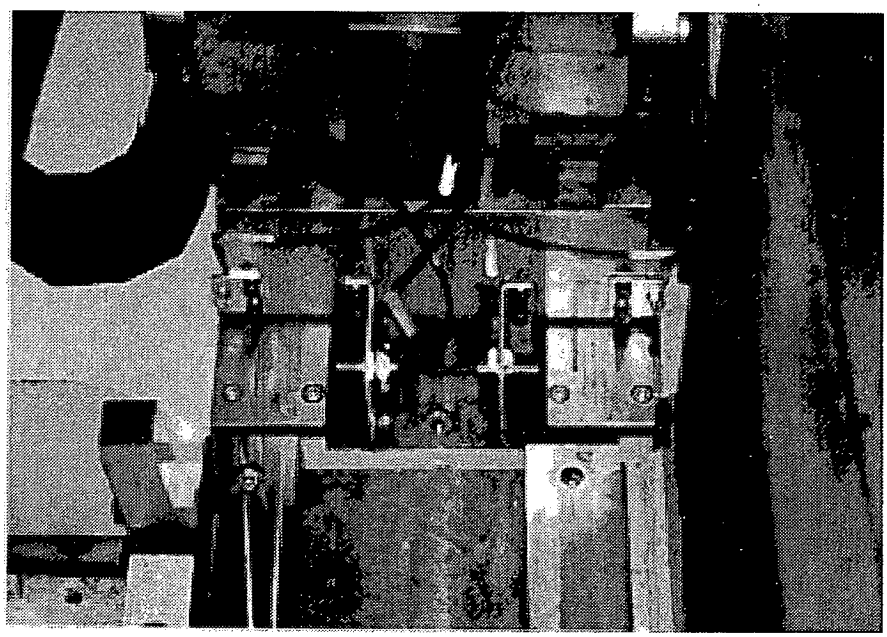

Fig. 3-24 Sensor Arrangement (Fork on SCC)

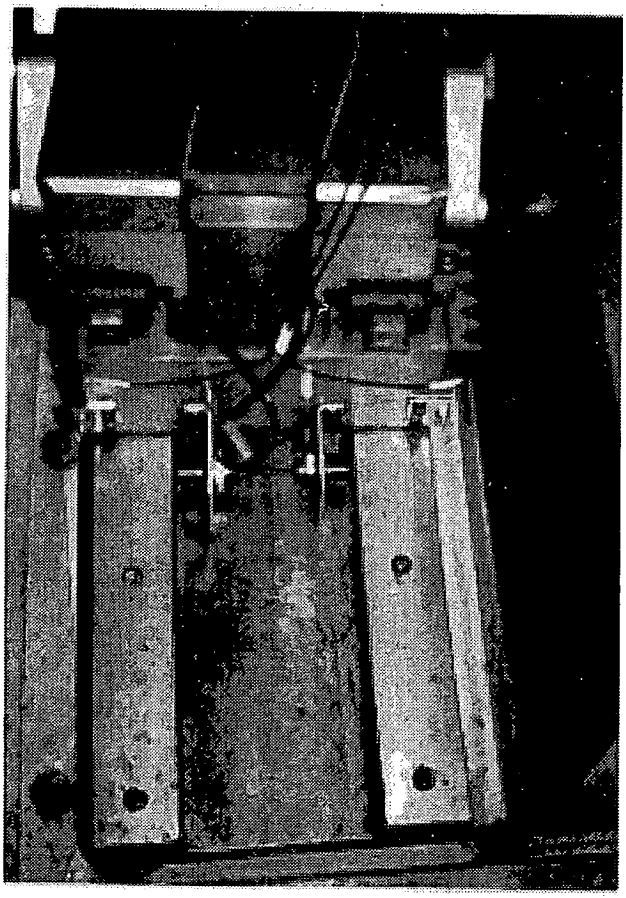

Fig. 3-25 Sensor Arrangement (Fork on Rail)

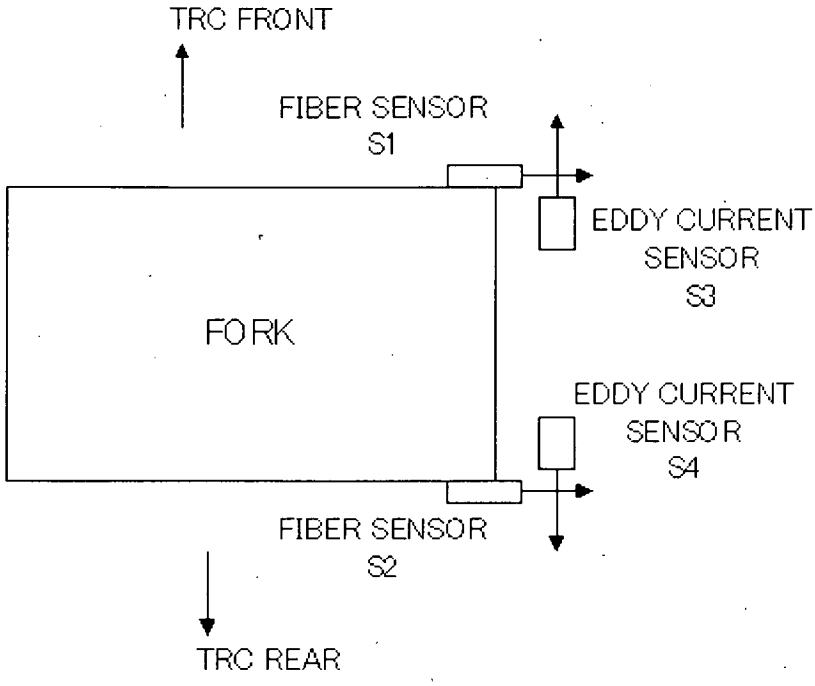

Fig. 3-26 Arrangement of Sensors

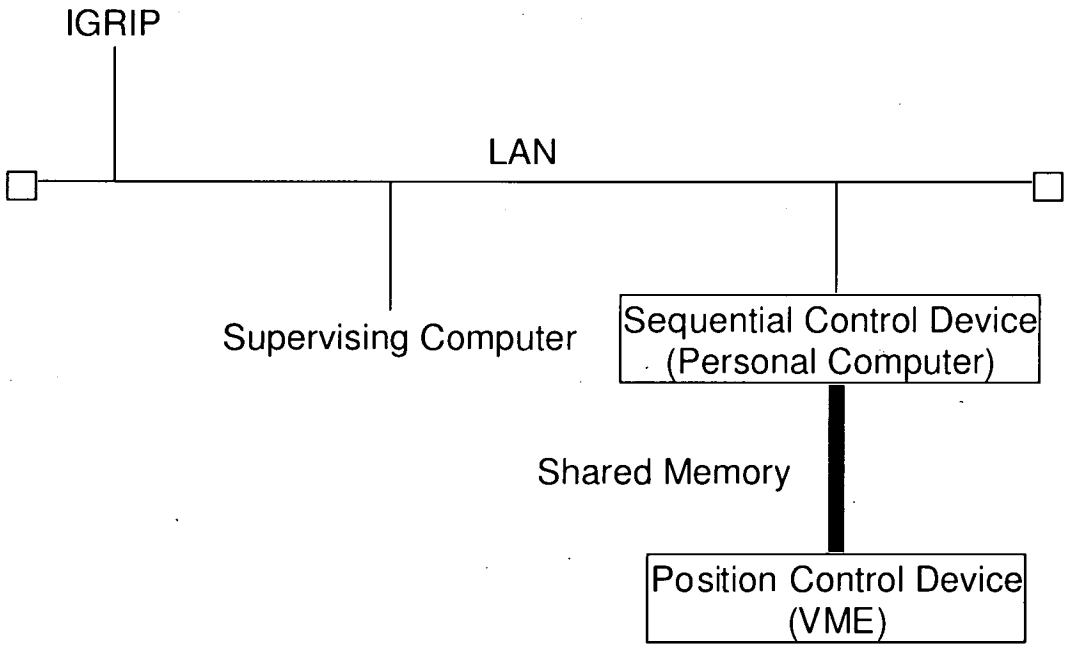

Fig. 3-27 Physical Configuration of Network Connection

From supervisor to PC

Command	**1 byte**
Dummy	**3 byte**
Data Length	**4 byte**
Data	**(Data Length)**

From PC to supervisor

Header	**6 byte**
Comment	**32 byte**
Position Data	**4 byte**

x 27

Fig. 3-28 General Format of Command

'R' (52 H)	Command
0	Dummy
4	Data Length
50	Data (executed program No.)

Fig. 3-29 Command "RUN"

'P' (50H)	Command
0	Dummy
0	Data Length

Fig. 3-30 Command "PAUSE"

'S' (53H)	Command
0	Dummy
0	Data Length

Fig. 3-31 Command "STOP"

Header	Source ID	101	6 byte	x 27
	Destination ID	100		
	No. of Channel	27		
Comment			32 byte	
Position Data			4 byte	

Fig. 3-32 Command "DATA"

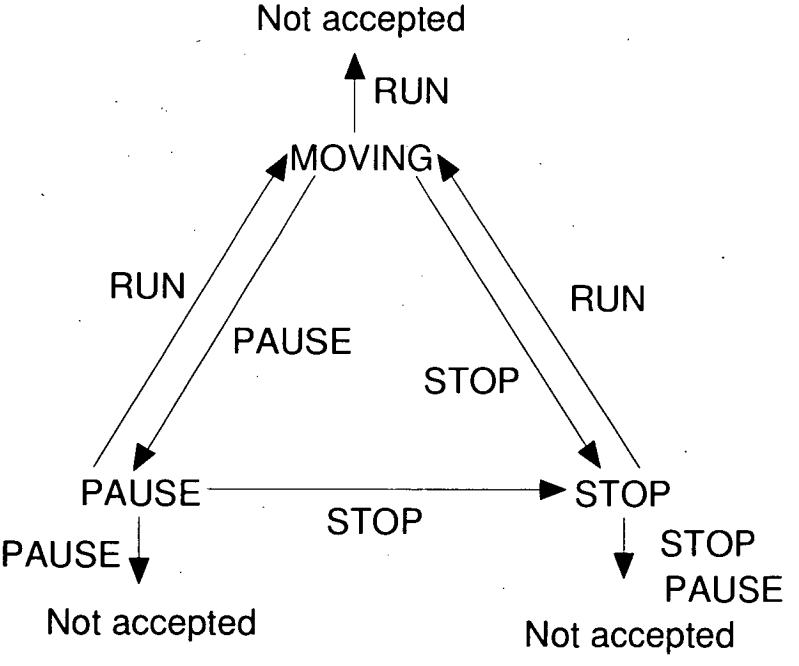

Fig. 3-33 Phase Transition

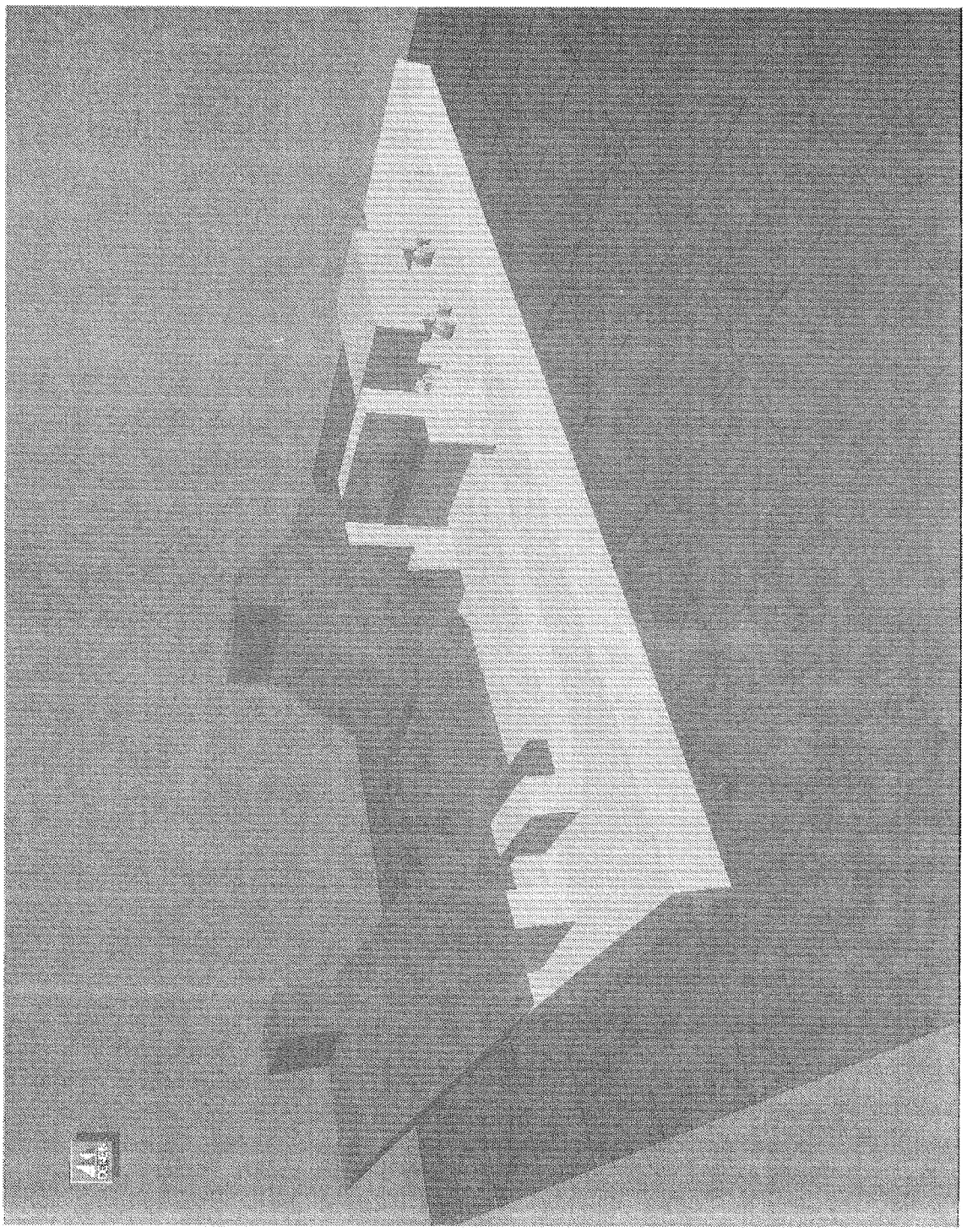

Fig. 3-34 IGRIP Model for SCM

4. CONCLUSION

The divertor cassette of the ITER is a quite heavy component, 25 tons of weight, and is required to be installed with high accuracy for positioning, less than 2 mm. The remote maintenance system for the divertor in the ITER was developed and satisfied all the requirements for it. Detailed results are described as follows.

(1) Link Mechanism for Transportation and Locking of Heavy Components

The two main functions of the maintenance system, transportation and locking, requires high output force and compactness. It was found that the link mechanism can satisfy both of these requirements through comparison with the other mechanisms. Therefore, this report investigated efficient arrangement of the mechanism concentrating on the parameters such as the angle of the link and the transfer efficiency of force. The result of investigation was reflected to the design of the jack-up system and the locking mechanism. The mechanical jack using the link mechanism achieved about 15 tons of lift-up force per a jack in the limited working space. The locking system using the link mechanism, which can be actuated by the small wrench, achieved final positioning accuracy of 0.03 mm while the initial positioning error of the 25-ton cassette was 5 mm.

As a result, this study enabled downsizing of the transporter and satisfied very strict requirement for positioning of the cassette in the ITER using the link mechanism.

(2) Assessment of "Fail-safe" Behavior and Rescue Procedures of the SCM

The fail-safe behavior was assessed for the SCC. It is clarified that the worst accident is the bring-back incompleteness of the fork because it made retraction of SCC impossible. The rescue procedures of the SCC were also studied. The rescue manipulators are effective to actuate the fork from the outside. They are put on the TRC and/or transported by the manipulator for blanket maintenance.

(3) Definition & Validation of Sensor Based Control of the SCM

The sensor-based control of the SCC was implemented for the radial movement of TRC and the toroidal movement of the fork by adopting optical fiber sensors and eddy-current-type distance sensors, respectively. The TRC can find the radial position with accuracy of 0.16 mm with the optical fiber sensors. The eddy-current-type distance sensor can find the abnormal approach of wall to the guiding roller of the fork. This function enables to avoid the bring-back incompleteness of the fork, which is found as the worst accident in the assessment mentioned above. Therefore, it can be said that the sensor-based control modifies the fail-safe behavior of the SCC.

(4) Validation of Human-machine Interfaces of the SCM

The SCM controller has been modified to enable the network communication with TCP/IP and the SCM can be controlled remotely. The human-machine interface of the SCM is prepared by the IGRIP. This function enables the operator to understand the situation in the vacuum vessel virtually, so that the control of the remote maintenance system becomes much easier and safer.

ACKNOWLEDGEMENTS

The author would like to acknowledge Drs. E. Tada, K. Shibanuma and K. Oka of the Japan Atomic Energy Research Institute for their continuous suggestions and encouragement.

The author also would like to acknowledge the contributions of Mr. K. Akou of the Kawasaki Heavy Industries, Ltd., and Mr. Y. Takiguchi of the Toshiba Corporation for their support.

REFERENCES

[1] "ITER EDA Agreement and Protocol", *ITER EDA Documentation Series* No. 1, IAEA, Vienna, 1992

[2] Martin, E., Burgess, T., Cerdan, G., Damiani, C., Duglue, D., Janeschitz, G., Maisonnier, D., Shibanuma, K., Sironi, M., Tada, E., Tesini, A., and Tivey, R., ''Design of the ITER divertor remote handling system,'' in *Proceedings of the 19th SOFT*, Lisbon, Portugal, September, 1996, pp. 1633-1636.

[3] "ITER Council Proceedings", *ITER EDA Documentation Series* No. 5, 53 IAEA, Vienna, (1992)

[4] "Technical basis for the ITER final design report, cost review and safety analysis", *ITER EDA Documentation Series* No. 16, IAEA, Vienna (1998)

[5] "ITER Council Proceedings", *ITER EDA Documentation Series* No. 15, IAEA, Vienna, (1999)

[6] Damiani, C., Cassarini, D., Gaggini, P.A., Scarcella, R., Tarantini, M., Fermani, G., Cerdan, G., Maisonnier, D., Sheppard, J., Millard, J., Blevins, J., Martin, E., Duglue, D., Tesini, A., and Tada, E., ''The Divertor Test Platform,'' in *Proceedings of the 19th SOFT*, Lisbon, Portugal, September, 1996., pp. 1709-1712.

[7] Fukatsu., S., Takeda, N., Kakudate, S., Martin, E., Burgess, T., Shibanuma, K., Maisonnier, D., and Tada, E., ''Development of locking and mover system for ITER divertor maintenance,'' in *Proceedings of the 19th SOFT*, Lisbon, Portugal, September, 1996, pp. 1657-1660.

[8] Takeda, N., Akou, K., Kakudate, S., Takiguchi, Y., Tada, E., Burgess, T., Shibanuma, K., Haange, R., Martin, E. and Janeschitz, G., "Development of Divertor Cassette Transporters for ITER," presented at *the 17th Symp. on Fusion Engineering*, San Diego, USA, 1997.

[9] Takeda, N., Akou, K., Takiguchi, Y., Oka, K., Kakudate, S., Tada, E., Burgess, T., Shibanuma, K., Martin, E., Damiani, C. and Cerdan, G., "Performance Test of Divertor Cassette Transporters for ITER," presented at *the 20th SOFT*, Marseille, France, 1998.

APPENDIX DETAILED DESIGN CALCULATIONS

A.1 Design Calculations for CC and CCC

A.1.1 Mechanical jacks

The loads on the inboard and outboard jacks are:

$F_{in} = W_{cassette}/2 \bullet D_{out}/(D_{in}+D_{out}) = 8{,}800$ kgf,

$F_{out} = W_{cassette}/2 \bullet D_{in}/(D_{in}+D_{out}) = 3{,}700$ kgf,

where

$W_{cassette} = 25{,}000$ kgf (Weight of the cassette),

$D_{out} = 1{,}085$ mm (Horizontal distance between the outboard jack and CoG),

$D_{in} = 455$ mm (Horizontal distance between the inboard jack and CoG).

The maximum axial force F_L on one link can be written as follows:

$F_L=F_{in}/(N\cos\theta)=1{,}324$ kgf,

where

$N = 8$ (the number of the links for one jack),

$\theta = 33.8$ degree (angle of the link when the cassette starts to be lifted).

Compression stress σ_L for a link is:

$\sigma_L = F_L/A = 1.5$ kgf/mm^2,

where $A = 900$ mm^2 (area of cross section of link)

Needed propulsive force F_B for nut to overcome the axial force F_L of the links is:

$F_B = (F_L N/2)\sin\theta = 2{,}946$ kgf.

Service life as rotation L_B can be calculated as follows:

$L_B = (C_a/(F_w \bullet F_a)^3)\times 10^6 = 0.22\times 10^6$ rev.,

where

$C_a = 2{,}683$ kgf,

$F_a = F_B = 2{,}946$ kgf (axial load),

$f_w = 1.5$.

It needs about 15 revolutions for jack to go up and down so the service life as cycle is about 15,000 cycles.

On the other hand, the rating fatigue life of the roller bearing of jack can be written as:

$L_{BR} = (C/P)^{10/3}\times 10^6 = 1.3 \times 10^6$ rev.,

where

$C = 6{,}400$ kgf (Basic load rating),

$P = XF_r + YF_a = 5{,}892$ kgf (Dynamic equivalent load),

$X = 0.4$, $Y = 2.0$ (Radial and axial load factors).

Needed torque for the ball screw can be written as follows:

$T_B = (F_B \bullet l)/(2\pi \bullet \eta) = 260$ kgf•cm,

where

$l = 0.5$ cm (Lead),

$\eta = 0.9$ (Efficiency).

The needed torque must be doubled because there is two nuts on the screw:

$T_{total} = 2T_B = 520$ kgf•cm.

Torsional stress in the shaft can be calculated as:

$\tau_{max} = (16T_{total})/(\pi d^3) = 2.5$ kgf/mm^2,

where $d = 22$ mm (Diameter of the shaft).

Rated torque actuating the shaft is:

$T = T_m Z_h \eta_h = 1{,}166$ kgf•cm,

where

$T_m = 24.3$ kgf•cm (Rated torque of motor),

$Z_h = 1/80$ (Reduction ratio of harmonic drive),

$\eta_h = 0.6$ (Efficiency of harmonic drive).

Rated rotation speed of the shaft is:

$N_s = N_m Z_h = 37.5$ rpm $= 0.625$ rps,

where $N_m = 3{,}000$ rpm (Rated rotation speed of the motor).

The time needed for the jack to move 20 mm is:

$t_{jack} = \Delta L/(lN_s) = 11.7$ sec,

where $\Delta L = 36.7$ mm (stroke of ball screw corresponds to that of jack).

After putting CC directly down on CCC, the load W is applied on the edge of the frame:

$W = (W_{CCC}/N_f + F_{in}/2)/2 = 2{,}389$ kgf,

where

$W_{CCC} = 3{,}000$ kgf (Weight of CCC excluding jacks weight),

$N_f = 8$ (Number of jack frames supporting the loads).

Bending stress of the frame at the root part described below is small compared with the stength of structural steel:

$\sigma = M/Z = Wl_1/Z = 6$ kgf/mm^2,

where

$l_1 = 30$ mm (Offset of weight),

$Z = bH^2/6 = 11{,}880\ mm^3$ (Modulus of section),

$b = 220$ mm (Frame length),

$H = 18$ mm (Frame thickness).

Deflection of the frame at the tip part can be calculated as:

$\Delta t = Wl_1^3/3EI = 0.01$ mm,

where

$E = 2.1\times10^4\ kgf/mm^2$ (Young's modulus),

$I = 6H^3/12 = 106{,}920\ mm^4$ (Geometrical moment of inertia).

The calculated results are summarized in **Table A-1**.

Table A-1 Result of Structural Calculation for Mechanical Jacks

Load Capacity of per a Jack F_{in}	8,800 kgf
Life of Ball Screw L_B	0.22×10^6 rev.
Life of Bearing L_{BR}	1.3×10^6 rev.
Time for 20 mm Jack up t_{jack}	11.7 sec

A.1.2 Wrenches and Locking Systems

Rated torque of the wrench is:

$T = T_m Z_h \eta_h = 1{,}248$ kgf•cm,

where

$T_m = 13$ kgf•cm (Rated torque of motor),

$Z_h = 1/160$ (Reduction ratio of harmonic drive),

$\eta_h = 0.6$ (Efficiency of harmonic drive).

Rated rotation speed of the wrench is:

$N_s = N_m Z_h = 18.75$ rpm $= 0.313$ rps,

where $N_m = 3{,}000$ rpm (Rated rotation speed of the motor).

Generated thrust force of screw bearing (THK DCM36) is:

$F_a = 2\pi\eta T/l = 3{,}528$ kgf,

where

$l = 0.6$ cm (Lead of screw),

$\eta = (1-\mu\tan\alpha)/(1+\mu/\tan\alpha) = 0.27$ (Efficiency),

$\alpha = 3.32°$ (Lead angle of screw),

$\mu = 0.15$ (Friction ratio).

Contact surface pressure is:

$p = F_a / F = 1.34$ kgf/mm^2,

where F = 2,632 kgf (Dynamic permissible thrust).

Sliding velocity at the tooth surface can be calculated as:

$V = (\pi D_o N_s)/\cos\alpha \times 10^3) = 1.94$ m/min,

where D_o = 33 mm (Effective diameter).

Referring the pV value chart, the both values satisfy the criterion.

Axial force in the link of the locking system is:

$F_l = F_a/(2\cos\theta_1) = 3{,}833$ kgf,

where $\theta_1 = 62.6°$ (Angle between the screw and the link).

Axial force in the locking pin is:

$F_p = F_l \sin\theta_1 - \mu F_l \cos\theta_1 = 3{,}050$ kgf.

Contact stress of the link composed of two plates is calculated as:

$\sigma_l = F_l/A_l = 2.0$ kgf/mm^2,

where A = 15×65×2 = 1950 mm^2 (Cross section area of the link).

Required pushing force to correct CC position in the radial direction is:

$F_C = \mu \times W_{cassette} = 7{,}500$ kgf,

where

$\mu = 0.3$ (Friction ratio),

$W_{cassette} = 25{,}000$ kgf (Weight of cassette).Thrust force of the pin to correct Pushing force in the radial direction applied by axial force F_p of the pin is:

$$F_{C1} = N_2\cos\theta_2 - \mu N_2 \sin\theta_2 = F_p \cdot (\cos\theta_2 - \mu\sin\theta_2)/(\sin\theta_2 + \mu\cos\theta_2)$$
$$= 1.35\, F_p = 4{,}117 \text{ kgf},$$

where

$F_p = N_2 \sin\theta_2 + \mu N_2 \cos\theta_2$.

The total pusing force 2 F_{C1} of 8,234 kgf is larger than required pushing force F_p of 7,500 kgf.

Reaction force F_R applied on locking pins induced by the disruption can be calculated as:

$F_R = Wo + Wo' = 52.1$ tonf,

where

Wu = 68 tonf (Upward force induced by the disruption),

Wo = 24.5 tonf (Outward force induced by the disruption).

Upward force Wu' excluding the weight of CC is described below:

$$W_u' = N_3 \cos\theta_3 + \mu N_3 \sin\theta_3 = W_u - W_{CC} \cdot 2/3$$

$$= 51.3 \text{ tonf},$$

where

W_{CC} = 25 tonf (Weight of CC),

2/3: Weight distribution rate on the inboard step

$\theta_3 = 45^\circ$ (Step angle)

Then the normal reaction force N_3 is as follows:

$$N_3 = \frac{W_u'}{\cos\theta_3 + \mu \sin\theta_3}$$

Outward force W_O' as a component of W_u' is as follows:

$$W_O' = N_3 \sin\theta_3 - \mu N_3 \cos\theta_3 = \frac{\sin\theta_3 - \mu\cos\theta_3}{\cos\theta_3 + \mu\sin\theta_3} \cdot W_u'$$

$$= 27.6 \text{ tonf}$$

The reaction force F_R causes the normal reaction force N_4 on the locking pin:

$$N_4\cos\theta_4 + \mu N_4 \sin\theta_4 = F_R/2 = 26.05 \text{ tonf}$$

N_4 can be caluclated as follows:

$$N_4 = \frac{1}{\cos\theta_4 + \mu\sin\theta_4} \cdot \frac{F_R}{2}$$

The axial force F_P' on the locking pins is as follows:

$$F_P' = N_4 \sin\theta_4 - \mu N_4 \cos\theta_4$$

$$= \frac{\sin\theta_4 - \mu\cos\theta_4}{\cos\theta_4 + \mu\sin\theta_4} \cdot \frac{F_R}{2}$$

$$= 1250 \text{ kgf}$$

Axial force F_L' applied on the link induced by the disruption is:

$$F_L' = \frac{F_P'}{\sin\theta_1} = 1287 \textit{ kgf}.$$

Axial force Fa' applied on the trapezoid screw

Fa' $= 2 \cdot F_L' \cdot \cos\theta = 610$ kgf

Maximum permissible static axial force of the screw is 8622 kgf.

Backward transmitting efficiency η_t' of the trapezoid screw is:

$$\eta_t' = \frac{\tan(\alpha - \lambda')}{\tan\alpha} \times 100 \ (\%) = -175\%$$

where

α : Lead angle of the screw = 3.32 degrees

λ' : static friction coefficient $=\tan^{-1}\mu' = 9.1$

$$\mu' = \frac{\mu}{\cos(\beta/2)} = 0.16$$

μ : Friction coefficient of solid lubrication = 0.15

β : Angle of the screw thread = 30 degrees

As shown above η_t' is negative and $\alpha - \lambda'$ is negative then the trapezoid screw can not be driven backward and can be self locked.

Rated output torque T of the wrench driven with the motor's rated torque and with the transmitting efficiency of 0.6 is described below.

T = 1,248 kgfcm

The loads P_1 to P_5 applied to the linear guide blocks shown in are as follows:

$$P_1 = \frac{1}{2}\left(\frac{T}{61} + \frac{T/2}{24}\right) = 232\,kgf$$

$$P_2 = \frac{1}{2}\left(-\frac{T}{61} + \frac{T/2}{24}\right) = 27.5\,kgf$$

$$P_3 = P_1 \times \frac{71}{164} + P_2 \times \frac{1}{164} = 102\,kgf$$

$$P_4 = \frac{P_1 + P_2}{2} + (P_1 + P_2) \times \frac{106}{61}$$

$$= 130 + 260 \times \frac{106}{61} = 582\,kgf$$

$$P_5 = \frac{P_1 + P_2}{2} - (P_1 + P_2) \times \frac{106}{61}$$

$$= 130 - 260 \times \frac{106}{61} = -322\,kgf$$

As shown above the maximum load of 582 kgf is applied on P4. Strength of the linear guide is evaluated as shown below.

$P_4 \cdot f_s = 1164$ kgf < 1377 kgf $= C_0$

where

f_s : Safety coefficient = 2 (small shocks supposed),

C_0 : Static rated load of the linear guide (type HSR15A) = 1377 kgf.

Moment M applied to the bearing supporting the output shaft of the reduction gear (Harmonic Drive gear) is as follows:

$M = 70\,W_{CP} + 145\,F_{CP} = 3{,}005$ kgfmm $= 3.0$ kgfm

where

W_{CP}: Weight of wrench head = 4.4 kgf,

F_{CP}: The maximum spring force of the vertical sliding mechanism = 18.6 kgf.

The strength of the mechanism is evaluated as shown below.

$M \bullet f_s = 3 \times 2 = 6$ kgfm < 9.3 kgfm $= M_0$

where

f_s: Safety coefficient =2 (not continuous operation with small shocks supposed)

M_0: Permissible moment of the gear (type CSF25) = 9.3 kgfm

Strengths of the joint pins and sleeves in Oldham's coupling are evaluated below. Shearing stress τ of the pin shown above and contact pressure P of the pin are as follows:

$$\tau = F_1/A = 195/78.5 = 2.48 \text{ kgf/mm}^2 < \tau_{max} = 18.9 \text{kgf/mm}^2$$

$$P = \frac{F_1}{S} = \frac{195}{51} = 3.8 \, kgf/mm^2 < \delta_{max} = 12 \text{ kgf/mm}^2$$

where

F_1: Couple of forces applied to the pin equivalent to the rated output torque T of the wrench $= \frac{T}{d_{H1}} = \frac{1248}{64} = 195 \, kgf$

d_V: Diameter of the pin = 10 mm

d_{H1}: Distance of between the couple of forces F_1 =64mm

A: Cross sectional area of the pin $= \pi d_v^2/4 = 10^2\pi/4 = 78.5$ mm^2

S: Projected area of the pin with 90 degrees angle as an effective area under the pressure $= \frac{d_V \pi \cdot 6.5}{4} = \frac{10\pi \cdot 6.5}{4} = 51 \, mm^2$

τ_{max}: Permissible shearing stress of structural carbon steel of S45C-H = 18.9 kgf/mm^2,

δ_{max}: Permissible contact pressure of structural carbon steel of S45C-H = 12 kgf/mm^2

Contact pressure P_O on the outer surface of the sleeves and contact pressure P_I on the inner surface of the sleeves are as follows:

$P_O = F_2/S_O = 320/141 = 2.3$ kgf/mm^2 < 4.4 kgf/mm^2 $= P_{AL}$

$P_I = F_2/S_I = 320/164 = 2.0$ kgf/mm^2 < 4.4 kgf/mm^2 $= P_{AL}$

where

S_O: Projected area of the sleeve's inner surface with 90 degrees angles as an effective area under the pressure = 141 mm^2

S_I: Projected area of the sleeve's outer surface with 90 degrees angles as an effective area under the pressure = 164 mm^2

F_2: Couple of forces applied to the sleeves equivalent to the rated output

$$\text{torque T of the wrench} = \frac{T}{d_{H2}} = \frac{1248}{39} = 320\ kgf$$

d_{H2} : Distance of between the couple of forces F_2 = 39 mm

P_{AL} : Permissible contact pressure of aluminum bronze

$= \delta_{0.2}$ (yield strength) $\times 1/7$ = 4.4 kgf/mm^2

The calculated results are summarized in **Table A-2**.

Table A-2 Result of Structural Calculation for Wrenches

Torque of Wrench T	1,248 kgf•cm
Radial Force Caused by Wrench F_{C1}	9,812 kgf
Radial Force Needed for Alignment F_C	7,500 kgf

A.1.3 Rollers

The maximum load on one roller is:

$F_r = F_{in}/8 + W_{CCC}/32$ = 1,210 kgf,

where W_{CCC} = 3,500 kgf (Weight of CCC).

Service life as rotation L_R can be calculated as follows:

$L_R = (f_T C/f_W P_c)^{10/3} \times 10^6 = 4.8 \times 10^6$ rev.,

where

f_T = 0.9 (Temperature factor at 150°C),

C = 3,220 kgf (Basic dynamic load rating),

f_W = 1.5 (Load factor for normal operation)

$P_c = F_r$ = 1,210 kgf (Dynamic equivalent radial load)

Service life as distance L_D is:

$L_D = \pi D_{roller} \times L_R = 1.2 \times 10^3$ km,

where D_{roller} = 80 mm (Diameter of roller).

According to Hertz's theory, width 2b of contact surface and depth z where shearing stress becomes maximum σ_{max} are calculated as follows:

$b = 3.04(F_r R/lE)^{1/2} = 1.09$ mm

$z = 0.786b = 0.44$ mm,

$\sigma_{max} = 2F_r/(\pi bl) = 78.6$ kgf/mm^2

where

R = 40 mm (Radius of roller),

l = 18 mm (Width of roller),
E = 2.1×10^4 kgf/mm^2 (Young modulus).

The calculated results are summarized in **Table A-3**.

Table A-3 Result of Structural Calculation for Rollers

Life of Bearing as Rotation L_R	4.8×10^6 rev.
Life of Bearing as Distance L_D	1.2×10^3 km
Maximum Shearing Stress σ_{max}	78.6 kgf/mm^2
Maximum Shearing Stress Depth z	0.44 mm

A.1.4 CC sliding mechanism with a pushing rod in the inboard locking system

CC can be slid outward so as to make a gap between CC and the inboard step by using the pushing rod which is driven simultaneously with unlocking operation.

Prior to the pushing rod operation, only outboard jacks are lifted by 0.6 mm so as to reduce friction at the outboard steps. Degrees of inclination is evaluated.
Inclination tan θ of CC is described below.

tan θ =1/4529

Height difference δ at the upper plate of the jacks caused by the inclination is as follows:

δ =500/tan θ =0.11mm,

where 500 is the upper plate length.

Reaction forces applied on the inboard step, R_A, and applied on the outboard jacks, R_B are as follows:

$$R_A = \frac{1085\times25}{2757} = 9.84\ tonf$$

$$R_B = \frac{1672\times25}{2757} = 15.16\ tonf < 8.8\times2$$

where 8.8 shown above is the rated lifting force of the jack as described before.

Required thrust force Fc of the pushing rod is as follows:

$F_c = R_A \times \mu$ =2952kgf,

where μ (= 0.3) is static friction coefficient.

Rated thrust force Fa generated by the pushing rod is described below.

$Fa = 2\pi \eta T / l = 3605 kgf$

where

T : Rated torque applied on the trapezoid screw = 1248kgfcm

l : Screw lead of type DCM28 = 0.5 cm

η : Transmitting coefficient of the screw

$$\eta = \frac{1 - \mu \tan\alpha}{1 + \mu / \tan\alpha} = 0.23$$

α : Lead angle of the screw = 3.57 degrees

μ : Friction coefficient with solid lubrication = 0.2

A.1.5 Mechanical connector with compliance

To keep positioning accuracy of CCC, mechanical connector must be rigid while CCC is pushed by TRC.

During an advance of CCC, the spring must keep initial length.

$$F_{move} \leqq F_{spring}, \quad (1)$$

where

F_{move} : Total required force of CCC and CC movement ,

F_{spring} : Pre-load of spring at the connector.

Here F_{move} can be calculated as follows:

$$Fmove = (W_{CC} + W_{CCC}) \times C_f / R_{ro}$$
$$= 285 \text{ kgf}, \quad (2)$$

where

W_{CC} : Weight of CC = 25,000 kgf

W_{CCC} : Weight of CCC = 3,500 kgf

C_f : Rolling friction coefficient = 0.02 ~ 0.04 cm

R_{ro} : Radius of CCC rollers = 4 cm

Then F_{spring} including margin is shown as follows.

$$F_{spring} \geqq F_{move} \times S_f = 428 \text{ kgf}, \quad (3)$$

where

S_f: Safety factor = 1.5.

The mechanical connector should be compliant while CCC is pushed by pushing rod of inboard locking system.

$$F_{rod} \geqq F_{CCC} + F_{slide} + F'_{spring}, \quad (4)$$

where

F_{rod} : Pushing rod force,

F_{CCC} : Rolling friction force of CCC with outboard jacks lifted up,

F_{slide} : Friction force of CC with outboard side jacked up by CCC.

Spring force is supposed to increase due to spring deflection of 5 mm with spring coefficient of 20 kgf / mm. Increased spring force compared with pre-load is:

$$F'_{spring} = F_{spring} + 20 \times 5 = 528 \text{ kgf}$$

F_{CCC} shown in (4) is obtained below.

$$F_{CCC} = (W_{CCC} + W_{CC\_out}) \times C_f / R_{ro}$$
$$\doteq 187 \text{ kgf}, \quad (5)$$

where

W_{CC_out}: Reaction force on outboard jacks = 15,160 kgf.

F_{slide} shown in (4) is obtained below.

$$F_{slide} = W_{CC\_in} \times \mu$$
$$= 2{,}952 \text{ kgf}, \quad (6)$$

where

W_{CC_in} : Shared load on inboard support = 9,840 kgf,

μ : Friction coefficient = 0.3.

Right side of (4) is as follows.

$$F_{CCC} + F_{slide} + F'_{spring} = 187 + 2952 + 528 = 3{,}667 \text{ kgf} \quad (7)$$

Pushing rod force driven with rated torque F_{rod_rated} is as follows.

$$F_{rod\_rated} = 3{,}605 \text{ kgf} \quad (8)$$

Pushing rod force F_{rod} can be more than F_{rod_rated} shown in (8) because torque of servo motor can be doubled from its rated torque in short periods.

A.1.6 Cable connection between CCC and CCC control device

Connectors are used at four location.

Components used in the cable connection are following:

- Connectors of the encoder cables and sensor cables are as follows:

  Type: 42DD series, of Harting Elektronik GmbH, conformed to CE marking

- Connectors of the motor cables are as follows:

  Type: 24DD series, of Harting Elektronik GmbH, conformed to CE marking

* The maximum length of the cables between the motors and their servo drivers must be less than 20 m.

- Cables of the encoders and sensors are as follows:

Type: UN-Li2YCY(TP), of U. I. Lapp GmbH & Co. KG, conformed to CE

marking, with twisted pair element wires of 8×2×0.34 mm, with shielding, and with measurement diameter of 11 mm

- Cables of motors are as follows:

Type : OE-110CY, of Lapp U. I. Lapp GmbH & Co. KG, conformed to CE marking, with element wires of 7×0.5 mm, with shielding and with measurement diameter of 10 mm

The number of cables are shown below.

– Two bundles of three cables for six motors

– Two bundles of three cables for six encoders

–A bundle of three cables for proximity sensors

A.2 Design Calculations for SC, SCC and TRC

A.2.1 Bi-directional fork transporter

(1) Rated transfer torque

Table A-4 shows the gear train values defined.

Table A-4 Gear train of bi-directional fork transporter

AC Servo motor	Harmonic Drive	1st gear Pinoin Gear wheel	2nd gear Pinion Gear wheel	Rack & pinion
1500W 3000rpm	CSF-40-160	m=5 b=30mm	m=5 b=35mm	m=5 b=35mm
Tm=48.7Kgfcm		PCD=10cm	PCD=8cm	PCD=13cm
*	Zh=1/160 Tha=46Kgfm	Zh1=26/20	Zh2=26/16	*
Rated Transfer torque	54.5Kgfm	67.4Kgfm	104Kgfm	1520Kgf

Tm:rated motor torque, Tha:maximum allowance torque of harmonic drive unit,

Zh1,Zh2:gear retio, *:blank

(2) Gear strength

Table A-5 shows gears strength of bi-directional fork transfer.

Table A-5 Gears strength of bi-directional fork transfer

unit:Kgf/mm^2

Location	type	Bend stress		Herz stress	
		Cal.	Limit	Cal.	Limit
1st gear	Pinion	15.9	33	138.4	162
	Gear wheel	14.8	33	121.4	162
2nd gear	Pinion	18.9	33	133.2	162
	Gear wheel	16.1	33	104.5	162
Rack&Pinion	Pinion	17.7	33	101.8	162
	Rack	10.5	33	119.0	122

(3) Applied loads of the fork roller

The applied loads to the fork rollers are calculated as follows.

Reaction force of inborad fork rollers $RF1 = \frac{1160}{2710} \times W1 = 14390Kgf$

Reaction force of outboard fork rollers $RF2 = \frac{1150}{2710} \times W1 = 10609Kgf$

RF1 is greater than RF2 depending on the position of center of gravity. Accordingly,the designed loads (Fr)is calculated to be 1439Kgf.

$$Fr = \frac{RF1}{N \times S} = 1439 Kgf$$

N(number of roller units): 1

S (number of rollers): 10

The maximum loads (Fr'), including the inboard fork dead weight, is calculated as follows.

$$Fr' = Fr + \frac{W3}{s'} = 1457 Kgf$$

W2(weight of the bi-directional fork):180Kgf

S'(sum of rollers): 10

(4) Hertz stress of the fork roller

Specifications of the fork roller are as follows:

Provider: THK

Product No.: NAST40ZZUUR

Material: SUJ2 (High carbon chromium bearing steel, JIS G 4805)

Hardness: HRC 58~64

Hertz stress σ_H can be calculated as follows:

$$\sigma_H = 0.418\sqrt{\frac{F_r' \bullet E}{l \bullet R}} = 72.0 kgf / mm^2$$

E (Young's modulus)=2.1 x 10^4 kgf/mm^2

I (wheel width) = 25.8 mm

R (wheel radius) = 40 mm

Fr' (maximum load force of fork)=1457 kgf

The yield strength of INCONEL 718, a candidate material for the rail, is about 100 kgf/mm^2 at 50 degree so the rail is enough strong. The endurance limit for Hertz stress can be calculated as follows:

$$\sigma_{H\lim} = 2.5 HRC(kgf / mm^2)$$

Therefore, the hardness of the rail must be larger than 28.8HRC.

A.2.2 Second cassette carrier (SCC)

(1) Radial rollers

- Maximum loads of the radial roller

Based on the loading condition. the maximum loads applied to the radial roller is

calculated as follows:

Reaction force to inborad carrier rollers $RF1 = \frac{1715}{2200} \times W1 = 19500Kgf$

Rreaction force to outboard carrier rollers $RF2 = \frac{485}{2200} \times W1 = 5500Kgf$

RF1 is greater than RF2, so maximum loads (Fr) is calculated as follows:

$Fr = \frac{RF1}{N \times S} = 2440Kgf$ N (number of roller units): 2

S (number of rollers): 4

Maximum force (Fr') including the dead weight of the SCC is calculated as follows.

$Fr' = Fr + \frac{W2}{S'} = 2703Kgf$ W2 (weight of the SCC): 4200Kgf

S'(sum of rollers): 16

- Hertz stress of the radial roller

Specifications of the radial roller are as follows:

Material: SCM435-Q (chromium molybdenum steel, JIS G 4105)

Hardness: HRC 35

Hertz stress σ_H can be calculated as follows:

$$\sigma H = 0.418 \times \sqrt{\frac{Fr' \cdot E}{I \cdot R}} = 38.8 \, Kgf/mm^2$$

Fr' (maximum load force of roller)=2703 Kgf

E (Young's modulus)=2.1 x 10^4 Kgf/mm^2

I (wheel width) = 110 mm

R (wheel radius) = 60 mm

The yield strength of INCONEL 718, a candidate material for the rail, is about 100 kgf/mm^2 at 50 degree so the rail is enough strong. The endurance limit for Hertz stress can be calculated as follows:

$$\sigma_{H\lim} = 2.5HRC(kgf/mm^2)$$

Therefore, the hardness of the rail must be larger than 15.5HRC.

(2) Connection of SCC to TRC (gripping structure)

- Mechanical connection

For disengagement/engagement of Second Cassette Carrier from/to tractor, the simple connection structure is required so facilitates easy connection SCC and TRC without position control. For this proposes, pins with hook and rollers are chosen as the gripping structure.

The normal traction force (Ft) and the initial traction force (Fi) required for transportation of cassette by the TRC are calculated as follows:

$$Ft = (W1 + W2) \cdot \frac{f}{R} = 197Kgf$$

$$Fi = Ft \cdot SF = 296Kgf \langle 3000Kgf$$

W 1: prototype regular cassettes weight 25000 Kgf

W 2: SCC weight (assumption) 4500 Kgf

R: radius of SCC radial rollers 60mm

f : misalignment by changing the contact surface 0.4mm

SF: safe factor 1.5

The bend force (M) $M = Fi \cdot l = 7620Kgfcm$

Fi: 3000 Kgf (the design specification)

l : Distance from the pin center to A part of hook

Section modulus (Z) of pin

$$Z = \frac{b \cdot h^2}{6} = 7500mm^2$$ b:side 30mm h:base 50mm

bend stress (σ) is 10.2Kgf/mm^2 which is bellow allowance.

$$\sigma = \frac{M}{Z} = 10.2 \, Kgf/mm^2$$

- Electrical connection

Electrical connectors for SCC motors and sensors are attached near the mechanical connection.

The electrical connectors are the general-purpose round connectors that can be easily retracted by manual operation.

A.2.3 Cassette locking mechanisms

(1) Basic design policy

The inboard rail is to fix the cassette by inserting tapered cotter so as to withstand the electromagnetic loads in the inward and downward direction during disruption.

The outboard rail is to locate the cassette into the final position by inserting straight pins, so as to provide radial flexibility for accommodate thermal expansion. The rail can support the electromagnetic loads applied in the downward direction. The pins support the upward electromagnetic loads.

(2) Locking structure

In the inboard locking system, a tapered big cotter is inserted into the rail for fixation of the cassette. By inserting the cotter, the cassette is slightly moved to the inward and downward due to the angle of taper, resulting in perfect contact to the rail.

In case of the outboard locking, on the other hand, the cassette is positioned correctly by inserting three straight pins: the center pin is to locate the cassette in the toroidal direction and other two pins is to locate the vertical position. In this arrangement, the downward electromagnetic loads can be sustained by the rail which keeping the flexibility in the radial direction for thermal expansion.

(3) Stress calculation of the locking mechanism

The pressure (Pq) and the shearing force (Fs) are calculated by assuming the inward (F1) and upward (F2) electromagnetic loads.

$$F1 = 110 ton$$

$F2 = 30 - 26 = 4 ton$ The disruption force in the upward direction: 30 ton
Regular cassette weight: 26 ton

The presser (Pq) is calculated as follows:

$$Pq = \frac{F1 + F2}{A} = 17\ Kgf/mm^2$$ A: contact surface of cotter 6615mm^2

The shearing force (Fs) is calculated as follows:

$$Fs = \frac{F1+F2}{B} = 6.4\,Kgf/mm^2$$ B: cross section 275mm*65mm

The pressure and the shearing force calculated are lower than the allowance.

A.2.4 Radial movement mechanism (TRC)

The TRC is to move the SCC with cassette to the radial directions by using rack&pinion mechanism.

(1) Main design specification

Weight: Less than 2 ton

Main components

- Main frame
- Rollers and driving mechanism for a radial movement
- Connecting (gripping) mechanism: more than 3ton in the traction proof

Sensors

- Proximity detectors to confirm the radial position: 2
- Over load limit switch: 2

Travelling speed: more than 400 mm/min

(2) TRC driving mechanism

- Rated transmission torque

Table A-6 shows the specification of the TRC gear train. Fugure5.14 shows the TRC gear arrangement.

Table A-6 TRC gear train

	AC servo motor	ball gear	harmonic drive	pinion gear	Rack & pinion
	750W 3000rpm	BR125 SH-20	CSF80-120	m=5 b=70mm	m=5 b=70mm

		Zs=1/20	Zh=1/120	PCD=150mm Zh1=45/30	PCD=225mm
Rated transfer torque	Tm= 24.3Kgfcm	4.2Kgfm	347Kgfm	494.5Kgfm	4176Kgf
Allowance maximum torque		7Kgfm	319Kgfm		

Tm: motor rated torque, Zs: ball gear reduction ratio, Zh Zh1: Harmonic drive reduction ratio

Transfer torque of ball gear

Fs: rated transfer torque of ball gear

$$Fs = \frac{Tm}{Zs} \cdot \eta s \cong 4.2 Kgfm$$

Tm: motor rated torque 24.3Kgfcm

Zs: ball gear reduction ratio 1/20

η s: ball gear efficiency 0.85

Transfer torque between motor and harmonic drive

Fh: rated transfer torque of harmonic drive

$$Fh = \frac{Fs}{Zh} \cdot \eta h = 347 Kgfm$$

Zh:harmonic drive reduction ratio 1/120

η h:harmonic drive efficientcy 0.7

Transfer torque between motor and pinion gear

Fp: rated transfer torque of pinion gears

$$Fp = \frac{Fh}{Zg} \cdot \eta g = 495 Kgfm$$

Zp:pinion gears reduction ratio 1.5

η p:pinion gears efficiency 0.95

Rated output of TRC

Wout:rated output of TRC

$$Wout = \frac{Fp}{R} \cdot \eta lp = 4176 Kgf$$

R:radius of final pinion gear

η lp:rack&pinion efficiency 0.95

Rated speed of TRC

$$Vout = 6120 \cdot \frac{Lmtr}{Wout} \cdot \eta = 9.8 mm/s$$

Vout:rated speed of TRC

Lmtr:AC servomotor reted output 750w

η :sum of gears efficiency 0.537

-Stress calculation of Gear

The calculated stress and Herz stress action on gear are summarized in Table A-7, together with their allowance.

Table A-7 TRC gear stress

unit:Kgf/mm^2

location		Bend stress		Herz stress	
		Cal.	Limit	Cal.	Limit
gear	Pinion	28.0	33.3	158.3	162
	Gear wheel	26.1	33.3	129.3	162
Rack&Pinion	pinion	16.5	33.3	79.6	162
	rack	14.2	33.3	85.0	122

- Stress calculation of TRC wheel

Based on the loading conditions, TRC moment (Mtrc) and upward force (Fr) by SCC weight can be calculated as follows:

$$Mtrc = Ftrc \cdot L1 = 418 Kgfm$$

Ftrc:TRC driving power 4176Kgf

L1:distance from radial rail to the connector 100mm

The forces of each wheel

$$Ra1 = Ra2 = \frac{Mtrc}{2 \cdot L3} = 209Kgf$$ L2:500mm L3:1000mm

Upward-torque of TRC

$Fr = F \cdot \tan\theta = 1520Kgf$ θ :pressure angle 20 deg

loads of P1 and P2

$$P1 = \frac{Ra1}{2} + \frac{W1 - Fr}{8} = 65Kgf$$

$$P2 = \frac{Ra2}{2} - \frac{W1 - Fr}{8} = 145Kgf$$

w1:TRC weight 1200Kgf

- Herz stress between TRC wheel and radial rail

As TRC wheel is 140mm in the wheel diameter and 127mm in the length, Herz stress σ_H in cylindrical plane is calculated as follows:

$$\sigma H = 0.418 \times \sqrt{\frac{Fr' \cdot E}{I \cdot R}} = 11.0Kgf$$

Fr' (maximum load force of wheel)=145 Kgf

E (Young' modulus)=2.1x10^4 Kgf/mm^2

I (wheel length) = 70 mm

R (wheel radius) = 127 mm

A. 3 Graphs Concerning Design Calculations for Link Mechanism

Figure A-1 shows relation between angle of link and horizontal stroke for the mechanical jack. Figure A-2 shows relation between angle of link and vertical position of the mechanical jack. Figure A-3 shows relation between vertical position and horizontal movement of the mechanical jack. Figure A-4 shows dependence of transfer efficiency of velocity on angle of link. Its dependence on q can be expressed as:

$f(\theta) = \cos\theta/(1+\sin\theta)$.

Fig. A-5 shows relation between link angle at top position and necessary link length.

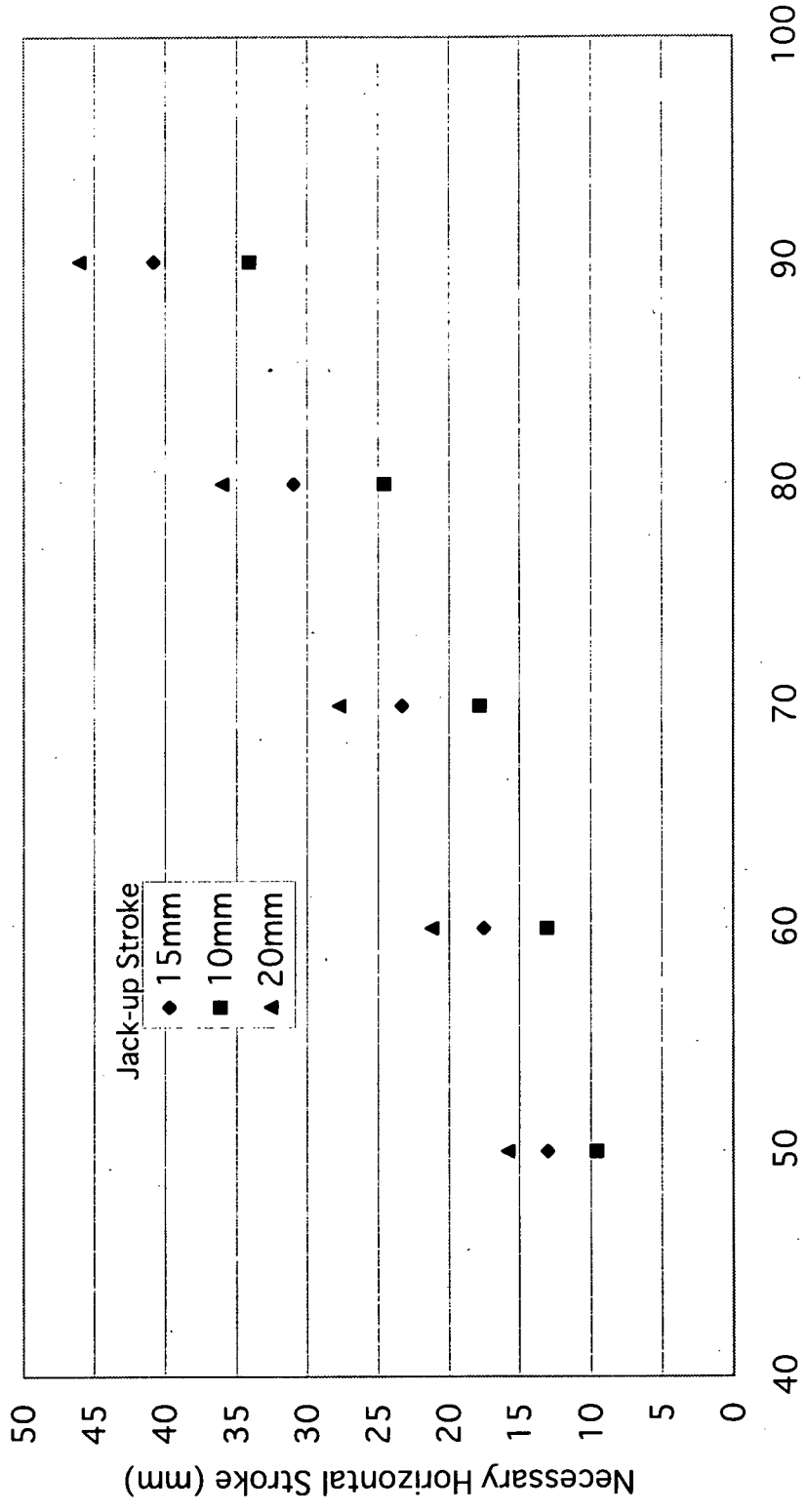

Fig. A-1 Relation between Angle of Link and Horizontal Stroke

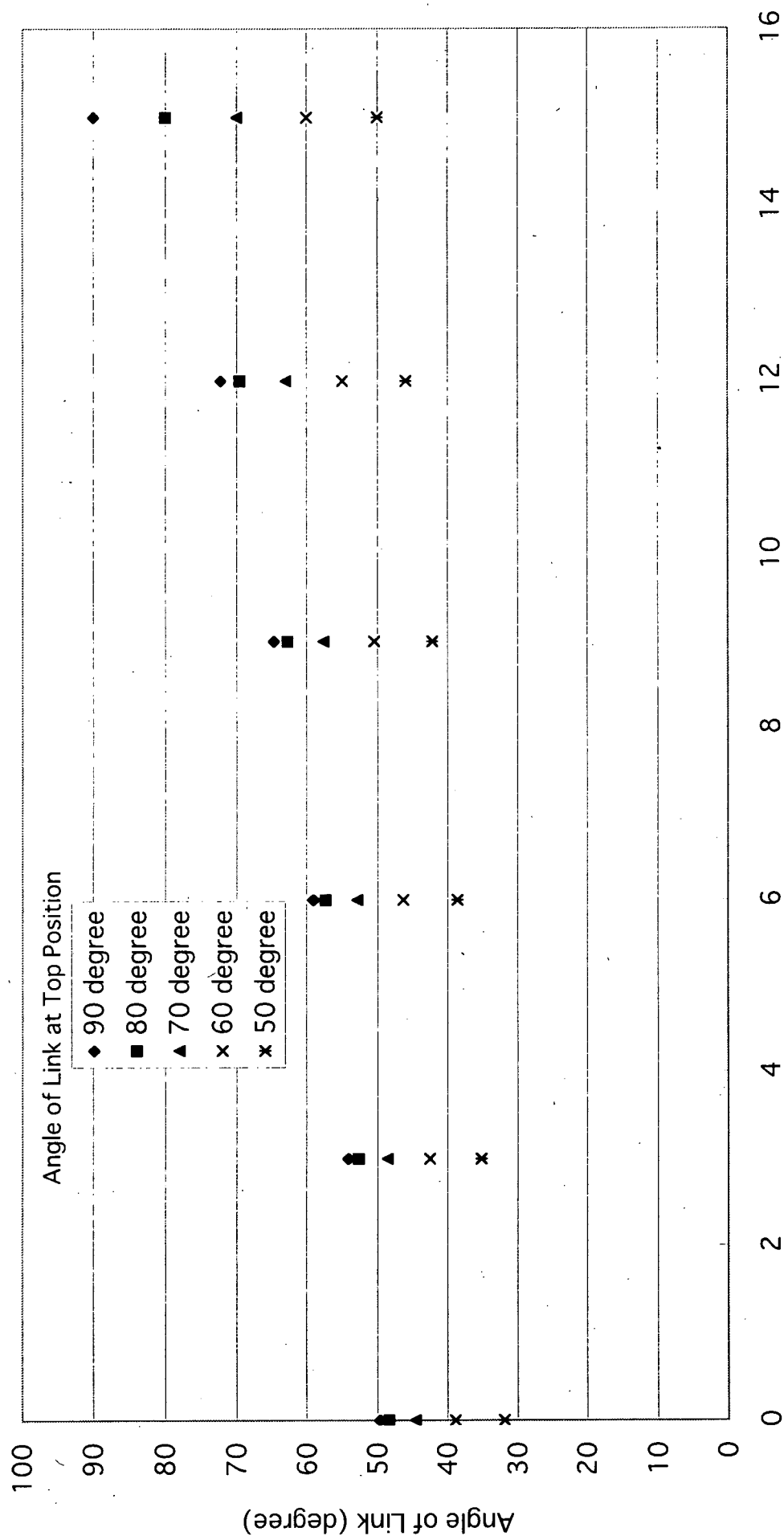

Fig. A-2 Relation between Angle of Link and Vertical Position

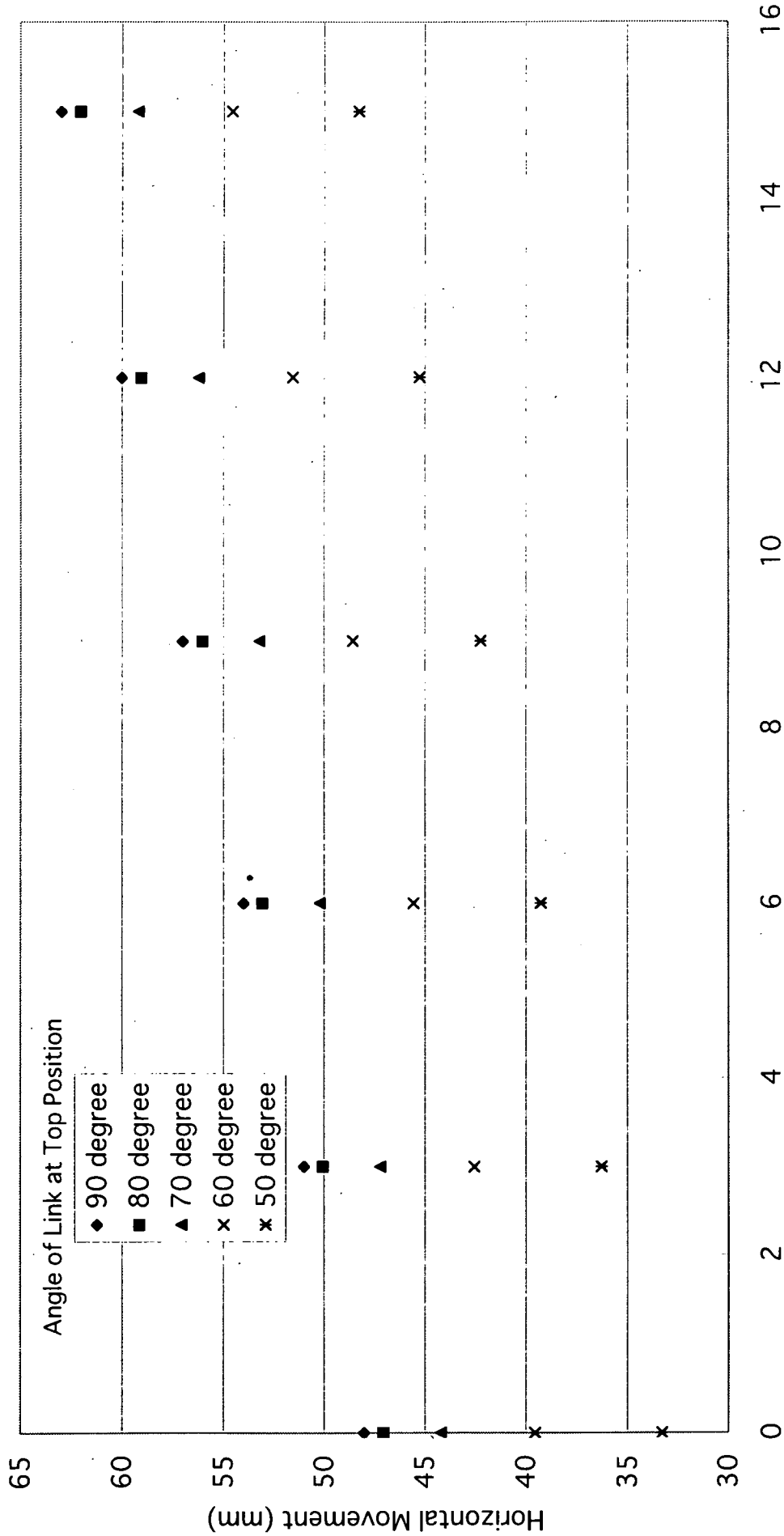

Fig. A-3 Relation between Vertical Position and Horizontal Movement

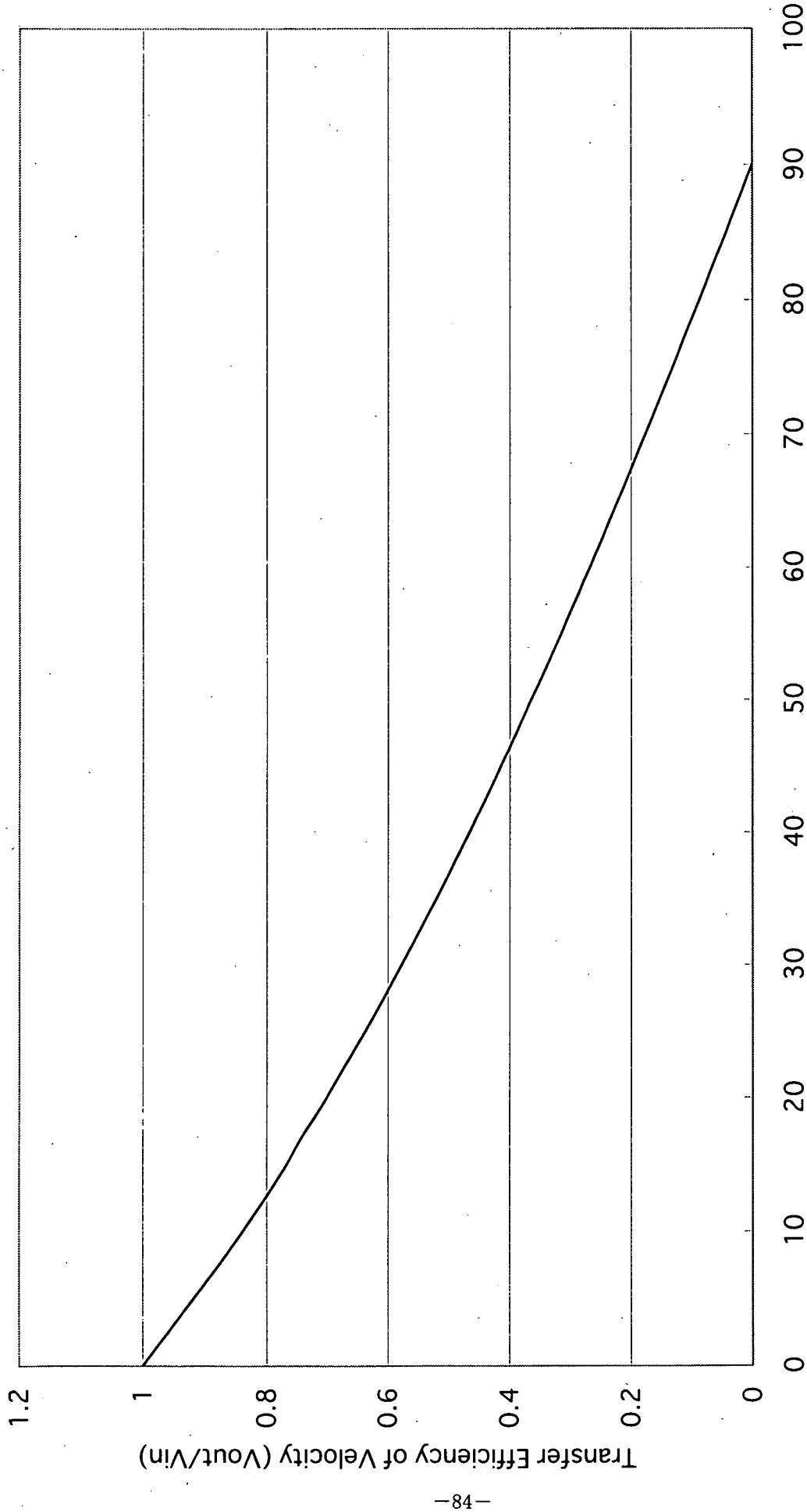

Fig. A-4 Dependence of Transfer Efficiency of Verlocity on Angle of Link

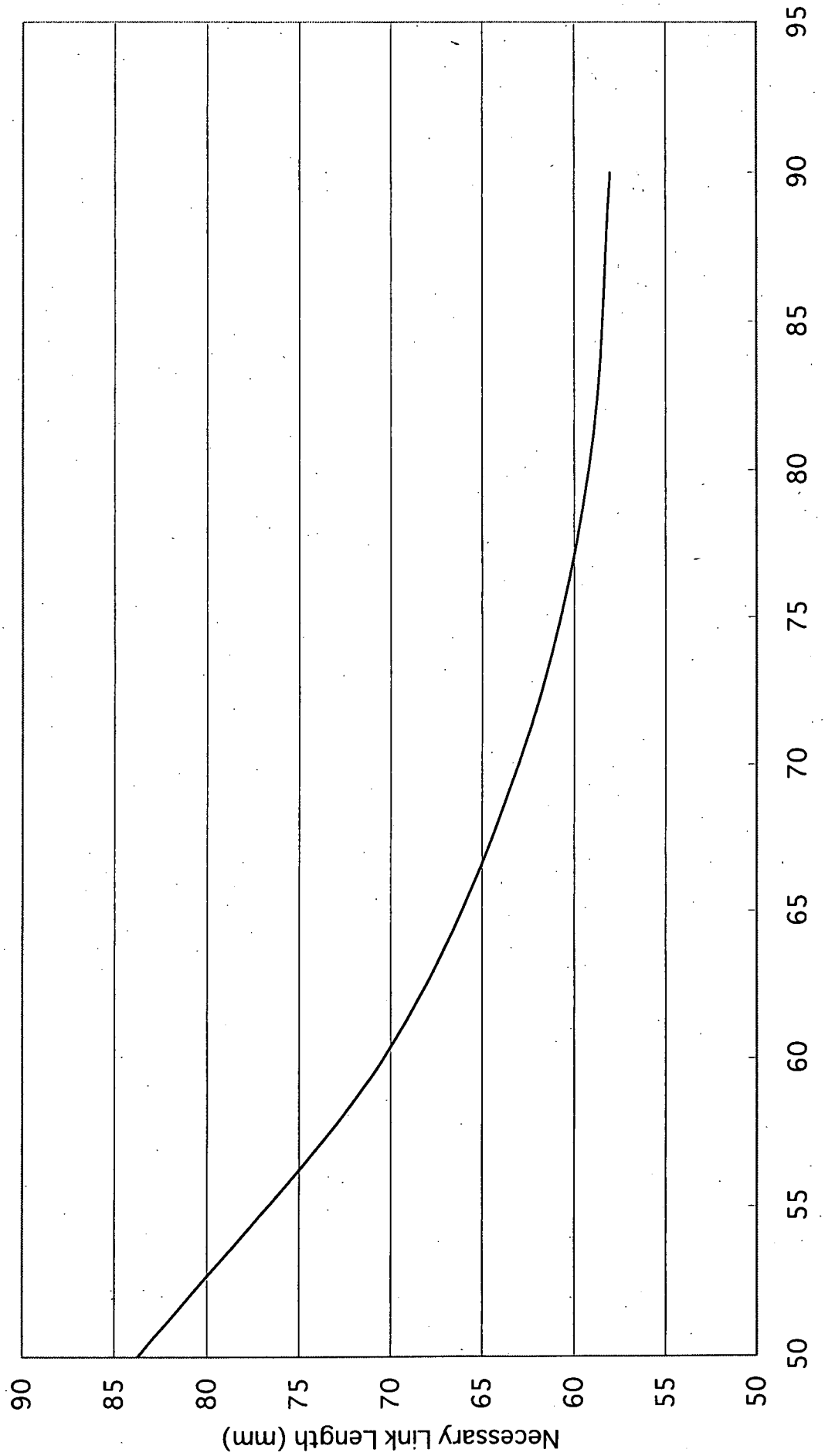

Fig. A-5 Relation between Link Angle at Top Position and Necessary Link Length

This is a blank page.

国際単位系 (SI)と換算表

表1　SI基本単位および補助単位

量	名称	記号
長さ	メートル	m
質量	キログラム	kg
時間	秒	s
電流	アンペア	A
熱力学温度	ケルビン	K
物質量	モル	mol
光度	カンデラ	cd
平面角	ラジアン	rad
立体角	ステラジアン	sr

表2　SIと併用される単位

名称	記号
分，時，日	min, h, d
度，分，秒	°, ′, ″
リットル	l, L
トン	t
電子ボルト	eV
原子質量単位	u

1 eV=1.60218×10^{-19}J

1 u=1.66054×10^{-27}kg

表3　固有の名称をもつSI組立単位

量	名称	記号	他のSI単位による表現
周波数	ヘルツ	Hz	s^{-1}
力	ニュートン	N	$m\cdot kg/s^2$
圧力，応力	パスカル	Pa	N/m^2
エネルギー,仕事,熱量	ジュール	J	N·m
工率，放射束	ワット	W	J/s
電気量，電荷	クーロン	C	A·s
電位，電圧，起電力	ボルト	V	W/A
静電容量	ファラド	F	C/V
電気抵抗	オーム	Ω	V/A
コンダクタンス	ジーメンス	S	A/V
磁束	ウェーバ	Wb	V·s
磁束密度	テスラ	T	Wb/m^2
インダクタンス	ヘンリー	H	Wb/A
セルシウス温度	セルシウス度	℃	
光束	ルーメン	lm	cd·sr
照度	ルクス	lx	lm/m^2
放射能	ベクレル	Bq	s^{-1}
吸収線量	グレイ	Gy	J/kg
線量等量	シーベルト	Sv	J/kg

表4　SIと共に暫定的に維持される単位

名称	記号
オングストローム	Å
バーン	b
バール	bar
ガル	Gal
キュリー	Ci
レントゲン	R
ラド	rad
レム	rem

1 Å=0.1nm=10^{-10}m

1 b=100fm^2=10^{-28}m^2

1 bar=0.1MPa=10^{5}Pa

1 Gal=1cm/s^2=10^{-2}m/s^2

1 Ci=3.7×10^{10}Bq

1 R=2.58×10^{-4}C/kg

1 rad=1cGy=10^{-2}Gy

1 rem=1cSv=10^{-2}Sv

表5　SI接頭語

倍数	接頭語	記号
10^{18}	エクサ	E
10^{15}	ペタ	P
10^{12}	テラ	T
10^{9}	ギガ	G
10^{6}	メガ	M
10^{3}	キロ	k
10^{2}	ヘクト	h
10^{1}	デカ	da
10^{-1}	デシ	d
10^{-2}	センチ	c
10^{-3}	ミリ	m
10^{-6}	マイクロ	μ
10^{-9}	ナノ	n
10^{-12}	ピコ	p
10^{-15}	フェムト	f
10^{-18}	アト	a

(注)

1．表1－5は「国際単位系」第5版，国際度量衡局1985年刊行による。ただし,1 eVおよび1 uの値はCODATAの1986年推奨値によった。

2．表4には海里，ノット，アール，ヘクタールも含まれているが日常の単位なのでここでは省略した。

3．barは，JISでは流体の圧力を表わす場合に限り表2のカテゴリーに分類されている。

4．EC閣僚理事会指令ではbar，barnおよび「血圧の単位」mmHgを表2のカテゴリーに入れている。

換算表

力	N(=10^{5}dyn)	kgf	lbf
	1	0.101972	0.224809
	9.80665	1	2.20462
	4.44822	0.453592	1

粘度　1 Pa·s(N·s/m^2)=10 P(ポアズ)(g/(cm·s))

動粘度　1m^2/s=10^{4}St(ストークス)(cm^2/s)

圧力	MPa(=10bar)	kgf/cm^2	atm	mmHg(Torr)	lbf/in^2(psi)
	1	10.1972	9.86923	7.50062×10^3	145.038
	0.0980665	1	0.967841	735.559	14.2233
	0.101325	1.03323	1	760	14.6959
	1.33322×10^{-4}	1.35951×10^{-3}	1.31579×10^{-3}	1	1.93368×10^{-2}
	6.89476×10^{-3}	7.03070×10^{-2}	6.80460×10^{-2}	51.7149	1

エネルギー・仕事・熱量	J(=10^7 erg)	kgf·m	kW·h	cal(計量法)	Btu	ft·lbf	eV
	1	0.101972	2.77778×10^{-7}	0.238889	9.47813×10^{-4}	0.737562	6.24150×10^{18}
	9.80665	1	2.72407×10^{-6}	2.34270	9.29487×10^{-3}	7.23301	6.12082×10^{19}
	3.6×10^6	3.67098×10^5	1	8.59999×10^5	3412.13	2.65522×10^6	2.24694×10^{25}
	4.18605	0.426858	1.16279×10^{-6}	1	3.96759×10^{-3}	3.08747	2.61272×10^{19}
	1055.06	107.586	2.93072×10^{-4}	252.042	1	778.172	6.58515×10^{21}
	1.35582	0.138255	3.76616×10^{-7}	0.323890	1.28506×10^{-3}	1	8.46233×10^{18}
	1.60218×10^{-19}	1.63377×10^{-20}	4.45050×10^{-26}	3.82743×10^{-20}	1.51857×10^{-22}	1.18171×10^{-19}	1

1 cal= 4.18605J（計量法）

= 4.184J（熱化学）

= 4.1855J（15℃）

= 4.1868J（国際蒸気表）

仕事率　1 PS(仏馬力)

= 75 kgf·m/s

= 735.499W

放射能	Bq	Ci
	1	2.70270×10^{-11}
	3.7×10^{10}	1

吸収線量	Gy	rad
	1	100
	0.01	1

照射線量	C/kg	R
	1	3876
	2.58×10^{-4}	1

線量当量	Sv	rem
	1	100
	0.01	1

(86年12月26日現在)

Research and Development of Remote Maintenance Equipment for ITER Divertor Maintenance